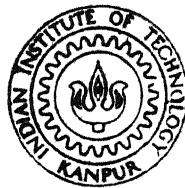# THEORETICAL INVESTIGATION OF
THE DEFORMATION PROCESS IN BLANKING

by

PRAKASHKUMAR BABULAL POPAT

DEPARTMENT OF MECHANICAL ENGINEERING
INDIAN INSTITUTE OF TECHNOLOGY KANPUR
APRIL, 1986

THEORETICAL INVESTIGATION OF
THE DEFORMATION PROCESS IN BLANKING

A Thesis Submitted

in Partial Fulfilment of the Requirements

for the Degree of

DOCTOR OF PHILOSOPHY

by

PRAKASHKUMAR BABULAL POPAT

to the

DEPARTMENT OF MECHANICAL ENGINEERING

INDIAN INSTITUTE OF TECHNOLOGY KANPUR

APRIL, 1986

Thesis
621.984
P91±

ME- 1986- D - POP- THE

TO

MY WIFE JYOTSNA

CERTIFICATE

This is to certify that the work entitled, 'THEORETICAL INVESTIGATION OF THE DEFORMATION PROCESS IN BLANKING' by Prakashkumar Babulal Popat has been carried out under my supervision and has not been submitted elsewhere for a degree.

(A. Ghosh)
Professor
Department of Mechanical Engineering
Indian Institute of Technology
Kanpur.

April, 1986

ACKNOWLEDGEMENTS

I am deeply indebted to my wife Jyotsna for her patienc
and understanding during this work, and to my children Dipal
Jagesh for brightening many a gloomy day by their love and
cheer. I am also thankful to my parents and my brother for
their encouragement for higher education.

At the end I am thankful to all those who helped me
directly or indirectly during my stay at I.I.T., Kanpur.

P.B. Popat

CONTENTS

List of Tables

List of Figures

Nomenclature

a	Nodal displacement vector
b	Vector of body force components
[B]	Strain displacement matrix
c	Punch-die clearance
c/t	Fractional punch-die clearance
c_o	Optimum punch-die clearance
$\dfrac{c_o}{t}$	Optimum punch-die clearance ratio
[D]	Stress-strain matrix
$[D^{ep}]$	Elasto-plastic stress-strain matrix
d	Blank diameter
$\det J_{ij}$	Determinant of Jacobian matrix of transformation
E	Elastic modulus
G	Shear modulus
H'	Strain hardening parameter
K	Element stiffness matrix
[K]	Global stiffness matrix
k	Yield shear stress
L	Length of cut or punch width
N	Shape function
[N]	Shape function matrix
NEL	Number of elements
P	Punch force
P_{max}	Maximum punch force

$\{Q\}$	Global load vector
q	Elemental nodal force vector
$\{R_L\}$	Nodal force vector
r	Externally applied concentrated load vector
S_s	Ultimate shearing strength
t	Sheet thickness
$\bar{t}$	Vector of traction components
$\{U\}$	Global vector of nodal displacements
u,v	Nodal displacement in x and y directions
σ	Stress
σ_o	Initial stress
σ_{av}	Average stress
σ_m	Hydraustatic stress component
σ_{yp}	Tensile yield stress
σ_x', σ_y'	Deviatoric stress components in x and y direction
σ_1, σ_2, σ_3	Three principal stresses
$\bar{\sigma}$	Effective stress
τ	Shear stress
ε	Strain
ε_o	Initial strain
ε_f	Local fracture strain
$\bar{\varepsilon}$	Effective strain
γ	Poisson's ratio

α_i, α_j Gaussian quadrature weights

δ/t Fractional punch penetration

$\dfrac{\Delta+c}{t}$ Fractional punch penetration at crack initiation

$\dfrac{\Delta+c}{t}_o$ Optimum punch penetration at crack initiation

Θ Diagonal angle of deformed continuum with y-axis

$\emptyset$ Direction of the maximum shear strain with y-axis.

SYNOPSIS

THEORETICAL INVESTIGATION OF THE DEFORMATION PROCESS
IN BLANKING

A Thesis Submitted
In Partial Fulfilment of the Requirements
for the Degree of
DOCTOR OF PHILOSOPHY
by
PRAKASHKUMAR BABULAL POPAT
Department of Mechanical Engineering
Indian Institute of Technology, Kanpur
April, 1986

The present work is an investigation of the sheet metal
deformation during blanking operation using finite element
analysis. Blanking, punching, trimming, shaving and other
operations for cutting metal sheets to shape using a die and a
punch, forms an important group of press operations. These are
the basic operations to several secondary operations such as
drawing, coining, etc.

Although blanking is one of the simplest and also one of
the well studied press operations, there are a number of un-
solved problems which are required to be taken up. While
reviewing the available literature on this process, it is found
that a large number of experimental and semi-experimental tech-
niques are used in the study of the process. But the reported
theoretical work is not exhaustive. The process of blanking is
unsteady and a closed form analytical solution to this operation
is not feasible.

The finite element method is used in the present analysis
because it is a versatile method and it is possible to predict
the distribution of stress, strain, strain-rate etc. with suffi-
cient accuracy using this technique. Based on the displacement

formulation, a general purpose elasto -plastic finite element programme is developed. The 'initial stress method' is used for the nonlinear analysis, with the material obeying von-Mises yield criterion. The parabolic isoparametric elements are used to discretize the continuum.

The deformation during the process is assumed to be a two-dimensional plane strain one. Displacement-controlled analysis is performed by suitably prescribing the displacement increments. The material is assumed to be linear elastic-linear strain-hardening type. A large number of computer runs are taken by varying the process parameters.

Punch-die clearance c, sheet thickness t, cutting conditions and the material properties such as elastic modulus E, Poisson's ratio γ, yield stress σ_{yp}, strain hardening parameter H' and local fracture strain ε_f are considered as the important parameters of the process. In this work the effects of the fractional punch-die clearance c/t, t, H' and ε_f on the punch force, punch penetration (at crack initiation), deformation pattern, optimum clearance etc. are investigated. The punch and the die surfaces are assumed to be flat, smooth and possess sharp edges.

A crack is introduced into the sheet by using the following crack initiation criterion. This states that, a crack is initiated at any point in the material where the effective

strain becomes equal to or greater than the specified local fracture strain of the material. It is also postulated that, the crack propagation direction coincides with the direction of the maximum shear strain at the crack initiating point. The execution of the programme is terminated as soon as an indication of the crack initiation is obtained. The results, thus obtained, are used to plot a number of graphs showing the effects of the various parameters, the deformation patterns, the strain distributions etc. From these an attempt has been made to find out the optimum punch-die clearance, maximum punch force, maximum punch penetration etc. for different combinations of the process parameters.

Based on this analysis it can be inferred that the maximum punch force is almost independent of the punch-die clearance. With larger value of H', the punch force required (for the same punch penetration) increases, and finally to initiate a crack more punch force is needed. The variation of sheet thickness is also found to yield similar results. But it is observed that variation of t and H' has very little effect on the percentage punch penetration for a given value of c/t ratio. The percentage punch penetration (at crack initiation) increases with the increase in c/t ratio and the ductility (ε_f) of the material. It is found that the above observations agree well with the experimental results obtained by previous researchers in this field.

When the clearance between the punch and the die is optimum, the cracks originated from the punch and the die corners meet each other after propagating along a straight line, resulting in a clean edge. As it was not possible to get crack propagation path from the finite element analysis the following presumption is made to get the optimum clearance. It states that when the clearance is optimum, the line passing through the corners of the punch and the die (at crack initiation) coincides with the direction of the maximum shear strain. By making use of this criterion optimum punch-die clearance for different values of ductility are obtained. From these an estimate of the maximum punch penetration for each value of the optimum clearance is also made. The results are examined critically and verified with the available experimental and theoretical results. It is found that they are in close agreement with the experimental results and the trends match with the previously obtained theoretical results. The optimum clearance reduces as the ductility of the metal is increased. So it can be concluded that the more ductile metals, e.g., aluminium require less punch-die clearance compared to the less ductile metals like mild steel, for satisfactory blanking. The optimum percentage punch penetration does not vary much with the ductility of the metal, and its value is found to remain around 30%, as obtained in previous experimental works.

Finally, to visualise the deformation mode of the material
in and around the clearance gap, the patterns of the nodal dis-
placements at each incremental step are plotted.   It is in-
fered that the material near the punch and the die corners
deforms most severely. This clearly brings out that the cracks
should initiate near the punch and the die corners as observed
in practice. Similar conclusion is also drawn from the strain
distribution contours which are plotted in the clearance gap,
i.e., the maximum value of strains occur near the punch and the
die corners for all cases considered.

At the end it is concluded that with the help of this
technique, it is possible to predict with sufficient accuracy
the values of the optimum punch-die clearance and the press
load required, without performing the experiments. Although
attempts have been made by other researchers to analyze theore-
tically the blanking process, but the results obtained by the
finite element analysis, proposed in this work, are found to be
much more accurate and the trends obtained regarding the effects
of the various parameters using this technique are in closer
agreement with the experimental work, when compared with pre-
vious theoretical work.

CHAPTER 1

INTRODUCTION

1.1 INTRODUCTION

The technology of sheet-metal press-work emerged with the development of steel industry, and to a large degree we owe our present standard of living to the production of stamped metal parts. A large number of metal parts are manufactured on press, which are being used in household goods, automobiles and other items.

Most of the operations for shaping sheet metal into finished products can be described as either cutting or forming operations. These are generally referred to as stamping, press-working or punch press working of sheet metal. Such processes are very economical as the desired shape, size and finish can be obtained without any significant loss of material. Moreover, a part of the input energy is fruitfully utilised in improving the strength of the product through strain hardening.

Blanking, punching, trimming, shaving and other operations of cutting metal sheets to shape using die and punch, forms a distinct group of press operations, the subdivision of which have much in common. This group is the largest among all the groups of press operations, the simplest and also the best

understood. The above mentioned operations are basic to several secondary operations such as drawing, coining etc. Still there are a number of unsolved problems and several complications which requires attention [1,2].

1.2 BASIC MECHANICS OF BLANKING

In punching and blanking processes [3], a finite volume from a sheet metal is removed by using a die and a punch. The shape and the size of the portion removed are determined by the geometry of the die and the punch. If the final product happens to be the removed portion, then the operation is termed as blanking; on the other hand, if the pierced sheet metal is the final product then the operation is called punching. However, the basic mechanics of metal removal is same in both the operations.

Fig. 1.1 shows a simple punching operation. The job is held by job holders to prevent any distortion and to provide a rigid support. The punch and the die corners are sharp, i.e., without any radius, as the objective in this process is to achieve rupture of the material. A clearance c is provided between the punch and the die. Hence the die diameter $d_d = d_p + 2c$ where d_p is the diameter of the punch.

The process of sheet metal blanking is studied with two different aims. In one case the emphasis is purely on the study of the mechanics of the deformation process, while in the
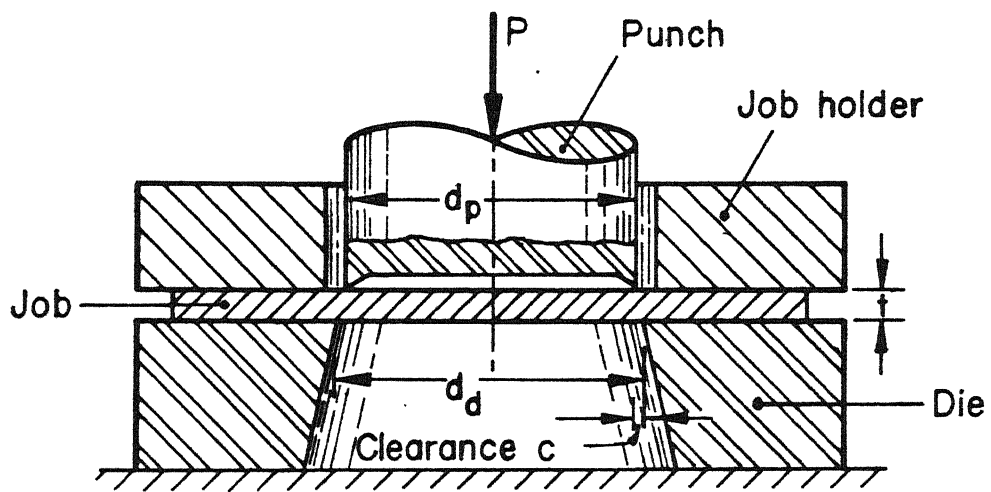
Fig.1.1 Details of punching process

other the effects of the various process parameters are studied. The most commonly accepted theory for blanking operation is based on the concept of shear failure of the material lying between the punch and the die. This theory results in a very simple formula to determine press load, which is given as follows :

$$P_{max} = L \times t \times S_s \qquad (1.1a)$$

or

$$P_{max} = \pi \times d \times t \times S_s \qquad (1.1b)$$

where

P_{max} = The maximum punch force to shear any shape with a sharp flat punch and a die having proper clearance between them.

L = Length of the cut, t = thickness of the metal,

d = Diameter of the blank,

S_s = Ultimate shearing strength of the metal.

In this theory it is not possible to incorporate the effects of the other process parameters such as the amount of clearance between the die and the punch etc.

Fig. 1.2 shows the nature of metal deformation as the punch penetrates into the workpiece. As the downward motion of the punch progresses, the workpiece material deforms and is pulled down by the punch movement causing the grains to

elongate near the punch corner B [3]. A similar type of deformation takes place near the other die corner D. When the grain elongation or the local natural strain in the surface fibre AB (of the workpiece) reaches a limiting value, the fibre ruptures. Since the local strain is maximum at the corner, a crack opens up at the punch corner. After this, with a slight movement of the punch, the inner fibres also get ruptured. Thus the fracture line BY propagates, following a path along which the successive inner fibres attain the fracture strain. A similar crack also propagates from the corner D (because of the symmetry of the deformation geometry). Now if the amount of clearance c is optimum, then the two fracture lines meet and a clean edge is obtained after the operation (Fig. 1.3a). If the clearance is too small, then the fracture lines miss each other and the secondary deformation takes place, resulting in an unclean edge (Fig. 1.3b). Fig. 1.3c shows what happens when the amount of clearance is too large, a significant amount of drawing action takes place and the quality of the workpiece is again quite poor.

1.3 PREVIOUS WORK

The first scientific paper on blanking appears to be that by Anthony [4] published in 1911. It describes a pressure recording apparatus suitable for use with a punching machine.
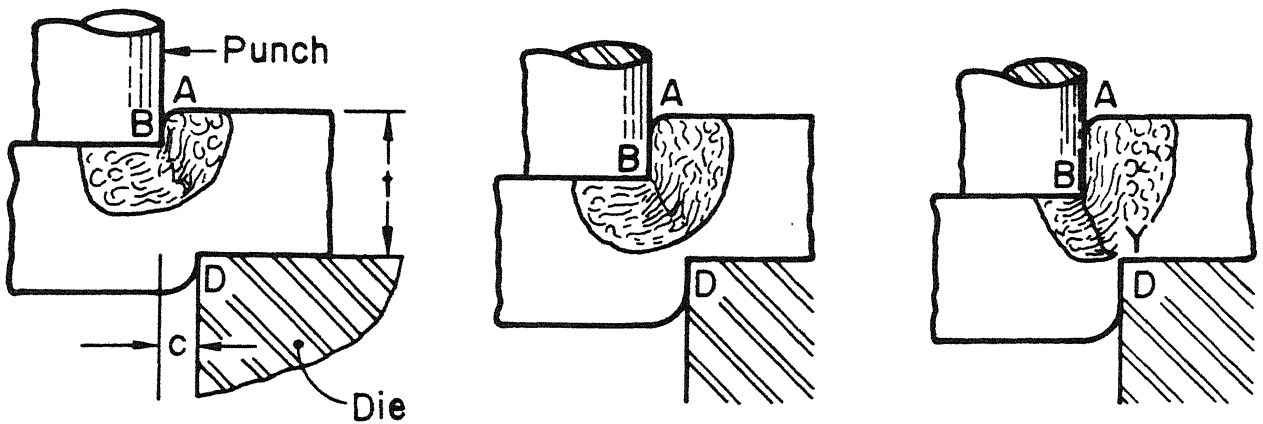
Fig.I.2 Deformation of workpiece with punch travel

(a)   (b)   (c)
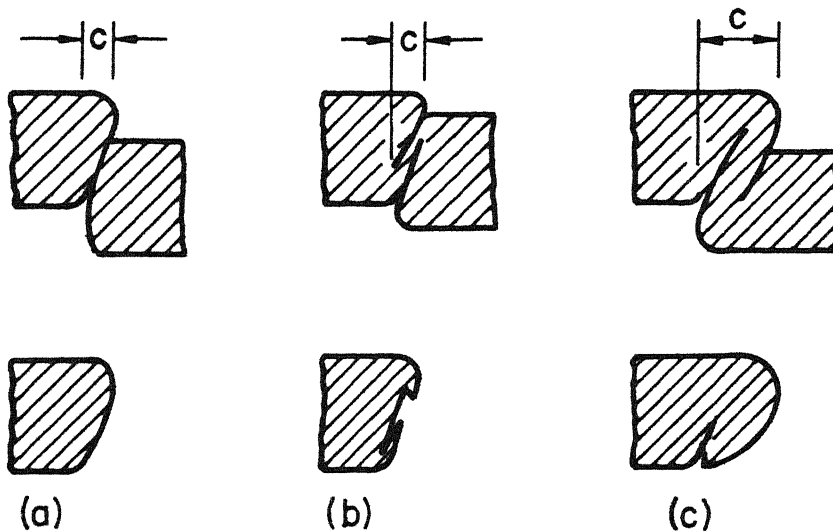
(a) Correct clearance, (b) Too little clearance
(c) Too large clearance

Fig.I.3 Fracture lines with different clearances

The principle of Emery testing machine was used in the design
of the said apparatus. The apparatus was designed to enable
an indicator diagram to be taken under the conditions of actual
shop practice by applying the mechanism to punching machinery
which were used during those days. The indicator being hydrau-
lically operated, there was possibility of reduction of pre-
ssure due to leakage if sufficient care was not taken. It is
also a wellknown fact that the indicators, used under such
conditions, are most likely to leak or stick and either con-
dition would affect the results. Of course, it is mentioned
that preventive action was taken by frequent calibration, which
removed any reduction in pressure due to leakage. It is added
that by the continued tapping of the indicator cylinder, irre-
gularity due to sticking of piston was almost entirely elimi-
nated and resulted in a high degree of precision. Such hydrau-
lic cum lever type indicators are only suitable for slow speed
operation. Chang and Swift [5] have reported a work in which
stresses, metal flow pattern, and crack propagation during the
shearing of metal bars of most industrial metals is studied by
performing experiments. The shearing of half inch thick metal
bars of different ductility were performed. The bars were
sheared by the process of double shear which resembled double
cropping operation. Some of the variables which were varied
during the operation are (i) clearance between the die and the
punch, (ii) the radius of cutting edges ground on the die and

the punch (i.e., dullness of the cutting edges), (iii) the
amount of prior tensile straining given to the bar before
experiment etc. The shearing load and the punch penetration
values, were obtained by means of a pressure gauge and a dial
indicator, respectively. Fig. 1.4 shows the typical load vs.
punch penetration curves obtained for various metals, from the
experiments. It is mentioned further that the development of
strain and progress of fracture were studied by subjecting
several specimens of each metal, to a different punch pene-
tration depths, i.e., one specimen was sheared to the point
of maximum load, while the others were sheared to the stages
intermediate between the point of maximum load and complete
fracture. By careful measurement of the deformed grid pattern
with the help of a travelling microscope, the distribution of
strain was obtained in each case. At the end, following
important conclusions were made. There are two different modes
of severence in a normal shearing operation, (i) ideally
ductile materials suffer bodily sliding action along the
line of shear and final severence occurs at full penetration
and (ii) materials which are not ideally plastic develop cracks
of tensile origin which tend to propagate at a small angle to
the line of shear. After this Chang [6] has done the experi-
ments on the shearing of metal blanks. In this work the
results of investigation on the effects of clearance, tool
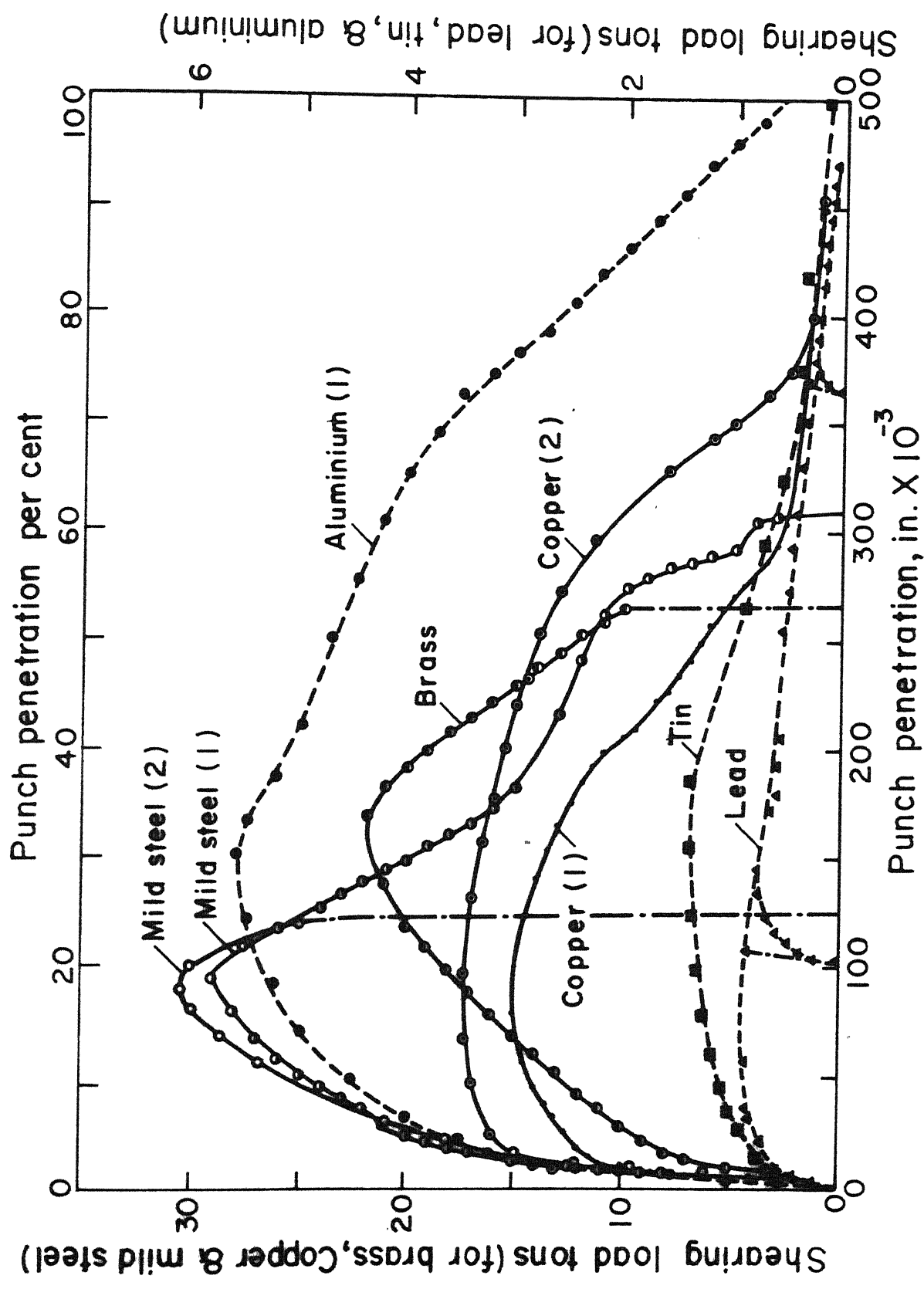
Fig. 1.4 Load penetration curves

shear and tool curvature in the shearing of circular blanks
is presented. The thickness of the various materials tested
were in the range of 0.036 to 0.5 inches. The variations in
the diameter of the tools employed were of the order of one
to six inches and the clearance between the punch and the dies
were varied between 0 to 58 percentage of the material
thickness. The conclusion which was reported is that the
basic modes of fracture in blanking with circular tools are
essentially the same as those found in the bar shearing
experiments. One of the observations made during the experi-
ments was that as the diameter of the tool was increased,
there was a systematic decrease in the nominal ultimate
shearing stress. This indicates that in the range of the
clearances used in industry, the shearing strength of the
material blanked is an inverse function of the tool diameter.
Another observation that was made is the nominal ultimate
shearing strength of all the metals tested except lead de-
creased with the increase of clearance. This effect was most
pronounced with the clearance less than 10%. For lead the
results obtained were rather uncertain. The work done in
blanking of mild steel decreased with the increase of clearance
initially and then remained steady or even increased with fur-
ther increase in clearance. A clearance in the range of 0% to
10% is recommended in order to obtain a clean fracture with
minimum work required to be done, while sheet blanking with
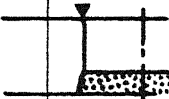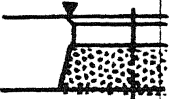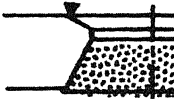
circular tools. It is further stated that the work required for shearing increases with the increase in the curvature of the tool. Also the fall in the maximum blanking load with increase in the angle of shear was found to be almost linear and recorded a reduction of about 75% in maximum load. Although the shear on the punch increases the punch penetration at maximum load and at failure, but it helps in smoothing out the operation by eliminating shocks.Crane [2] has given a detailed discussion on the effects of the various parameters on the shearing process, which are similar to those observed by the previous workers mentioned above. It is mentioned that the shearing process in a punch and a die resembles testing the specimen in tension very closely. But it is stated that any definite relationship between stresses in blanking and tensile test was not found. Biegel [7,8] has studied the effects of variation in the clearance between the punch and the die on the forces and work required during stamping operation. Experiments were performed using a single circular punch (without providing any shear) in combination with seven different dies. By mounting the punch to a strain gauge type dynamometer the force-time trace was obtained on an oscilloscope and the same was recorded by a Polaroid Land Camera. This measuring method is quite superior to that using mechanical cum hydraulic autographic recorders. Finally it was concluded that the maximum shearing force is a function of the area of the material being

sheared, the material strength and is independent of clearance.
But the amount of work required for shearing is a function of
the shear area, material strength and also the clearance. At
the end it is mentioned that to reduce the wear and tear of the
punch and the die, the tool material must have high strength,
good wear resistance and should be completely free of imper-
fections in the region of cutting edges. Hugo [9] describes
the stamping die performance and quality levels of parts pro-
duced. In general there are two methods of measuring stamping
die performance viz., one based on the number of parts produced
per press run and the other based on the number of parts pro-
duced per sharpening grind. Five classes of cut edge characteri-
stics were recommended for measuring the quality levels of the
parts produced (Table 1.1). These five classes viz., A,B,C,D
and E can be distinguished in terms of the type of the burr
produced (i.e., tensile, compressive, extrusion or combined),
and the amount of roll over (i.e., minimum, moderate, large or
very large). It is added as the punch-die clearance is in-
creased the part quality level shifts from type A to type E.
Also by limiting the productivity measurements in terms of
burr height for each class the individual effects of the many
contributing factors in the stamping operation can be properly
evaluated. Although this is a good technique to assess the
quality of stamped metal parts, but it is difficult to measure
burr height of each and every stamping in mass manufacture.

Table 1.1

Five Cutting Edges for Measuring Part Quality Levels
Punch-to-Die Clearances

	A	B	C	D	E
Cutting Edges .002 to .006 Corner Breakdown Burr and Burnished Length Increases as Cutting Edges Break Down Duration of Run Longer Runs as Clearance Increases	Burr: Tensile and Compressive Min. Roll-Over	Burr: Tensile and Compressive Min. Roll-Over	Burr: Tensile Moderate Roll-Over	Burr: Tensile Large Roll-Over	Burr: Tensile and Extrusion Very Large Roll-Over
	Double Shear	Secondary Shear	General Purpose Hole	Ejector Punches Required	
Material	Total Clearance in Percent of Material Thickness				
Aluminum—hard —soft	1– 2 1– 2	10–12 4– 8	18–20 12–16	25–28 16–20	40 pct max. 34 pct max.
Brass—½ hard —annealed	1– 2 1– 3	6–10 4– 6	12–16 12–16	18–22 16–20	48 pct max. 42 pct max.
Bronze, phosphor	3– 5	7–10	20–24	25–27	50 pct max.
Copper—½ hard —annealed	2– 4 1– 2	6–10 4– 8	12–16 10–14	18–22 16–18	50 pct max. 50 pct max.
Lead	3– 5	8–12	13–15	16–20	44 pct max.
Magnesium	1– 2	3– 5	7– 9	10–14	32 pct max.
Stainless steel	2– 4	6–10	18–22	25–27	46 pct max.
Steel, CRS (1020) high carbon	2– 4 5–10	10–14 22–26	16–20 28–32	23–25 34–38	42 pct max. 50 pct max.

Some researchers have applied visioplasticity technique of analysis during blanking operation. This is a good semi-experimental method to visualise the deformation of the metal sheet as the punch penetrates into the sheet metal. The formability of metal can also be judged from such an analysis. Keeler [10,11] has used circular grid system to evaluate sheet metal formability. It is claimed that circular grids permit immediate and simple measurement of the maximum elongation of the sheet at any location. The grids were marked on the sheet by electrochemical etching. As the material was strained, a circle became an ellipse whose major and minor axes were measured. Knowing the diameter of the original circle the strains were calculated. Santos and Organ [12] in the beginning of the analysis have given a brief review of the principles involved in determining strains and stresses during the observation of the deforming grid. The equations for relating incremental deformations of grid, in two dimensions of an originally orthogonal cartesian grid, to the incremental plane strain are stated and explained. Two approaches are described for calculating the strain increments from the measurement of distorted grid as follows :

(i) The incremental displacement U, at a grid point is deduced. This U is resolved into components u and v which are parallel to the x and y axis respectively, from which the curves of variation of u and v w.r.to x and y both are plotted.

Then the resulting slopes $\frac{\partial u}{\partial x}$, $\frac{\partial u}{\partial y}$, $\frac{\partial v}{\partial x}$ and $\frac{\partial v}{\partial y}$ are used to obtain infinitesimal strains in the x and y directions, i.e., $\delta\varepsilon_x$, $\delta\varepsilon_y$ and $\delta\gamma_{xy}$. This method involves graphical or numerical differentiation and therefore demands the application of the tedious process of smoothing .

(ii) In the second method the local strain components are determined directly by noting the relative distortions along convenient axes. Then the direction cosines of these axes with respect to the x and y axes are determined. Finally the strains are transformed w.r. to the x and y.

This second method was used for calculation of strains in the work reported. It is claimed that there was no previous study of the ductile fracture processes using the visioplasticity method, although attempts were made only to give the qualitative idea of the distribution of deformation patterns. Fig. 1.5 and Fig. 1.6 show the proposed slip line fields for initial and lateral stages of the process respectively. It was found that deformation mechanism implied in the resulting slipline field was in accordance with the published observations on the behaviour of the material, subjected to that process. Kasuga and others [13,14] reported application of visioplasticity method combined with strain gauge technique during blanking of circular specimens. The grid was photoetched on one half of the specimen which was in two halves, and the strain
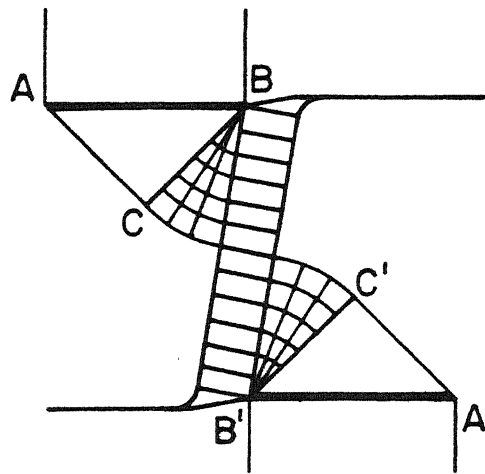
Fig.I.5   Proposed slip-line field for initial stage
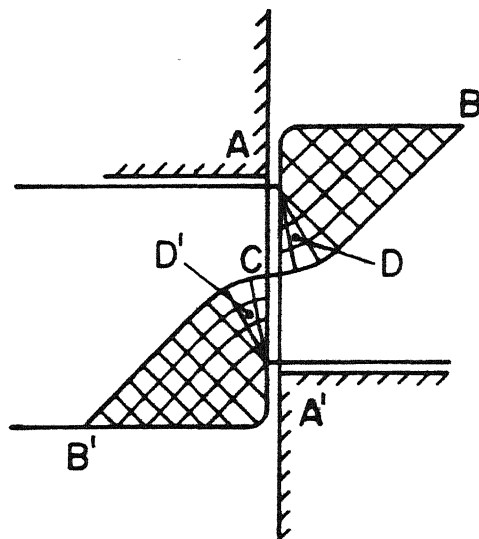
Fig.I.6   Proposed slip-line field for an advanced stage

gauges were applied on the upper and the lower surfaces.
This technique made it possible to get the flow pattern of
the metal through out the whole specimen, and even in the
elastic region. A technique of the virtual displacement of
punch was also applied for the analysis of metal flow. From
the results of this analysis it is reported that as the
clearance becomes larger, the danger of crack initiation at
less penetration increases. A simplified shearing model with
scissor like tools was also proposed. The general drawback of
using the visioplasticity method is that the process is to be
interrupted after small penetration of the punch. Also blanking
being nonsteady state process in which metal is continuously
strained, the visioplasticity technique may not reflect the
correct behaviour of the metal during the process.

The critical review of the progress of research in the area
of slow and fast blanking at ambient and high temperatures is
presented by Johnson and Slater [15]. Only the literature
available in English was reviewed. It is claimed that there
were relatively few papers which add significantly to the under-
standing of the effects of the parameters involved in the blank-
ing process. It is mentioned that modern blanking practice aims
at producing the finished products which do not require any fur-
ther machining or finishing. There is a demand for high rate of
production together with a high degree of accuracy, good edge
finish and consistency in production. Only experiments under

laboratory conditions are performed at extremely slow or quasi-static conditions which give rise to a mean shear strain rate of the order of 10^{-4} to 10^{-3} s^{-1}. Fig. 1.7 shows a schematic representation of punch force-punch displacement diagram. It is said that cracks are developed from the punch and the die corners after the blanking force reaches a maximum value and they propagate towards each other. After performing the dimensional analysis of the parameters involved in circular blanking at constant strain rate the following expression is given :

$$P_{max}/\tau \; dt = \emptyset[(c/t) \cdot (d/t)] \qquad\qquad (1.2)$$

where

        d = diameter of the blank

        t = thickness of sheet metal

        c = punch-die radial clearance

        τ = current shear stress of the material

    P_{max} = maximum blanking force required .

It is further stated that eq. (1.2) may be used to study the dependence of maximum blanking force and energy required on various parameters. Following conclusions were made from a number of experiments performed and review of literature :
(i) Maximum quasi-static blanking force is independent of the radial clearance but there is a rising characteristic as the percentage radial clearance approaches zero, (ii) With the

Punch force

Maximum punch force

B

Initiation of crack propagation

C

Secondary cracks probably formed

A

Elastic phase

Plastic deformation with strain hardening.

Further plastic deformation but shear area decreases

Frictional resistance between
(a) Blank and hole
(b) Punch and hole
(c) Blank and die

D

E

Frictional resistance mainly between blank and hole

Separation of blank from sheet

F

Frictional resistance mainly between punch and hole

O

Stripping of sheet from punch

Punch displacement

G

H

Fig. I.7 Schematic representation of punch force – punch displacement autographic diagram

increase in the ratio of tool diameter to material thickness, the maximum blanking force per unit sheared area decreases. Regarding the effect of speed on the process it is stated that generally greater energy is required for dynamic blanking in comparison to quasi-static process. This can be attributed mainly to the effect of strain-rate on the yield shear stress of the material, if it is assumed that the mode of plastic deformation and the fracture are independent of speed. As regards the phenomenological features of the blanking process it is commented that the blanking of closed contour is a complex non steady-state process involving a triaxial stress system. It is well known that the process of producing blank with a die and a punch involves both plastic deformation and fracture; out of the two the former is reasonably well understood, but not the latter. It was observed that by providing small radius to the tool, the effect on the quasi-static blanking force was almost negligible. Further it is mentioned that the non-dimensional edge taper is approximately directly proportional to the percentage radial clearance. When the blanking of mild steel is carried out at high speed it was observed that there was a considerable reduction in distortion of the blanked piece in terms of 'doming' and 'dishing'. In the later half of the reported work, the results of the axisymmetric blanking at elevated temperatures is described.

Tatsuo and others [16,17] have reported the work of circular punching, two sided cutting and blanking using profiled tools, which was undertaken mainly to investigate the effect of profile on the resistance to shear and the quality of the sheared surface obtained. It is concluded that the material under the punch is deformed by indentation of punch in the early stages of the process, then a sort of forward-backward extrusion and ultimately by the usual process in punching of small holes.

Blanking, bending and deep drawing are some of the most important techniques in press working. Among these techniques the plastic deformation of the sheet material in the process of bending and deep drawing has been studied well. However, for blanking process, where the material in the narrow region between the edges of the die and the punch flow unsteadily, literature on theoretical analysis available is not adequate. The theoretical work done on blanking by Maeda [21] is reported by Jimma [18,19] and Masuda and Jimma [20] together with their own work. Jimma applied theory of limit analysis for the theoretical investigation of the blanking process. The process of circular blanking was considered, and the theory of plane strain deformation was used, assuming the material to be a non-hardening plastic rigid body. It is reported that the process was analysed in two parts. In part I of the analysis following work is described :

(i) The sheet material was separated into several regions of
constant stress by using the straight lines of discontinuity,
and the statically admissible field was analysed. (ii) The
lower limit of blanking force against each punch penetration
was calculated. (iii) An estimate of the development of crack
in blanking process is explained.

In part II of the analysis, the plastic deformation of the
sheet material in the blanking process was divided into four
stages, viz., the first stage (obtuse plane or shear drop),
the second stage   (bright plane), the third stage (depre-
ssed plane) and the fourth stage where the separation due to
slip off occurs in the material, after the complete penetra-
tion of the punch into the sheet. All these four modes of
deformation for ideally ductile metal is shown in Fig. 1.8.
Thereafter the kinematically admissible velocity field in the
material was analysed for each stage and the upper limit of
blanking force against punch penetration was calculated. Follow-
ing hypothetical mechanism is also mentioned regarding the ini-
tiation and growth of the microcrack during the process. Micro-
cracks occur first in the material near the tool edges where the
strain hardenability of the material become too low after severe
distortion. When the microcrack moves from the tool tip to the
side of the tool the normal stress across the plane of the crack
becomes tensile and, thus, microcrack opens up. The conditions
put forward for a microscopic crack to develop are : (i) the

23

(a) The first stage

Obtuse plane (Shear droop)

(b) The second stage

Bright plane

O
O'

(c) The third stage

Depressed plane

(d) The fourth stage
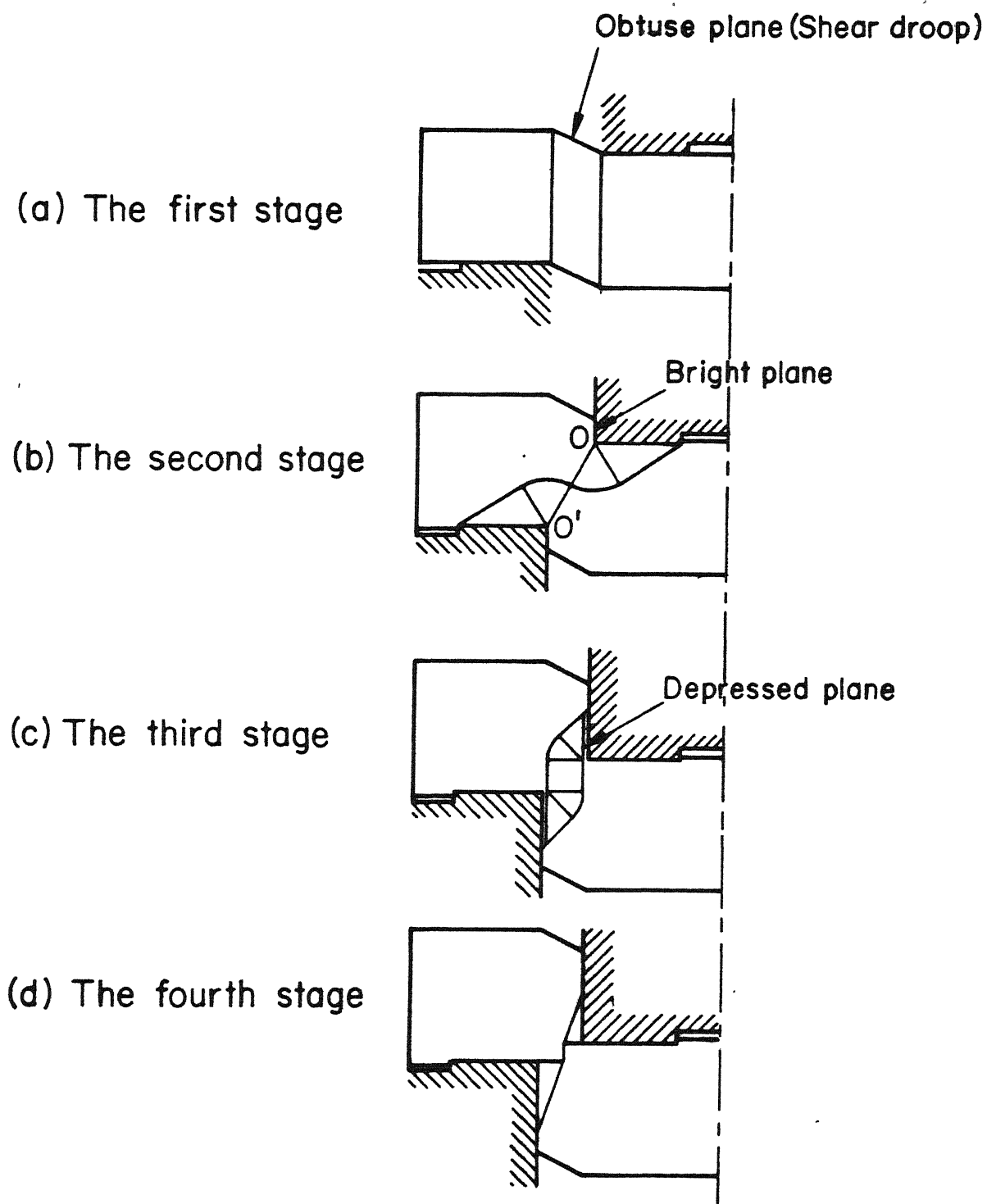
Fig.1.8 Four modes of deformation in the shearing processes of ideally ductile metals

shearing strain along the slip plane near tool edges should reach a limiting value at rupture, and (ii) the normal stress across the plane of microcrack should become zero. Finally a number of experiments were performed to verify the theoretical predictions and results which were obtained are reported to be quite satisfactory.

It is observed from the literature reviewed so far that no one has put forward any explicit mathematical relation connecting the material properties, sheet thickness, and clearance, with the maximum blanking force, etc. Ghosh and others [22,23] have put forward a simple model for the deformation of the metal in the clearance gap during the blanking operation, from which a mathematical expression connecting the variables of the process has been tried. It is mentioned that the metal fibres rupture when the local strain in the material reaches a critical value, and using this concept it is claimed that a theoretical relationship between the optimum clearance and the other parameters has been developed.

Some parts of the said analysis is presented here. The relation between the active strain, ε_1' and the locally observed strains ε_1 and ε_2 was assumed to be related through the following expression [24],

$$\varepsilon_1' = 4/3\left(\varepsilon_1 - \frac{1}{2} \mid \varepsilon_2 \mid \right) \tag{1.3}$$

This was simplified for the case of blanking, and the criteria for fracture was taken as

$$\varepsilon_1 = \varepsilon_f \qquad (1.3a)$$

or

$$e_1 = e_f \qquad (1.3b)$$

where e_f is the engineering fracture strain of the material blanked. Fig. 1.9 shows the details of the assumed deformation pattern for optimum clearance, when fracture has just started at point B. From the said figure and assuming linear variation of strains along the fibres it was shown that

$$e_B = \pi - 2 + \frac{2\Delta}{c_o} \qquad (1.4)$$

where e_B is the observed engineering strain at B and c_o is the optimum clearance.

Similarly the expression for strain at S was obtained as

$$e_S = \frac{\pi - 2 + (2\Delta / c_o)}{1 + (2\Delta / \pi c_o)} \qquad (1.5)$$

The relation between the work thickness and the optimum clearance was shown to be given by

$$\frac{t}{c_o} = (\frac{1 + 1.5 e_f}{0.63 + 1.32 e_f})(1 + e_f) + 0.5 e_f + 0.43 \qquad (1.6)$$
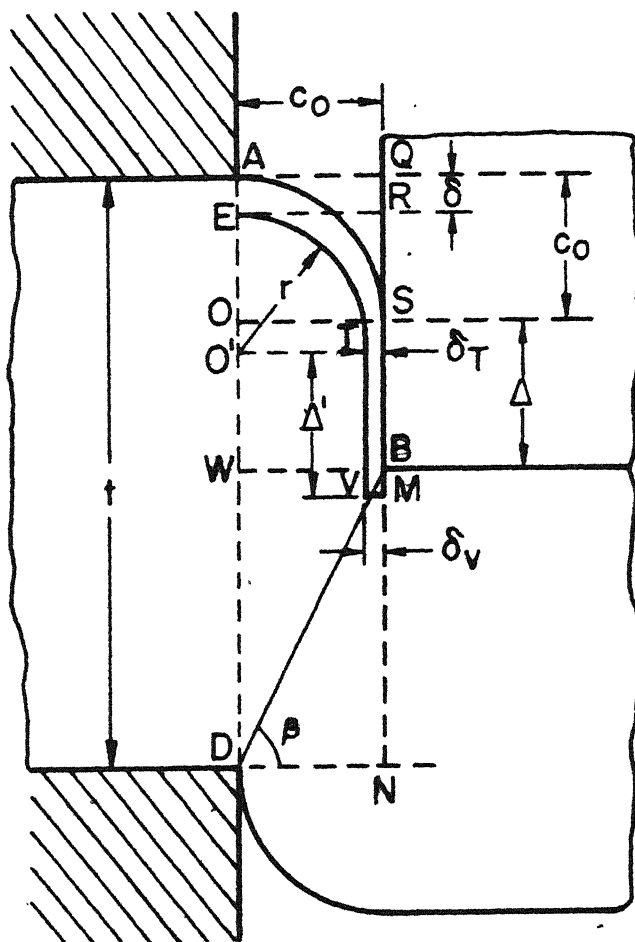
Fig.I.9 Geometry of deformation of two
fibres at a distance δ apart

The penetration of the punch $(\Delta + c_o)/t$ was expressed as

$$\frac{\Delta + c_o}{t} = \frac{0.43 + 0.5\ e_f}{\dfrac{(1+1.5\ e_f)(1+e_f)}{0.63+1.32\ e_f} + 0.5\ e_f + 0.43} \qquad (1.7)$$

The value of natural fracture strain $\varepsilon_f = \ln(e_f+1)$ was substituted and the final expressions were given as

$$\frac{t}{c_o} = 1.36\ \exp(\varepsilon_f)\ \left[\frac{2.3\ \exp(\varepsilon_f-1)}{2\ \exp(\varepsilon_f)-1}\right] \qquad (1.8)$$

and

$$\frac{\Delta + c_o}{t} = \frac{1}{2.45}\ \left[\frac{1.9\ \exp(\varepsilon_f)-1}{2.56\ \exp(\varepsilon_f)-1}\right] \qquad (1.9)$$

The assumed pattern of the variation of punching force with punch travel is shown in Fig. 1.10. It is mentioned that the maximum punching force is attained just when the fracture starts and drops very rapidly with the progress of the punch. The maximum force (Fig.1.11) was given by the following equation :

$$P_{max} = \sigma_{av}\ c_o\ L \qquad (1.10)$$

where L = punch width

σ_{av} = average stress

From the same figure the work required, W, for the punching operation was expressed as
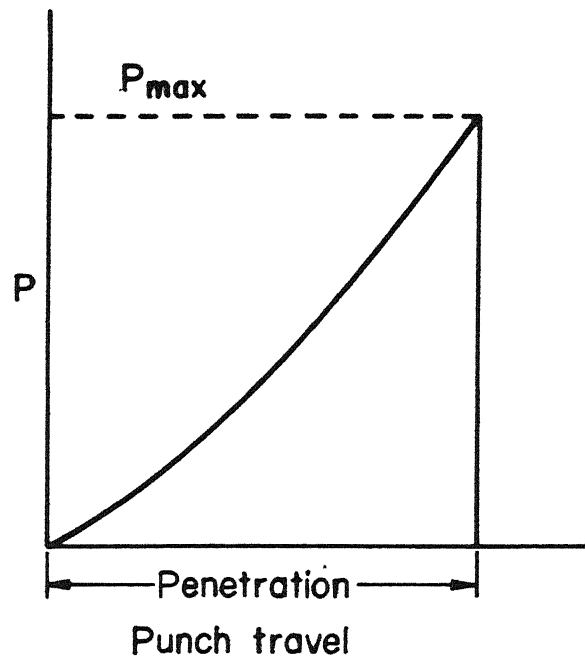
Fig.1.10 Variation of the load with punch travel
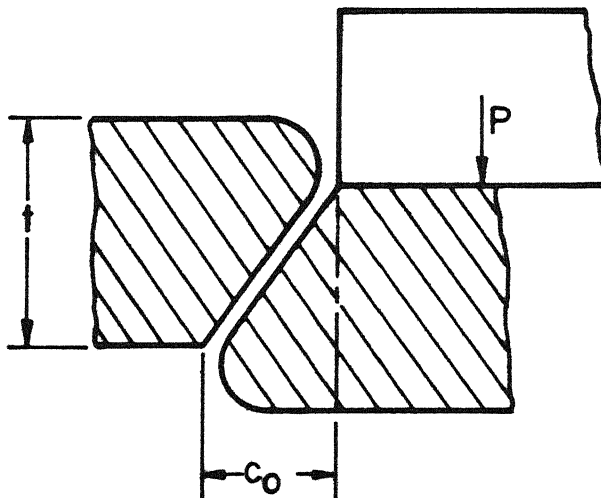
Fig.1.11 Separation of the blank from the workpiece

$$W = \frac{1}{2} P_{max} \, tp \qquad\qquad (1.11)$$

where

$$p = \text{the penetration} = \frac{(\Delta + c_o)}{t}$$

Then the values of the optimum clearance c_o and penetration depth $(\Delta + c_o)$ in terms of the sheet thickness, for different values of ductility (ε_f) of the material were calculated using the above equations. Some of the calculated values are given below :

ε_f	1	1.5	2.0	2.5
c_o/t	0.215	0.133	0.082	0.05
$\dfrac{(\Delta + c_o)}{t}$	0.278	0.289	0.296	0.30

It was concluded from the results that depending on the ductility of the material the clearance varies from about 5 to 20% of the sheet thickness. It is suggested that for the blanking of more ductile material optimum clearance required is less, which was also observed by other workers in this field. Regarding the percentage penetration at fracture it was about 30% of sheet thickness and increased very slowly with the ductility of the metal. For the verification of the proposed model, Popat [25] performed a large number of experiments using a simple solid punch and variable clearance die set up. Two die halves

were mounted on two adjustable members running in a dovetail slide, the required clearance was set using the screw and nut assembly and feeler gauges. The punch force-punch travel pattern was obtained on the storage oscilloscope screen using a load cell below the die and a LVDT fixed onto the press ram. Further it is mentioned that to decide the value of optimum clearance, all the fractured pieces obtained at various clearances were examined simultaneously, the optimum clearance being indicated by the cleanness of the edge produced. A two-sided cutting was performed on sheet materials with different ductilities and thicknesses, at various clearances. It is mentioned that the following observations were made from the results of the experiments.

(i) The optimum percentage clearance remains almost constant for any one material, since the fracture strain is independent of the thickness, and it changes only with the ductility of the material. The Fig. 1.12 shows the variation of optimum clearance with fracture strain, for the values obtained from experimental results and those obtained using equation (1.8). The nature of the variation for the experimental and theoretical curves seems to match well. In the similar way the values of the percentage penetration obtained from equation (1.9) and those from the experimental results are plotted on the same graph, they are also found to be in good agreement. But while comparing the values of the maximum punch force measured
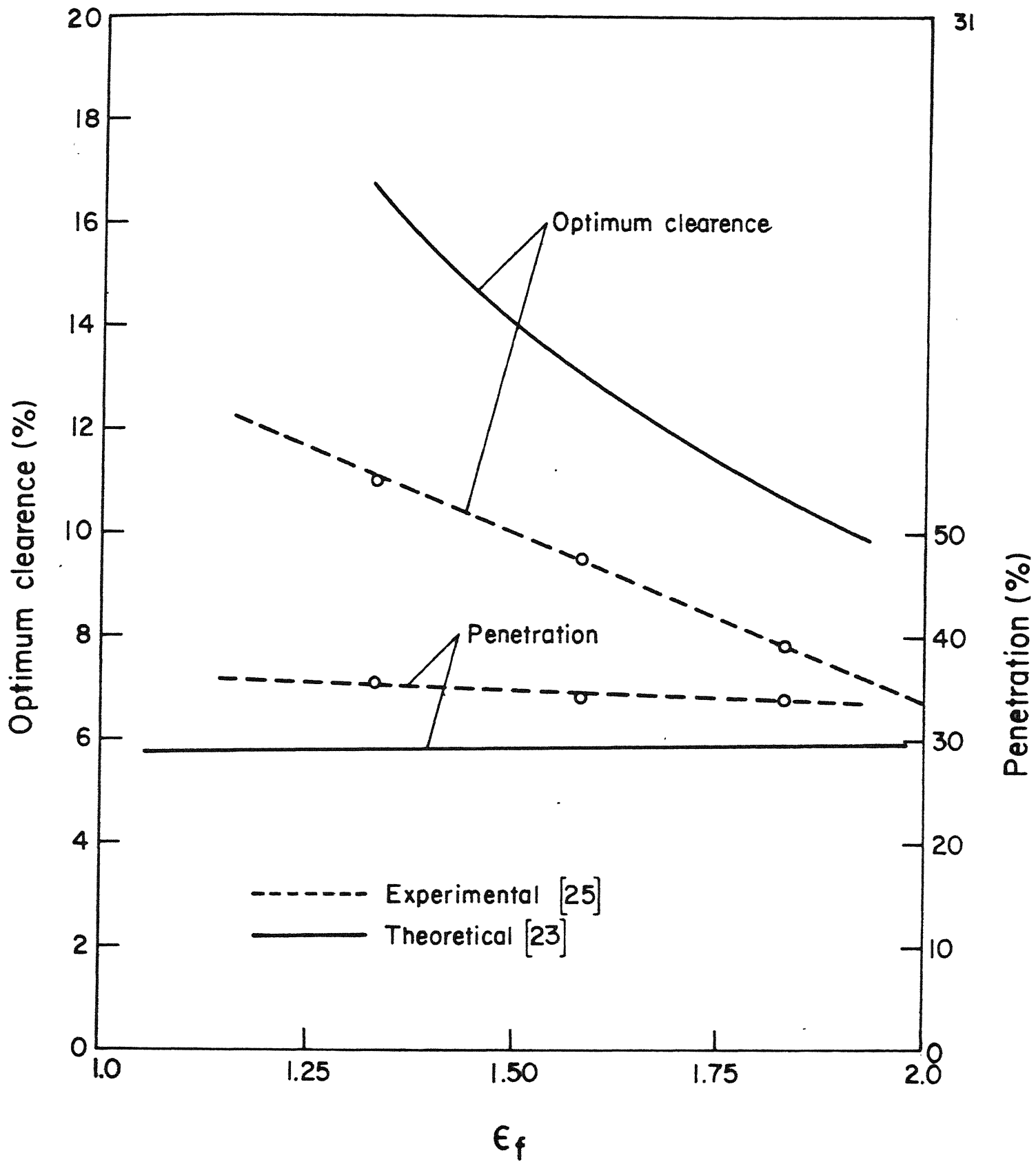
Fig. I.I2 Variation of the optimum clearence and penetration with fracture strain.

experimentally and calculated using equation (1.10), it was found that theoretical predicted values were higher than the experimentally found values. This was attributed to the fact that rupture of fibres is not simultaneous, which was an assumption while deriving the theory, but the rupture is continued during the finite interval of time. Close agreement between the theoretically predicted and experimental values was shown, after inserting some corrections using energy criterion.

It has been noticed that from sixties onwards with the advent of High Energy Rate Forming (H.E.R.F.) methods, which are suitable for ambient and high temperatures, most of the research on blanking is diverted to fast blanking. The H.E.R.F. methods have offered the possibility of fast blanking with reduction of unit production times, improvements in the sheared edge of the blank produced and reduction in the amount of energy required to effect the plastic deformation during the process. References 26 to 31 are devoted to the investigations on H.E.R.F. methods applied to blanking operation.

Other works [32,33] have been devoted to manufacturing and other aspects.

1.4 OBJECTIVE AND SCOPE OF THE PRESENT WORK

The main objective of this work is to develop a finite element model for analysing the elastic-plastic deformation during blanking operation. The finite element method is selected

for the analysis because it is a versatile method and it is possible to predict with sufficient accuracy the distribution of stress, strain, strain-rate, etc. for a complicated problem. It is intended to prepare a displacement based finite element programme employing 'initial stress method' for this nonlinear problem.

The punch-die clearance is the most important parameter of blanking process. When the clearance is adequate (optimum), the cracks initiating from the punch and the die corners will meet resulting in clean edges. The amount of the work required to be done for complete separation of the blank will also be minimum. In such processes there is severe plastic deformation before fracture. Thus a suitable crack initiation criterion based on the value of a combination of the strains is to be identified. Then a criterion for determining crack propagation direction will also be postulated which will be necessary for estimating the optimum punch-die clearance.

In addition to the fractional punch-die clearance, the material properties and the sheet-thickness are also considered to be important process parameters. During the analysis a parametric study is being undertaken to determine the effects of each one of the above on the maximum punch force required, punch penetration at crack initiation, optimum clearance etc.

To provide an overall idea about the deformation process the distributions of principal and effective strains in the clearance zone will be shown, with the progress of the punch. The deformation pattern and its variation with punch penetration will also be presented.

In order to verify the correctness and accuracy of the results obtained from the analysis, these are to be compared with the results of the previous experimental and theoretical works. A more extensive study is required to actually determine the complete crack path with the progress of the punch and is not included in the present work. It will be shown that an attempt is being made for getting the crack path. But it is felt that to obtain the correct crack path it requires different type of the element and a very fine mesh to discretize the continuum. This will result in a very big size of the stiffness matrix and a large number of equations to be solved at each iteration.

Although stresses, strains etc. are calculated assuming small deformation theory to be applicable, it is possible to take the large deformations into account by modifying the nodal coordinates, calculation of new stiffness matrix etc. after each displacement increment. Similarly with the necessary alterations in the finite element model, the effects of the punch shear, frictional conditions at the tool-work interface,

clamping forces,strain rate etc. could be implemented into the analysis.

The present work is restricted to the two dimensional analysis of blanking operation. But in order to take into account the process of close contour blanking, a more rigorous three dimensional analysis should be performed using this technique.

CHAPTER 2

GENERAL THEORY OF FINITE ELEMENT METHOD

2.1 INTRODUCTION

The finite element method is much more versatile compared
to other solution methods described earlier, and it is possible
to analyse a complicated problem using this technique. There-
fore, in recent years it has been also applied in the field of
metal forming and sheet metal cutting [34 to 45]. With its use
stress, strain, strain-rate and temperature distribution can be
predicted more accurately, and hardness, ductility and grain
homogenity can be deduced.

This chapter briefly outlines the theory of finite element
displacement formulation, as applied to the solution of problem
of statics. Displacement formulation of elements used in the
analysis of plane strain situation is described, using eight
noded isoparametric elements. The two dimensional finite ele-
ment displacement formulation of an elastic continuum is ex-
plained. Methods of solution of plasticity problems using
elasto-plastic analysis is stated in short. The two most
commonly used yield criteria are described. The expressions for
the elasto-plastic stress-strain matrix using von-Mises yield
criterion are stated for the 3-dimensional as well as for plane
strain situations. At the end, the steps during a typical

load/displacement increment is   summarised for the elasto-
plastic analysis using 'initial stress method'.

2.2   FINITE ELEMENT METHOD

In many situations an adequate engineering model of the
system is obtained by replacing the system by a finite number
of well defined components.   Such problems are called dis-
crete problems.   In contrast to this are the continuous sys-
tems in which the formulation leads to differential equations
or equivalent statements, which imply an infinite number of
elements [46].   Even if the number of elements is very large,
the discrete problems can be solved readily now with the
advent of digital computers.   The various discretisation
methods suggested from time to time to solve the realistic
continuum problem both by engineers and mathematicians, all
involve approximations which approach the true continuum solu-
tion as the number of discrete variables increase.

The discretization of continuum problems has been
approached differently by mathematician and engineers.   The
first have developed general techniques applicable directly
to differential equations governing the problem, such as a
fiting difference technique.   On the other hand, engineers
often approach the problem more intuitively by creating an
analogy between real discrete elements and finite portion of a
continuum domain.

finite

It is for the engineering 'direct analogy' view that the term 'finite element' has been born. Clough appears to be first to use this term, which implies in it a direct use of standard methodology applicable to discrete systems.

Finite element method (FEM) is now very well described in a number of books [46 to 50]. However, it is briefly outlined here to keep continuity of the discussion. FEM is a numerical discretisation procedure by the use of which a wide range of complex boundary value problems can be analysed. Elastic, non-linear elastic and elasto-plastic constitutive relations can be implemented within finite element framework in a straight forward manner.

In FEM, the region of interest is divided into a finite number of simply connected sub-domains or elements. An approximate functional value of the solution is assumed over the sub-domain so that the parameters, say u_i (i = 1, ..., n) of the function becomes the unknown of the problem.

2.2.1 Physical Interpretation of FEM

The basic concept is derived from structural analysis. Here every structure is approximated as a physical assemblage of individual structural components or finite elements. The elements are interconnected at a finite number of nodes and sometimes along the boundaries of the element. Assuming the approximate behaviour of individual elements, the behaviour of

the entire system can be analysed. After assembling the individual elements, the necessary boundary conditions are imposed, with primary nodal values as unknowns. Solution of the resulting set of equations yield the system response.

Considering the nature of each individual component in an element, the relationship between the primary variable u^e and the forcing function Q^e, for a linear system can be written as [46]

$$Q_i^e = K_{ij}^e \, u_j^e + Q_{oi}^e \qquad (2.1)$$

repetitive indices indicating summation.

Connection among elements can be established using,

(a) one set of variables, u_j, for the assembled system, i.e., the condition of continuity

$$u_j = u_j^e \qquad (2.2)$$

(b) the equilibrium of the second set of variable Q_i^e, at each node and equating it to zero,

$$\sum_{e=1}^{NEL} Q_i^e = 0 \qquad (2.3)$$

in which, NEL, is the number of elements considered. Using equations (2.1) to (2.3), the resulting equations can be written as

$$[K] \ \{u\} + \{Q\} = 0 \tag{2.4}$$

in which

$$[K] = K_{ij} = \sum_{e=1}^{NEL} K_{ij}^{e} \tag{2.5}$$

and

$$\{Q\} = Q_{oi} = \sum_{e=1}^{NEL} Q_{oi}^{e} \tag{2.6}$$

2.2.2 Finite Element Displacement Formulation of an Elastic Continuum

The special features of the problem are given below [51] :

(a) The continuum is separated by imaginary lines or surfaces in a number of 'finite elements'.

(b) The elements are assumed to be interconnected at a discrete number of nodal points situated on their boundaries. The nodal displacements will be the basic unknowns.

(c) A set of functions is chosen to define uniquely the state of displacement within each finite element in terms of nodal displacements.

(d) The displacement functions now define uniquely the state of strain within each element in terms of nodal displacements. These strains, together with any initial strains and constitutive properties of the material will define the state of stress throughout the element and hence along the boundaries.

(e) A system of forces concentrated at the nodes and equilibrating the boundary stresses and any distributed load, is determined.

Once this stage is reached, the solution procedure follows the standard discrete system pattern. The above procedure involves a series of approximations. Ensuring displacement compatibility between adjacent elements may not be possible always, though within each element it is obviously satisfied. Concentrating the equivalent forces at nodes, equilibrium conditions are satisfied in the overall sense only.

The displacements can be expressed as

$$u = \Sigma N_i a_i^e = [N_i, N_j, \ldots,] \begin{Bmatrix} a_i \\ a_j \\ \vdots \end{Bmatrix}^e = N a^e \qquad (2.7)$$

where u = displacement at any point within the element

N = prescribed function of position called shape function

a^e = nodal displacement vector for a particular element.

The strain vector, ε , can be obtained with displacements known at all points within the element. Dropping subscript for element,

$$\varepsilon = B a \qquad (2.8)$$

For a linearly elastic constitutive law,

$$\sigma = D (\varepsilon - \varepsilon_o) + \sigma_o \qquad (2.9)$$

where

ε_0 = initial strain matrix

D = symmetric matrix

σ_0 = initial residual stresses.

$$q^e = \begin{Bmatrix} q_i^e \\ q_j^e \\ \vdots \end{Bmatrix}$$ = nodal force vector which are statically equivalent to the boundary stresses and distributed loads on the elements .

To make the nodal forces statically equivalent to the actual boundary stresses, and distributed loads, the simplest procedure is to impose an arbitrary virtual displacement and to equate the external and internal work done by the various forces and stresses during that displacement (i.e.)

$$\delta a^{e^T} q^e = \delta a^{e^T} [\int_{V^e} B^T \sigma d(vol) - \int_{V^e} N^T b d(vol)$$

$$- \int_{A^e} N^T \bar{t} \, d(Area)] \qquad (2.10)$$

where

b = vector of body force components

$\bar{t}$ = vector of traction components.

As this relation is valid for any value of virtual displacement,

$$q^e = \int_{V^e} B^T \sigma d(vol) - \int_{V^e} N^T bd(vol) - \int_{A^e} N^T \bar{t} \, d(Area) \qquad (2.11)$$

$$q^e = K^e a^e + f^e \qquad (2.12)$$

$$K^e = \int_{V^e} B^T DBd(vol) \qquad (2.13)$$

$$f^e = -\int_{V^e} N^T bd(vol) - \int_{A^e} N^T \bar{t} \, d(Area) - \int_{V^e} B^T D \varepsilon_0 \, d(vol) +$$

$$\int_{V^e} B^T \sigma_0 \, d(vol) \qquad (2.14)$$

External concentrated forces may exist at the nodes denoted by vector

$$r = \begin{Bmatrix} r_1 \\ r_2 \\ \vdots \\ r_n \end{Bmatrix} \qquad (2.15)$$

Equation (2.7) when applied to the whole structure will give,

$$u = \bar{N} a \qquad (2.16)$$

in which a is nodal displacement vector for all the nodal points.

Similarly,

$$\varepsilon = \overline{B}\, a \tag{2.17}$$

Dropping the bar superscript

$$\delta a^T r = \int_V \delta\, u^T b\ dV + \int_A \delta\, u^T\, \overline{t}\ dA - \int_V \delta\, \varepsilon^T\, \sigma\ dV \tag{2.18}$$

Substituting, equations (2.16), (2.8) and (2.9), once again a system of linear equations are obtained.

$$Ka + f = r \tag{2.19}$$

$$K = \int_V B^T DB\ dV \tag{2.20}$$

$$f = -\int_V N^T b\ dV - \int_A N^T\, \overline{t}\ dA - \int_V B^T D\, \varepsilon_o\ dV + \int_V B^T\, \sigma_o\ dV \tag{2.21}$$

The integrals are taken over the whole volume V and over the whole area A on which the tractions are given,

$$K_{ij} = \Sigma\, K_{ij}^e \quad , \qquad f_i = \Sigma\, f_i^e \tag{2.22}$$

$$\int_V N^T b\ dV = \Sigma \int_{V^e} N^T b\ dV \tag{2.23}$$

$$\int_V N^T\, \overline{t}\ dA = \Sigma \int_{A^e} N^T\, \overline{t}\ dA \tag{2.24}$$

The same is true for other elements in the equation (2.20) and (2.21).

2.3 DISPLACEMENT FORMULATION OF THE ELEMENT USED

The unique description of the displacement within each element in terms of nodal values at boundary points or internal points of the element is the basic step in any displacement finite element formulation and can be expressed as

$$u = N a^e$$

where N is the matrix of shape functions.

If the shape function chosen to describe the element geometry are identical to those used to prescribe function (displacement) variation, then the element is termed iso-parametric. The basic procedure in the isoparametric finite element formulation is to express the element coordinates and element displacements in the form of interpolation functions using natural coordinates system of the element. The functional property of the interpolation function N_i is that its value in the natural coordinate system is unity at node i and zero at all other nodes. The formulation given below follows general pattern of derivation suggested by Bathe and Wilson [47] and Zienkiewicz [46]. For a two dimensional element interpolation functions for eight noded case is given below.

$$N_1 = \frac{1}{4}(1-s)(1-t_1) - (\frac{1}{2}) N_5 - (\frac{1}{2}) N_8$$

$$N_2 = \frac{1}{4}(1+s)(1-t_1) - (\frac{1}{2}) N_5 - (\frac{1}{2}) N_6$$

$$N_3 = \frac{1}{4}(1+s)(1+t_1) - (\frac{1}{2}) N_6 - (\frac{1}{2}) N_7$$

$$N_4 = \frac{1}{4}(1-s)(1+t_1) - (\frac{1}{2}) N_7 - (\frac{1}{2}) N_8 \qquad (2.25)$$

$$N_5 = \frac{1}{2}(1-s^2)(1-t_1)$$

$$N_6 = \frac{1}{2}(1-t_1^2)(1+s)$$

$$N_7 = \frac{1}{2}(1-s^2)(1+t_1)$$

$$N_8 = \frac{1}{2}(1-t_1^2)(1-s)$$

A quadratic variation of displacement and geometry are assumed for this element and it has 16 displacement degrees of freedom (Fig. 2.1).

Cartesian coordinates x,y and natural coordinates s, t_1 are related as follows :

$$x = N_1 x_1 + N_2 x_2 + N_3 x_3 + N_4 x_4 + N_5 x_5 + N_6 x_6 + N_7 x_7 + N_8 x_8 \qquad (2.26a)$$

$$y = N_1 y_1 + N_2 y_2 + N_3 y_3 + N_4 y_4 + N_5 y_5 + N_6 y_6 + N_7 y_7 + N_8 y_8 \qquad (2.26b)$$

where N_1 to N_8 are given in equation (2.25).
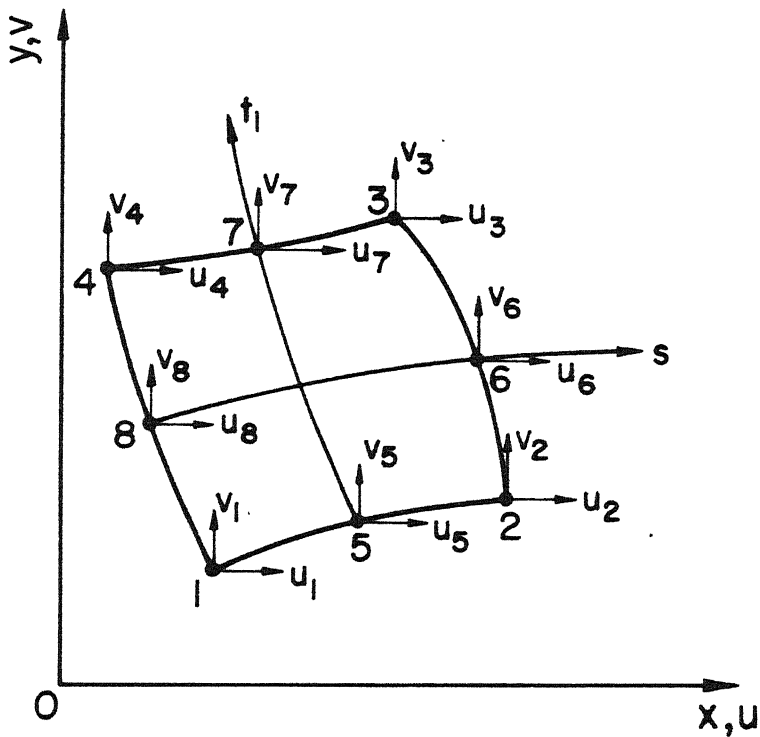
(a) Local co-ordinate system
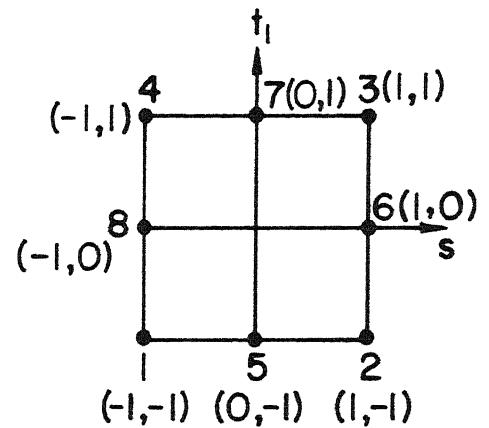
(b) Natural co-ordinate system
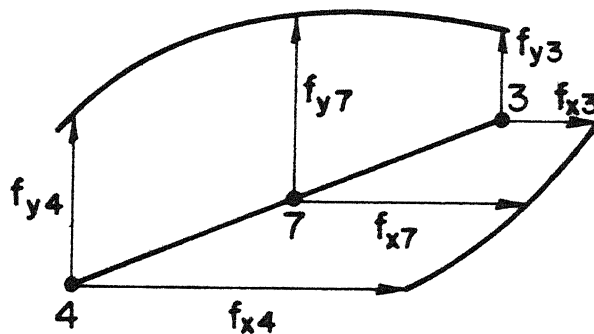
(c) Parabolic variation of surface traction on straight edge 43

Fig.2.1 Eight noded parabolic isoparametric element for two dimensional analysis

Similarly, the displacements expressed in terms of nodal values are :

$$u = N_1 u_1 + N_2 u_2 + N_3 u_3 + N_4 u_4 + N_5 u_5 + N_6 u_6 + N_7 u_7 + N_8 u_8$$
$$(2.27a)$$

$$v = N_1 v_1 + N_2 v_2 + N_3 v_3 + N_4 v_4 + N_5 v_5 + N_6 v_6 + N_7 v_7 + N_8 v_8$$
$$(2.27b)$$

Along the edge of the element the variation of displacement is quadratic.

Writing equation (2.27) in matrix notation

$$\{u\} = [N] \{a\}$$

$$\{a\}^T = [u_1 v_1 \quad u_2 v_2 \quad u_3 v_3 \quad u_4 v_4 \quad u_5 v_5 \quad u_6 v_6 \quad u_7 v_7 \quad u_8 v_8] \qquad (2.28)$$

Element strain vector for plane strain case is

$$\{\varepsilon\}^T = [\varepsilon_{xx} \quad \varepsilon_{yy} \quad \gamma_{xy}] \qquad (2.29a)$$

$$\text{where} \quad \varepsilon_{xx} = \frac{\partial u}{\partial x}, \quad \varepsilon_{yy} = \frac{\partial v}{\partial y}, \quad \gamma_{xy} = \frac{\partial v}{\partial x} + \frac{\partial u}{\partial y} \qquad (2.29b)$$

The strains at any point within the element is obtained knowing the nodal displacement, by

$$\{\varepsilon\} = [B] \{a\} \qquad (2.30)$$

where B is the strain displacement matrix given by

$$[B] =$$

$$
\begin{bmatrix}
\dfrac{\partial N_1}{\partial x} & 0 & \dfrac{\partial N_2}{\partial x} & 0 & \dfrac{\partial N_3}{\partial x} & 0 & \dfrac{\partial N_4}{\partial x} & 0 & \dfrac{\partial N_5}{\partial x} & 0 & \dfrac{\partial N_6}{\partial x} & 0 & \dfrac{\partial N_7}{\partial x} & 0 & \dfrac{\partial N_8}{\partial x} & 0 \\[2mm]
0 & \dfrac{\partial N_1}{\partial y} & 0 & \dfrac{\partial N_2}{\partial y} & 0 & \dfrac{\partial N_3}{\partial y} & 0 & \dfrac{\partial N_4}{\partial y} & 0 & \dfrac{\partial N_5}{\partial y} & 0 & \dfrac{\partial N_6}{\partial y} & 0 & \dfrac{\partial N_7}{\partial y} & 0 & \dfrac{\partial N_8}{\partial y} \\[2mm]
\dfrac{\partial N_1}{\partial y} & \dfrac{\partial N_1}{\partial x} & \dfrac{\partial N_2}{\partial y} & \dfrac{\partial N_2}{\partial x} & \dfrac{\partial N_3}{\partial y} & \dfrac{\partial N_3}{\partial x} & \dfrac{\partial N_4}{\partial y} & \dfrac{\partial N_4}{\partial x} & \dfrac{\partial N_5}{\partial y} & \dfrac{\partial N_5}{\partial x} & \dfrac{\partial N_6}{\partial y} & \dfrac{\partial N_6}{\partial x} & \dfrac{\partial N_7}{\partial y} & \dfrac{\partial N_7}{\partial x} & \dfrac{\partial N_8}{\partial y} & \dfrac{\partial N_8}{\partial x}
\end{bmatrix}
$$

$$(2.31)$$

For plane strain the elasticity (stress-strain) matrix can be written as

$$
[D] = \frac{E}{(1+\gamma)(1-2\gamma)}
\begin{bmatrix}
1-\gamma & \gamma & 0 \\[2mm]
\gamma & 1-\gamma & 0 \\[2mm]
0 & 0 & \dfrac{1-2\gamma}{2}
\end{bmatrix}
\qquad (2.32)
$$

The matrices to be evaluated are the stiffness matrix K, the body force vector, and the surface load vector for distributed loads at the boundary. The matrices in general are evaluated by numerical integration, using Gaussian quadrature formula. For the plane strain condition thickness being unity, the matrix K can be obtained as

$$
[K] = t \sum_{i=1}^{n} \sum_{j=1}^{n} \alpha_i \alpha_j F_{ij} \qquad (2.33a)
$$

$$
F_{ij} = B_{ij}^{T} \, D \, B_{ij} \, \det J_{ij} \qquad (2.33b)
$$

in which n is the number of integration points in each
direction, det J_{ij} is the determinant of the Jacobian matrix
of transformation

α_i , α_j are Gaussian quadrature weights

F_{ij} are the function values to be evaluated at sampling
     points s_i, t_{1j} .

For the evaluation of stiffness matrix of the element, a
2 x 2 numerical integration is used. The function values are
evaluated at 4 sampling points and summed upto get the stiffness
matrix of the eight nodes element.

2.4 ELASTO-PLASTIC ANALYSIS

The difference in elastic and plastic behaviour under
uniaxial stress is clearly brought out in Fig. 2.2. In non-
linear elastic behaviour, the stress can be expressed as a
function of strain as $\sigma = \sigma(\varepsilon)$. The main difference of
plasticity formulation from nonlinear elastic formulation is,
such an explicit relationship is not evailable. Although the
stresses at any level of strain have to lie on or within the
current yield surface, the exact value of each component
cannot be determined.

2.4.1 Development of Numerical Techniques for Plasticity
        Analysis

Theoretical as well as practical interest in plasticity
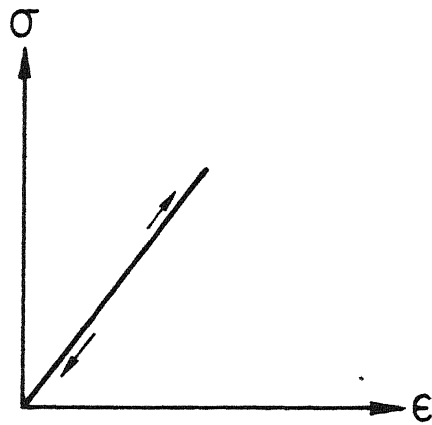
a. Linear elastic
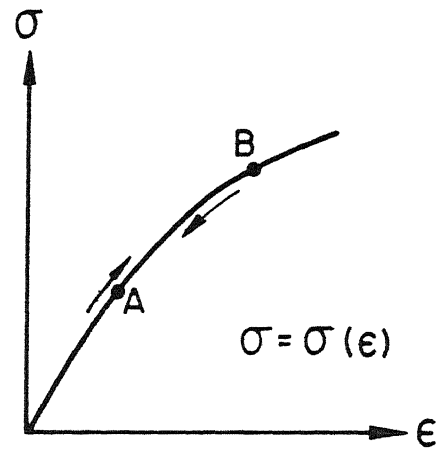
b. Non-linear elastic

$\sigma = \sigma (\epsilon)$
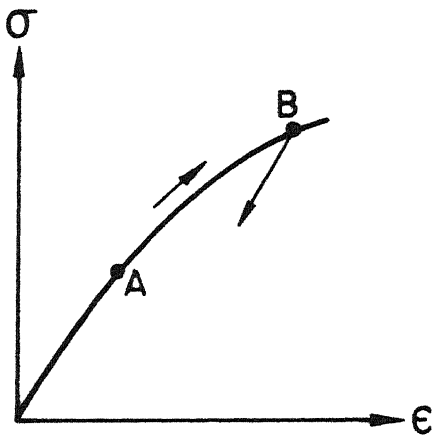
c. Strain hardening
plasticity
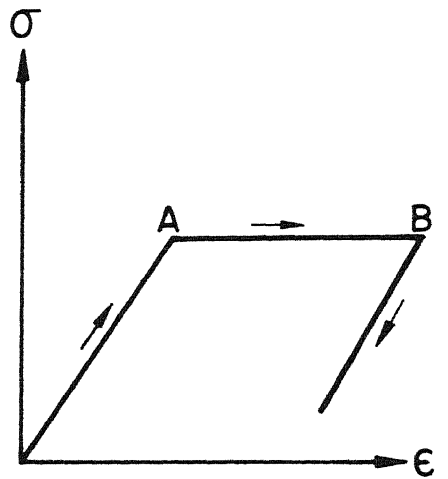
d. Ideal plasticity

Fig. 2.2 Elastic and plastic behaviour under
uniaxial stress

has stimulated much work in the numerical solution of elasto-plastic problems by the FEM and other procedures [52]. The literature on small strain displacement elastic-plastic solution using FEM is now large [53 to 63]. Only the difference lie between the apparent forms of the nonlinear solution algorithms used, and the form of constitutive relations postulated.

The common computational approach used with incremental theory of plasticity in finite element method are :

(i)   incremental tangent stiffness approach,

(ii) 'initial strain' method, and

(iii) 'initial stress' method [48,62].

In the first method the change of material constitutive matrix forming element stiffness, assembling and inverting an overall stiffness matrix for each step of analysis is to be carried out. In 'initial strain' and the 'initial stress' approaches, in all iterations a simple resolution of constant linear elastic problem is carried out. The 'initial stress' method is suitable for solution of ideal plasticity or for strain hardening formulations.

2.4.2 Yield Criteria

A yield criteria is a hypothesis concerning the limit of elasticity under any possible combination of stresses. The suitability of any proposed yield criteria must be checked by

conducting experiments.

If a point in a ductile material is subjected to the principal stresses σ_1, σ_2, σ_3 and is represented by a Mohr Circle, and if the principal stresses are changed to $(\sigma_1+\sigma_m)$, $(\sigma_2+\sigma_m)$ and $(\sigma_3+\sigma_m)$, then the size of Mohr circle, for this new state of stress, remains same but is shifted by a distance σ_m along the σ-axis. The additional stresses σ_m make up a hydrostatic (tensile or compressive) stress system. It is found that the absolute size of the Mohr circle alone determines the limit of elasticity and is independent of its position. This is to say that the yield criteria is a function of $(\sigma_1-\sigma_2)$, $(\sigma_2-\sigma_3)$ and $(\sigma_3-\sigma_1)$ and is independent of hydrostatic stress component $(\sigma_1+\sigma_2+\sigma_3)/3$.

Thus yielding occurs when some scalar function of the principal stress differences reaches a critical magnitude, mathematically :

$$f(\sigma_1-\sigma_2,\ \sigma_2-\sigma_3,\ \sigma_3-\sigma_1) = \text{constant} \tag{2.34}$$

Tresca Yield Criteria

Perhaps the simplest function imaginable which satisfies equation (2.34) is of the form

$$\sigma_i - \sigma_j = \text{constant} \tag{2.35}$$

Equation (2.35) interprets when largest of the three magnitudes $\sigma_1-\sigma_2$, $\sigma_2-\sigma_3$, $\sigma_3-\sigma_1$ attains a critical constant value (for a given material) yielding begins.

This was first suggested by Tresca in 1864. It states: 'yielding occurs when the greatest absolute value of any one of the three maximum shear stresses in the material reaches a certain value'.

Applying this criteria for a state of pure shear and simple tension following relation could be derived :

$$|\sigma_1-\sigma_3| = \sigma_{yp} = 2\,k \tag{2.36}$$

where σ_{yp} is tensile yield stress and k is a yield shear stress.

Von-Mises Yield Criteria

Another admissible function, which satisfies equation (2.34) is of the form

$$(\sigma_1-\sigma_2)^2 + (\sigma_2-\sigma_3)^2 + (\sigma_3-\sigma_1)^2 = \text{constant} \tag{2.37}$$

In this type of function, each of the principal stresses contributes to yielding. This function was proposed by Huber (1904) and von-Mises (1913) and by J.C. Maxwell in a letter to Kelvin in 1856 [64]. The criteria was then interpreted by Hencky as 'yielding begins when the shear strain energy reached a critical value'.

The value of the constant in equation (2.37) can be again determined from the simple tension yielding, i.e., $\sigma_1 = \sigma_{yp}$, $\sigma_2 = 0$, $\sigma_3 = 0$ and pure shear yielding, i.e., $\sigma_1 = -\sigma_3 = k$, $\sigma_2 = 0$. Hence yield criteria becomes

$$(\sigma_1-\sigma_2)^2 + (\sigma_2-\sigma_3)^2 + (\sigma_3-\sigma_1)^2 = 2\sigma_{yp}^2 = 6k^2 \qquad (2.38)$$

For a general state of stress (σ_x, σ_y, σ_z, τ_{xy}, τ_{yz}, τ_{zx}), the von-Mises criteria becomes

$$\frac{1}{\sqrt{2}} [(\sigma_x-\sigma_y)^2 + (\sigma_y-\sigma_z)^2 + (\sigma_z-\sigma_x)^2 + 6(\tau_{xy}^2 + \tau_{yz}^2 + \tau_{zx}^2)]^{\frac{1}{2}} = \sigma_{yp}$$

$$(2.39)$$

In Fig. 2.3a and Fig. 2.3b both the yield criteria are represented in principal stress space and π plane respectively.

2.4.3 Elasto-Plastic Stress-Strain Matrix

Hooke's law for the isotropic elastic material can be written in matrix form as

$$\{\sigma\} = [D] \{\varepsilon\} \qquad (2.40)$$

where [D] is given by equation (2.32) for the plane strain condition.

By now it has been well established that the plastic deformations are incremental. Yamada and Yoshimura [53] have developed a plastic stress-strain matrix (Elasto-Plastic Matrix)
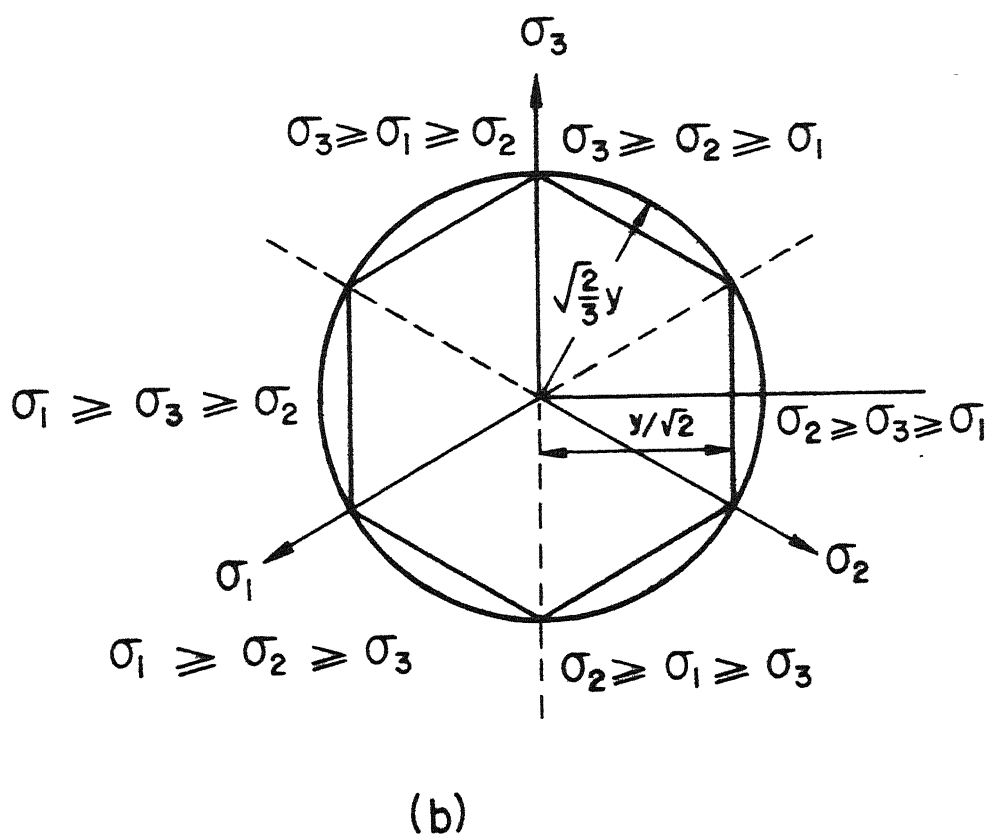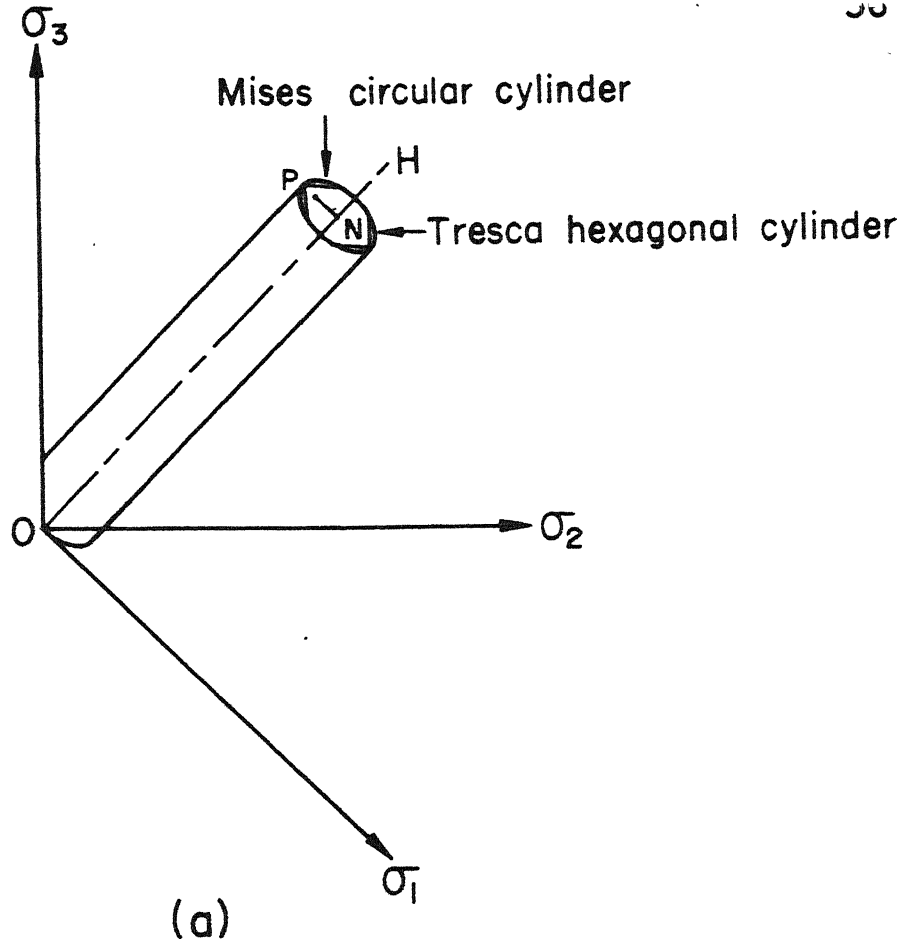
Fig. 2.3 Stress space representation of yield criteria

by inverting the Prandtl-Ruess equations obeying the von-Mises yield criterion. This symmetric plastic stress-strain matrix is given by following equation

$$[D^{ep}] =$$

$$\frac{E}{1+\gamma} \begin{bmatrix} \frac{1-\gamma}{1-2\gamma} - \frac{{\sigma_x'}^2}{S} & & & & & \\[2mm] \frac{\gamma}{1-2\gamma} - \frac{\sigma_x'\sigma_y'}{S} & \frac{1-\gamma}{1-2\gamma} - \frac{{\sigma_y'}^2}{S} & & & & \\[2mm] \frac{\gamma}{1-2\gamma} - \frac{\sigma_x'\sigma_z'}{S} & \frac{\gamma}{1-2\gamma} - \frac{\sigma_y'\sigma_z'}{S} & \frac{1-\gamma}{1-2\gamma} - \frac{{\sigma_z'}^2}{S} & & & \\[2mm] -\frac{\sigma_x'\,\tau_{xy}}{S} & -\frac{\sigma_y'\,\tau_{xy}}{S} & -\frac{\sigma_z'\,\tau_{xy}}{S} & \frac{1}{2} - \frac{\tau_{xy}^2}{S} & & \\[2mm] -\frac{\sigma_x'\,\tau_{yz}}{S} & -\frac{\sigma_y'\,\tau_{yz}}{S} & -\frac{\sigma_z'\,\tau_{yz}}{S} & -\frac{\tau_{xy}\,\tau_{yz}}{S} & \frac{1}{2} - \frac{\tau_{yz}^2}{S} & \\[2mm] -\frac{\sigma_x'\,\tau_{zx}}{S} & -\frac{\sigma_y'\,\tau_{zx}}{S} & -\frac{\sigma_z'\,\tau_{zx}}{S} & -\frac{\tau_{xy}\,\tau_{zx}}{S} & -\frac{\tau_{yz}\,\tau_{zx}}{S} & \frac{1}{2} - \frac{\tau_{zx}^2}{S} \end{bmatrix}$$

$$(2.41)$$

here
$$S = \frac{2}{3}\,\bar{\sigma}^2\,(1+ \frac{H'}{3G}), \quad \bar{\sigma} = \frac{1}{\sqrt{2}}\,[(\sigma_x-\sigma_y)^2 + (\sigma_y-\sigma_z)^2 + (\sigma_z-\sigma_x)^2$$
$$+ \; 6(\,\tau_{xy}^2 + \tau_{yz}^2 + \tau_{zx}^2)\,]^{1/2}$$

or the plain strain case, the $[D^{ep}]$ will reduce down to the follow-
ng matrix :

$$[D^{ep}] = \frac{E}{1+\gamma} \begin{bmatrix} \frac{1-\gamma}{1-2\gamma} - \frac{\sigma_x'^2}{S} & & \\ \frac{\gamma}{1-2\gamma} - \frac{\sigma_x'\sigma_y'}{S} & \frac{1-\gamma}{1-2\gamma} - \frac{\sigma_y'^2}{S} & \\ -\frac{\sigma_x'\tau_{xy}}{S} & -\frac{\sigma_y'\tau_{xy}}{S} & \frac{1}{2} - \frac{\tau_{xy}^2}{S} \end{bmatrix} \qquad (2.42)$$

where

$$S = \frac{2}{3}\bar{\sigma}^2 \left(1 + \frac{H'}{3G}\right) = \frac{2}{3}\bar{\sigma}^2\left(1 + \frac{2(1+\gamma)H'}{3E}\right).$$

2.4.4 The 'Initial Stress' Computational Method

In the 'Initial stress method' [51] the solution of the non-linear problem is approached in a series of approximations. During a load/displacement increment, a purely elastic problem is solved, determining an increment of strain $\{\Delta \epsilon\}$ and stress $\{\Delta\sigma'\}$ at every point of the continuum. For the increment of strain found from the analysis, the stress increment in general will not be correct. If $\{\Delta\sigma\}$ is the true increment of stress possible for the given strain than the situation can only be maintained by a set of body forces, equilibrating the initial stress system given by $\{\Delta\sigma'\} - \{\Delta\sigma\}$. At the second stage of the computation, this body force system can be removed by allowing the structure, (with unchanged elastic properties) to deform further. An additional set of strain and corresponding stress increments are

caused. Once again these are likely to exceed those permissible by the nonlinear relationship and the redistribution of equilibrating body forces has to be repeated. If the process converges then within an increment the full nonlinear compatibility and equilibrium conditions will be satisfied. In each cycle, since the same elastic problem is solved only partial inversion of the elastic equations is needed.

For the elastic-plastic situation, the steps during a typical load/displacement increment can be summarised as follows [56] :

1. Increment of displacement is applied. Elastic increments of strains $\{\Delta \varepsilon'\}_1$ and elastic increments of stress $\{\Delta \sigma'\}_1$ which corresponds are found.

2. $\{\Delta \sigma'\}_1$ is added to stresses existing at start of increment, $\{\sigma_0\}$, to obtain $\{\sigma'\}$, and thus $\bar{\sigma}'$. Check whether $\bar{\sigma}' < \sigma_{yp}$. If the condition is satisfied only elastic strain changes occur and the process is stopped. If the condition is not satisfied proceed to the next step.

3. If $\bar{\sigma}' \geq \sigma_{yp}$ and if $\bar{\sigma}'_0 = \sigma_{yp}$ (the element has yielded at start of iteration), $\{\Delta\sigma\}_1$ is found by $\{\Delta \sigma\}_1 = [D^{ep}] \{\Delta\varepsilon'\}_1$ where $[D^{ep}]$ is computed using $\{\sigma'\}$. Stresses which are supported by body forces are evaluated.

$$\{\Delta \sigma''\}_1 = \{\Delta \sigma'\}_1 - \{\Delta \sigma\}_1 \qquad (2.43)$$

Current stress is

$$\{\sigma\} = \{\sigma'\} + \{\Delta \sigma''\}_1 \qquad (2.44)$$

Current strain is

$$\{\varepsilon\} = \{\varepsilon'\} + \{\Delta \varepsilon'\}_1 \qquad (2.45)$$

4. If $\bar{\sigma}' > \sigma_{yp}$, but $\bar{\sigma}'_o < \sigma_{yp}$, i.e., elastic-plastic
    transition is occurred in that iteration, a factor [65]
    equation (2.46) is found and then the intermediate stress
    value is found out at which yield begins. The increment in
    stress is computed by the relation, $\{\Delta \sigma\}_1 = [D^{ep}] \{\Delta \varepsilon'\}_1$
    starting from that point. Then proceed as in step 3.

$$\text{Factor} = \frac{\bar{\sigma}' - \sigma_{yp}}{\bar{\sigma}' - \bar{\sigma}'_o} \qquad (2.46)$$

5. Nodal forces are computed corresponding to the equilibrat-
    ing body forces. These are given by

$$\{R_L\}_1^e = \int [B^T] \{\Delta \sigma''\}_1 \, d(\text{vol}) \qquad (2.47)$$

Elemental nodal force are added to get the complete nodal
force vector $\{R_L\}$.

6.   The problem is resolved using the original elastic pro-
     perties and the load system $\{R_L\}$ to find $\{\Delta\sigma'\}_2$ and
     $\{\Delta\varepsilon'\}_2$.

7.   Current values are found.

8.   Steps 2 to 6 are repeated.

The cycling can be stopped when the appropriate conver-
gence criterion specified is satisfied.

2.4.5   Convergence in Finite Element Method

Since finite element method is an approximate numerical
procedure for solution of engineering problems, like any other
approximate numerical techniques, the question of convergence,
rate of convergence and accuracy of the method are of great
importance.

During the procedure in developing finite element method
employing variational, residual or virtual work methods, the
key equations involve integrals over the domain (and also in
some cases over the boundary),it is seen from equations (2.20)
and (2.21). If each of these integrals tends to its exact
value as the element size decreases to zero the finite element
method would yield solution which correspondingly tends to the
exact solution. So the requirements for any displacement for-
mulation can be stated as follows [48] :

(a)   The displacement model must be continuous within the
      elements and the displacements must be compatible between
      the adjacent elements.

(b)   The displacement model should include the rigid body dis-
      placements of the element.

(c)   The displacement model should include constant strain
      states of the element.

Element formulations which satisfy criterion (a) is called
compatible or conforming and formulations which satisfy (b) and
(c), are called complete.

The adoption of an incremental plasticity theory and itera-
tive solution technique, such as used in 'initial stress
method' leads to errors due to size of increment and finite
values of criteria for convergence specified. Convergence
criteria specified in a solution, indicate whether the non-
linear equations describing the behaviour of the material when
subjected to increment of load/displacement have been solved
with sufficient accuracy. This is achieved by comparing the
change in some aspect of the solution between iterations and
terminating the procedure once this change has become suffi-
ciently small.

Nayak   and Zienkiewicz [61], and Rowe and Davis [66]
have described some of the convergence criteria for load based

analysis and displacement based analysis. The convergence criteria imposed in this work is on the change in the absolute magnitude of largest term in load correction vector between the iterations, compared as a percentage of the absolute magnitude of largest term in load correction vector at that instant calculated by equation (2.47).

CHAPTER 3

FINITE ELEMENT ANALYSIS OF BLANKING

3.1 INTRODUCTION

This chapter describes the finite element formulation of
sheet blanking operation, which is considered as a two dimen-
sional process occurring under plane strain conditions. Eight-
noded isoparametric quadrilateral elements are used for the
analysis and a 2x2 numerical integration is employed for cal-
culation of stresses and strains . A list of the assumptions
made and the description of the data which is necessary for the
execution of the programme is also mentioned, together with the
solution procedure. The criteria used to determine crack ini-
tiation and crack propagation direction are also stated. The
finite element code was verified by a punch indentation pro-
blem [61]. A short description of the main programme and
important subroutines is given in Appendix A.

3.2 PROBLEM DESCRIPTION

The actual blanking operation is normally a closed con-
tour sheet metal cutting process involving a 3-dimensional
deformations which is rather difficult to analyze. For the
present analysis the process is simplified as a two dimensional
under plane strain conditions, just similar to the two sided
bar cropping operation. In a simple blanking operation

(Figure 3.1) a strip of thickness t is cut along the sides AA and BB with a sharp edge punch and die set having the clearance c. As the punch moves down the sheet metal deforms, initially the deformation being elastic in nature and with the further movement of the punch, material deforms plastically. When the penetration of the punch reaches a certain critical value, cracks start at the die and the punch corners. With the further movement of the punch the cracks propagate inside eventually leading to the separation of portion of the sheet metal under the punch (known as a blank), from the rest of the strip. It is known that the severest deformations occur in the clearance gap. In the present work an attempt has been made to obtain the distribution of stress and strain fields in the clearance gap so as to determine the crack path and the variation of punch load with punch travel.

3.3 FINITE ELEMENT FORMULATION

The process of sheet blanking is analyzed using the finite element method with the following assumptions.

(i) The blanking process is a two dimensional occurring under the plane strain conditions.

(ii) The process is quasi-static with the punch moving at slow speed and hence the effect of the strain rate is neglected.
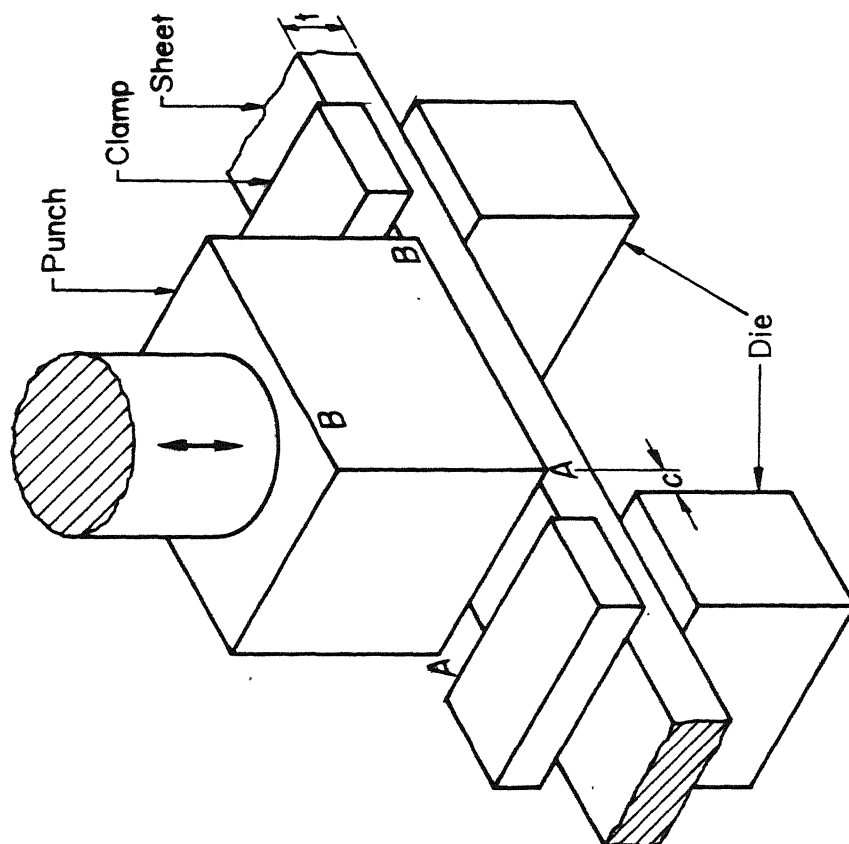
Fig.3.1 Schematic diagram of blanking operation

(iii)   The bottom surface of the punch and the top surface of the die are flat and smooth, and their edges are sharp.

(iv)   The cutting conditions are identical at the punch and the die edges.

(v)   Small deformation theory is applicable for the purpose of calculating stresses and strains.

(vi)   The material of the sheet is isotropic, linear elastic linear strain hardening type obeying von-Mises yield criterion.

Fig. 3.2 shows the two dimensional blanking process. The deformation pattern is symmetric about the centre line X-X and, hence, half of the sheet needs to be analysed, say region ABCD (beyond the deformation in the sheet is assumed negligible). The detailed model of the region ABCD is shown in Fig. 3.3, in which for convenience two rigid blocks separated by the distance c (clearance gap),are moving in opposite directions. In the present work displacement controlled analysis is performed and at each increment of displacement the two blocks move equally in opposite directions.

The following geometric boundary conditions are specified for the present work (refer Fig. 3.3).

(i)   The boundary sides AB and CD are fixed in the x-direction and free in the y-direction.
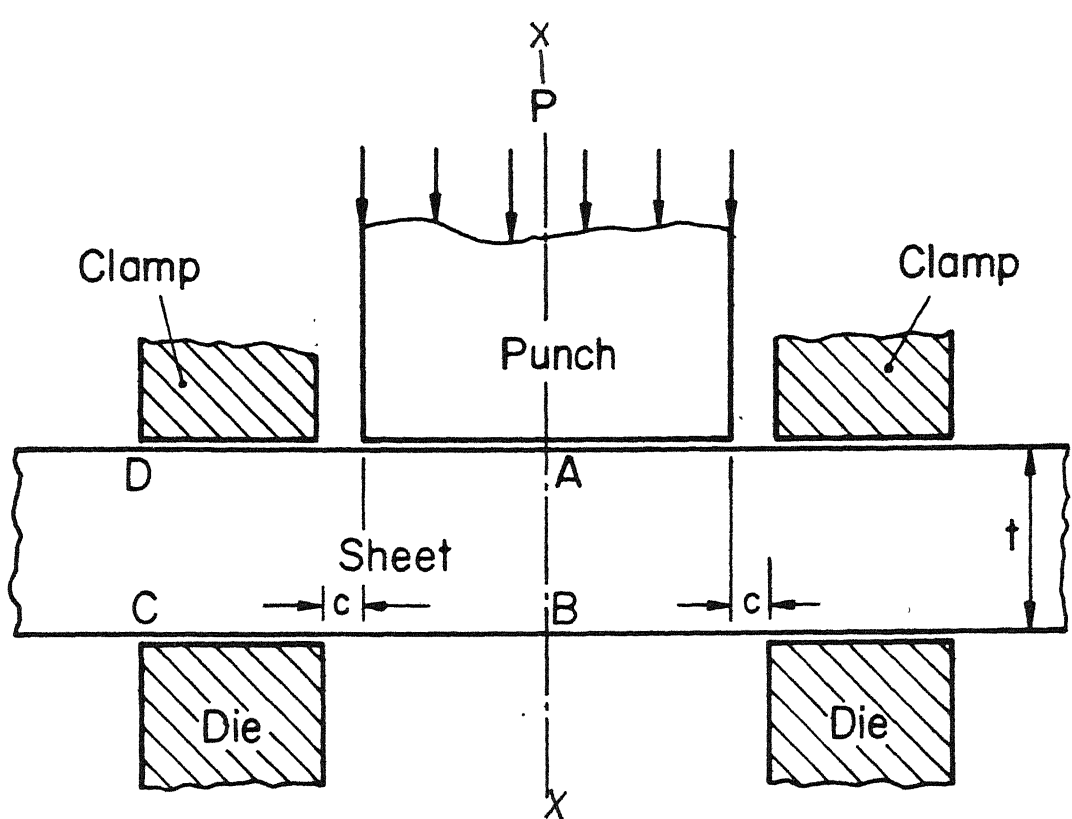
Fig.3.2 Two dimensional blanking operation
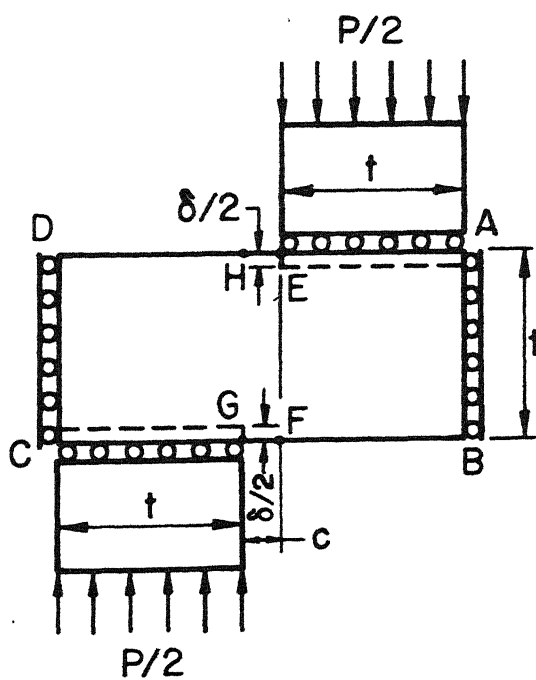
Fig.3.3 Detailed model of blanking

(ii)   The boundary side EA is free in the x-direction and uniform downward displacement is specified in the y-direction.

(iii) The boundary side CG is free in the x-direction and uniform upward displacement is specified in the y-direction.

3.3.1   Element Type and Step Size

A general purpose elastic-plastic finite element programme using 'initial stress method' was developed on DEC-1090 computer system for the analysis of the present problem.

The element selected for the discretization of the continuum was eight noded two dimensional isoparametric element which is already described in Sec. 2.3.·   For this type of parabolic element the variation of displacement is quadratic within the element and hence the variation of stresses and strains is linear.

In this incremental cum iterative technique of elastic-plastic finite element analysis the size of the increment and the number of iterations to be performed within an increment will affect the results obtained. For this work the values of the displacement specified in first displacement step is such that yielding just begins. Because of the antisymmetry, two gauss points yields whose effective stress just equals the yield stress of the material. It has been observed [46] that by using the 'initial stress method' for the nonlinear material problems, even if the large values of load/displacement

increments are specified, the results obtained are quite satis-
factory. From the kind of the mesh selected for this analysis
the total number of degrees of freedom comes out to be around
800, which requires large computer storage and the longer exe-
cution time for the programme. Thus it was decided to give
the total displacements required to be applied (till the indi-
cation of the crack initiation is obtained), in about 5 to 8
steps, depending upon the local fracture strain value specified.

3.3.2 Criteria for Crack Initiation and Crack Propagation Direction

Shaw and Avery [24] have mentioned that metal forming and
sheet cutting (i.e., cold working) operations involve severe
plastic deformation in general, i.e., the material is strained
much above the elastic point. The sheet blanking operation is
also one of the cold working processes, during which it is
observed that with the penetration of the punch into the sheet,
the metal lying between the punch and die (in the clearance gap)
deforms severely and finally the crack develops and propagates.
Crack initiation is a local phenomenon and here it is postula-
ted that crack is initiated at any point where the effective
strain ($\bar{\varepsilon}$) just exceeds the local fracture strain value (ε_f)
of the material. In the present analysis the effective strain
is calculated, from the values of the individual strains, using
following expression for 2-D plane strain case

$$\bar{\varepsilon} = 2/3 \ [\ \varepsilon_{xx}^2 + \varepsilon_{yy}^2 + 0.5 \ (\frac{\gamma_{xy}}{2})^2]^{1/2} \qquad (3.1)$$

This $\bar{\varepsilon}$ was then compared with the local fracture strain, ε_f, of the material, i.e., if $\bar{\varepsilon} \geq \varepsilon_f$ then the crack is assumed to be initiated at that point. If $\bar{\varepsilon} < \varepsilon_f$ at all the points then the next increment of displacement is applied and process repeated.

As the shearing strains are predominant in the blanking process, blanking is also referred to as a process of shearing. This was observed from the results (presented later in Chapter 4) of the finite element analysis, i.e., the shearing strains comes out to be higher than values of the normal strains. Thus here, it is postulated that the direction of the crack propagation is the same as the direction of the maximum shear strain at crack initiation point.

3.4   INPUT DATA STRUCTURE

The required finite element mesh was initially generated using an automatic mesh generation programme which is a revised version of the Durocher and Gasper's [67] programme. The following data was supplied as input to the elasto-plastic programme for the purpose of analysis.

(i)   Total number of nodes and elements, number of nodes per element, number of displacement prescribed boundary nodes, order of numerical integration, number of degrees of freedom at

each node, maximum number of iterations for each displacement step, bandwidth of the matrix etc.

(ii) Material properties, i.e., the values of the elastic modulus, Poisson's ratio, yield stress, strain hardening co-efficient and local fracture strain. These values are taken from references[25], and [34].

(iii) Nodal data which includes the node number and, x and y coordinates of the node, for all the nodes.

(iv) The element data in which the element number is given and the nodal connectivities of the element, for all the elements.

(v) The boundary node number on which geometric boundary condition is known or prescribed and the type of the boundary condition, i.e., either free, fixed or some prescribed displacement, for all nodes having geometric boundary conditions.

3.5 PROGRAMME TESTING

The solution algorithm of the general purpose elasto-plastic finite element programme using 'initial stress method' is already described. The programme which was developed is applied initially for the solution of a punch indentation problem [61], whose results are known. Fig. 3.4 shows a rigid punch indenting into a metal specimen whose material properties have been varied from isotropic strain hardening ($H' = 0.1E$), ideally plastic ($H' = 0$), to strain softening case($H' = -0.1E$).

The problem being symmetric about the centre line X-X of the punch,only half the continuum ABCD is analysed. For this purpose the region ABCD is divided into 107 nodes and 28 parabolic isoparametric elements as shown in Fig. 3.5. For every incremental displacement step the mean punch pressure has been calculated, from which the pressure-displacement curves are drawn as shown in Fig. 3.6, for various values of H'. As it can be seen from the graphs in the said figure, that the results of the present analysis match with those given by Nayak and Zienkiewicz [61]. For the case of ideally plastic situation the collapse load predicted by slip line solution [68] also matches with the finite element solution, which can be seen from the same figure.
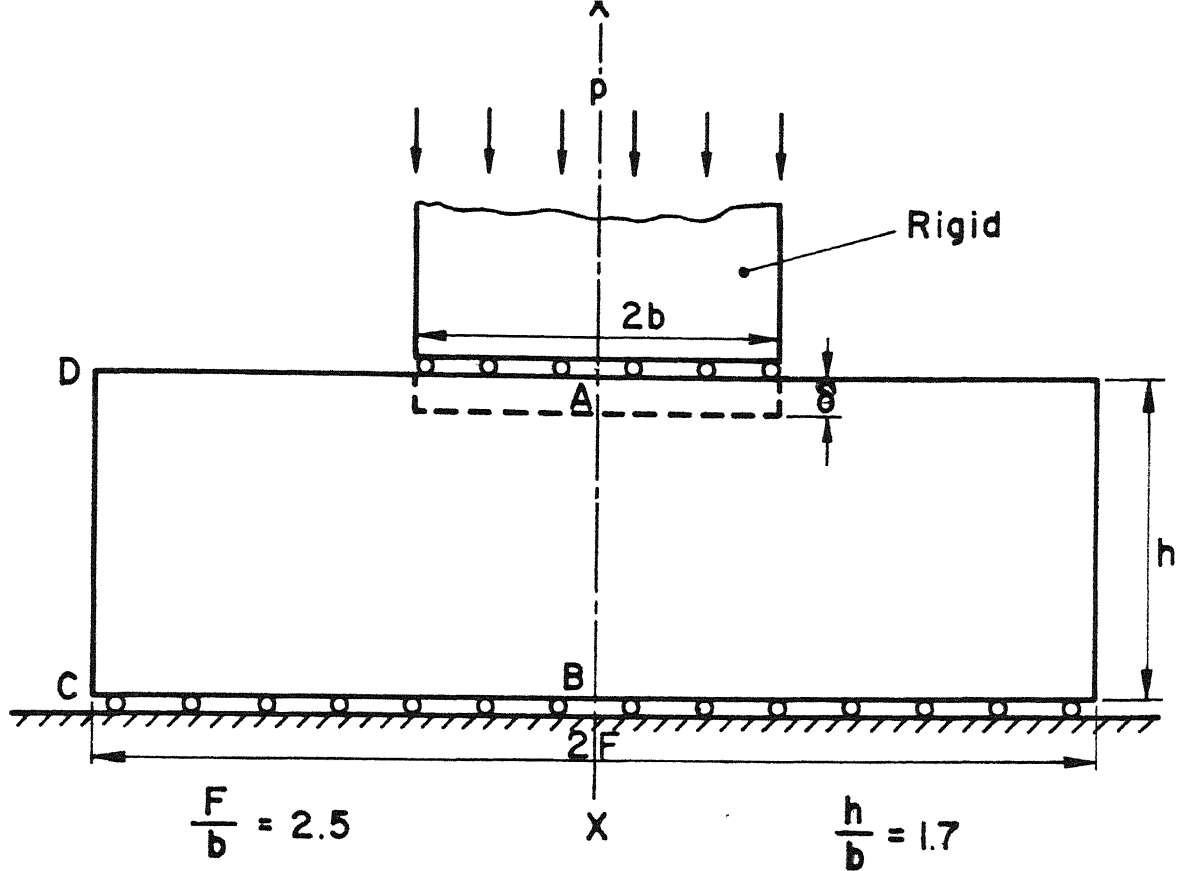
Fig. 3.4 Plane strain punch indentation problem
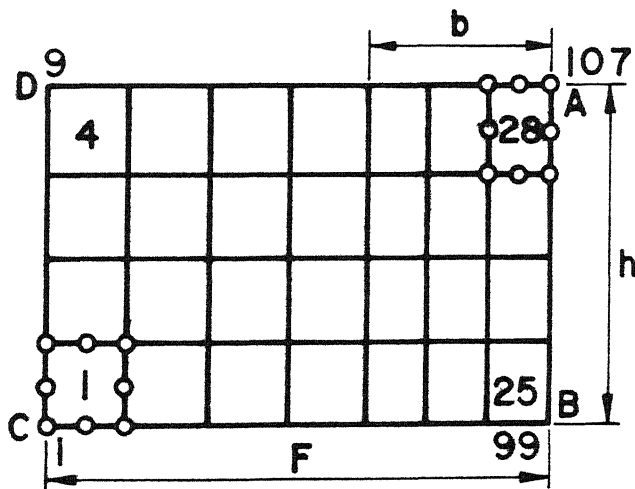
Number of elements = 28

Number of nodes = 107

Fig. 3.5 Discretization of region ABCD
(of Fig. 3.4)
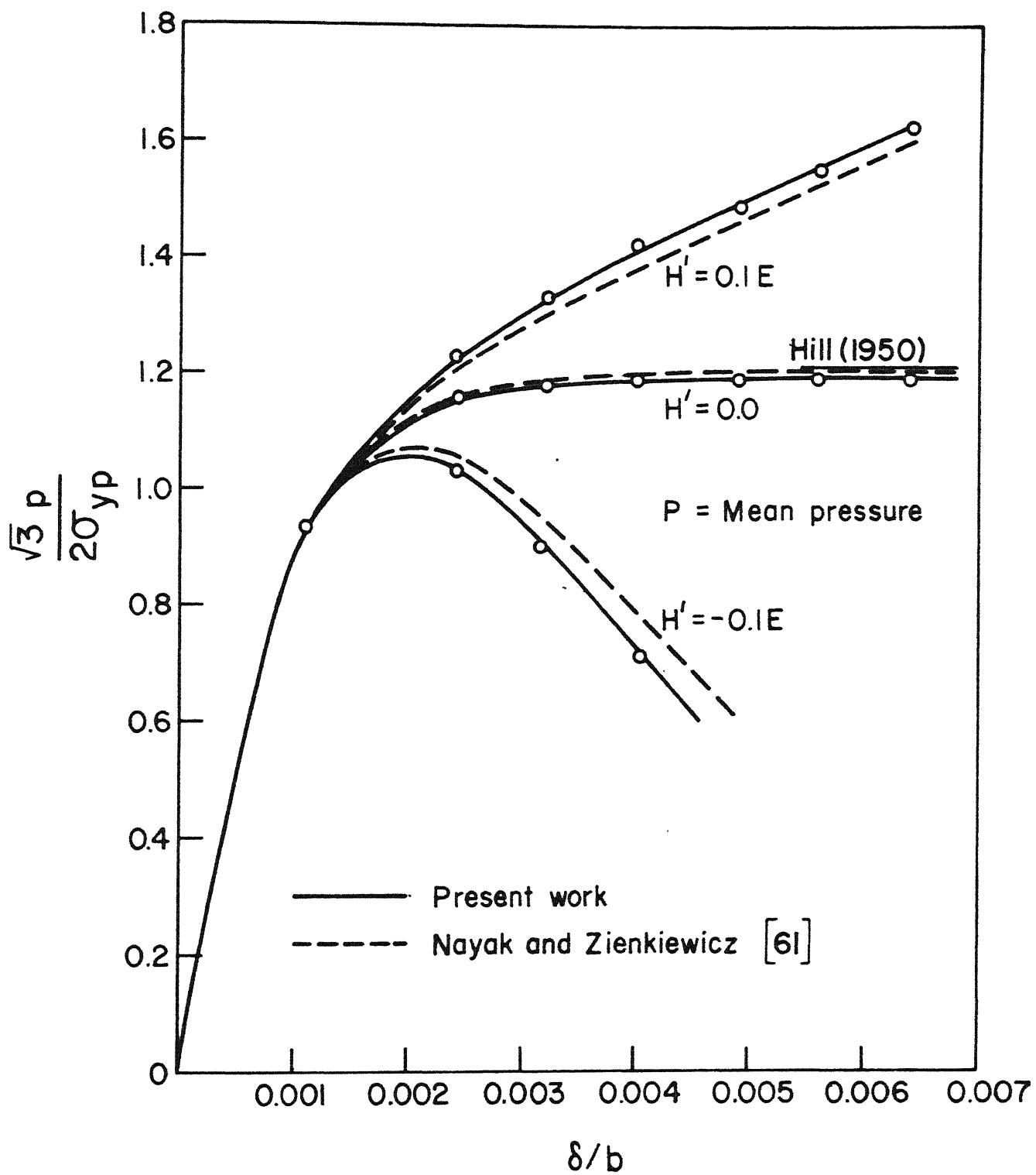
Fig. 3.6 Punch pressure-punch displacement curves for punch indentation problem.

CHAPTER 4

RESULTS AND DISCUSSION

4.1 INTRODUCTION

This chapter presents an analysis of the results obtained for the blanking problem using the elasto-plastic 'initial stress' finite element programme. The continuum is discretized into 396 nodes and 117 eight noded quadrilateral elements. The main variables for this problem are the material properties $E, \gamma, \sigma_{yp}, H'$ and ε_f (the material is assumed to remain isotropic during the process), the sheet thickness t and the fractional punch-die clearance c/t. In the present work a large number of computer runs are taken, keeping the values of $E = 12500 \times 10^7$ N/m^2, $\gamma = 0.34$ and $\sigma_{yp} = 8 \times 10^7$ N/m^2 as constant throughout the analysis. The values of other variables are changed i.e., H' is varied from 25×10^7 N/m^2 to 100×10^7 N/m^2, ε_f from 1.1 to 1.59, t from 1.47×10^{-3} m to 6.0×10^{-3} m and c/t from 0.03 to 0.20 respectively; at a time only the value of one variable is changed. The CPU time required for one run on the average comes to about 40 to 45 minutes on DEC-1090 computer system. Initially the effect of the various variables on the punch force-punch penetration pattern is analysed. Then from these results the fractional punch penetration ($\frac{\Delta + c}{t}$) required at crack initiation is obtained for all

the cases and these are discussed. The punch force required to initiate the crack is taken as the maximum punch force, P_{max} and effects of various parameters on it are studied. From the values of the principal strains and their directions, for various c/t ratios and ε_f, an indication of the optimum clearance ratio is obtained and the dependance of the optimum clearance ratio on the ductility of the material (ε_f) is brought out. Finally an attempt is made to explain the mode of metal deformation and distribution of strains, at various stages of punch penetration, in the punch-die clearance gap. The convergence criterion specified is, the change in absolute maximum value of residual load vector between iterations as one percent of its absolute maximum value, in the present work.

4.2 RESULTS AND DISCUSSION

Fig. 4.1 shows the finite element discretization of the region ABCD of Fig. 3.3 together with the geometric boundary conditions. As mentioned earlier the discretization is obtained using automatic mesh generation programme. The same mesh was employed for the complete analysis of the problem but with the numerical values of thickness (t) and clearance (c) varied as and when required. This mesh is selected after checking the results of some sample runs with different meshes. A mesh finer than the used here was not selected, because that would lead to more number of degrees of freedom (with the present mesh the

total degrees of freedom is about 800). This means with finer
mesh there is higher band width of the global stiffness matrix,
larger number of equations to be solved at each iteration etc.,
thus requiring higher computation time. The size of the mesh
is also restricted because it is decided to take a good number
of computer runs by varying different parameters.

Displacement controlled analysis is performed i.e., equal
and opposite vertical displacements $\delta/2$ are specified on sides
AE and GC (Fig. 4.1) of the continuum, during each displacement
increment step. The output of the computer run gave the value
of the equivalent vertical load $P/2$ corresponding to $\delta/2$.
Thus, the value of load P (called punch force) was obtained
against the percentage displacement $((\delta/t)\times100)$ also called
the punch penetration, at each increment. The increments of
applied displacement is continued till the crack initiated in
any of the element (i.e., the crack initiation criterion
stated earlier is satisfied). The punch force corresponding
to percentage penetration upto crack initiation $((\frac{\Delta + c}{t})\times100)$
is called maximum punch force. From these results the varia-
tion of punch force-punch penetration and other plots are
drawn.

4.2.1 Punch Force-Punch Penetration Characteristics

Fig. 4.2 shows a set of such plots where the percentage
clearance $(\frac{c}{t} \times 100)$ is taken as 3,6,8.5,14 and 20,respectively,

with the values of sheet thickness, strain hardening parameter and local fracture strain taken as 1.47×10^{-3} m, 25×10^{7} N/m^{2} and 1.25, respectively (Table 4.1a). Figures 4.3, 4.4 and 4.5 show similar sets of plots as the previous one with the values of H' as 50×10^{7} N/m^{2}, 75×10^{7} N/m^{2} and 100×10^{7} N/m^{2} respectively (Tables 4.1b, 4.1c and 4.1d). In Figures 4.6 and 4.7 the value of thickness for a set of variation of percentage clearance is taken as 3×10^{-3} m and 6×10^{-3} m respectively (Table 4.2), keeping the other parameters constant.

From the above plots it is observed that within the range of clearances used, with the increase in percentage clearance, for the same amount of punch force the punch penetration increases. Again with the same amount of percentage clearance, as the H' is increased the curve moves upwards, i.e., the punch force required for same amount of penetration of the punch, increases. This is because with higher H', the material is more strain hardened and its ductility reduces, thus, demanding more force for plastic deformation. The similar observation is made (i.e., the punch force increases) with the increase in sheet thickness. This is because the amount of material in the clearance gap increases as the thickness is increased and so requires more force.

4.2.2 Punch Penetration at Crack Initiation

In Fig. 4.8 a set of curves is shown in which the percentage

Table 4.1 Punch Penetration vs Punch Force at Different Fractional Clearances ($t=1.47 \times 10^{-3}$ m)

$E = 12500 \times 10^7$ N/m^2, $\gamma = 0.34$, $\sigma_{yp} = 8 \times 10^7$ N/m^2, $\varepsilon_f = 1.25$

a. $H' = 25 \times 10^7$ N/m^2

c/t=0.03		c/t=0.06		c/t=0.085		c/t=0.14		c/t=0.20	
$(\delta/t) \times 100$	P_N	$(\delta/t) \times 100$	P_N	$(\delta/t) \times 100$	P_N	$(\delta/t) \times 100$	P_N	$(\delta/t) \times 100$	P_N
0.02	33.3	0.02	33.0	0.02	33.8	0.02	34.0	0.03	34.3
0.11	106.6	0.12	125.4	0.13	125.0	0.15	123.2	0.16	121.8
0.57	208.2	0.63	186.4	0.67	173.6	0.75	159.0	0.84	153.9
2.88	239.5	3.18	218.6	3.39	207.4	3.78	188.6	4.24	176.1
14.45	335.0	15.93	317.4	16.99	308.2	18.91	288.4	21.22	275.2
23.67	354.0	28.69	364.8	30.59	353.6	35.64	343.8	38.25	320.6

b. $H' = 50 \times 10^7$ N/m^2

c/t=0.03		c/t=0.06		c/t=0.085		c/t=0.14		c/t=0.20	
$(\delta/t) \times 100$	P_N	$(\delta/t) \times 100$	P_N	$(\delta/t) \times 100$	P_N	$(\delta/t) \times 100$	P_N	$(\delta/t) \times 100$	P_N
0.02	31.3	0.02	33.0	0.02	33.8	0.02	34.1	0.03	34.3
0.11	128.3	0.12	126.7	0.13	126.2	0.14	124.4	0.16	102.8
0.57	214.7	0.63	198.3	0.67	181.2	0.75	166.4	0.84	160.2
2.88	263.9	3.18	247.2	3.39	234.8	3.77	216.2	4.24	203.4
14.45	457.4	15.93	448.0	16.99	434.2	18.91	418.2	21.25	404.2
23.34	505.8	28.58	531.2	30.59	544.6	35.64	546.8	41.82	556.4

c. $H' = 75 \times 10^7$ N/m^2

c/t=0.03		c/t=0.06		c/t=0.085		c/t=0.14		c/t=0.20	
$(\delta/t) \times 100$	P_N	$(\delta/t) \times 100$	P_N	$(\delta/t) \times 100$	P_N	$(\delta/t) \times 100$	P_N	$(\delta/t) \times 100$	P_N
0.02	33.3	0.02	33.3	0.02	33.8	0.02	34.1	0.03	34.3
0.11	109.8	0.12	127.9	0.13	127.4	0.15	125.5	0.16	123.9
0.57	220.4	0.63	205.0	0.67	188.3	0.75	172.5	0.84	166.4
2.89	288.4	3.18	272.2	3.39	261.2	3.78	242.4	4.24	230.2
14.45	578.6	15.93	574.0	16.99	586.0	18.91	545.4	21.22	531.4
23.70	667.4	28.05	919.6	30.47	737.4	36.31	758.6	41.82	764.6

d. $H' = 100 \times 10$ N/m^2

c/t=0.03		c/t=0.06		c/t=0.085		c/t=0.14		c/t=0.20	
$(\delta/t) \times 100$	P_N	$(\delta/t) \times 100$	P_N	$(\delta/t) \times 100$	P_N	$(\delta/t) \times 100$	P_N	$(\delta/t) \times 100$	P_N
0.02	33.3	0.02	33.3	0.02	33.8	0.02	34.1	0.03	34.3
0.11	131.2	0.12	129.0	0.13	128.5	0.15	126.5	0.16	104.8
0.56	225.6	0.63	213.4	0.67	195.7	0.75	178.3	0.84	172.1
2.88	313.2	3.18	297.8	3.40	288.2	3.78	269.0	4.24	256.4
14.44	699.4	15.93	699.6	16.99	696.4	18.91	672.8	21.22	657.6
24.04	834.0	27.79	886.4	30.47	917.0	35.91	950.8	41.82	972.8

Table 4.2 Punch Penetration vs Punch Force Variation at Different Fractional Clearances ($t=3\times10^{-3}$m; 6×10^{-3}m)

$E=12500\times10^{7}$ N/m^2, $\gamma = 0.34$, $H'=25\times10^{7}$ N/m^2, $\varepsilon_f=1.25$,

$\sigma_{yp}=8\times10^{7}$ N/m^2

a. $t = 3\times10^{-3}$ m

c/t=0.03		c/t=0.06		c/t=0.085		c/t=0.14		c/t=0.20	
$(\delta/t)\times100$	P_N	$(\delta/t)\times100$	P_N	$(\delta/t)\times100$	P_N	$(\delta/t)\times100$	P_N	$(\delta/t)\times100$	P_N
0.02	65.6	0.02	68.6	0.02	69.2	0.02	69.7	0.03	70.2
0.11	257.8	0.12	256.7	0.13	255.3	0.15	251.7	0.16	249.7
0.59	414.0	0.64	367.8	0.68	352.4	0.75	327.5	0.85	313.3
2.94	466.4	3.22	441.4	3.40	422.2	3.79	390.9	4.26	362.9
14.73	665.9	16.14	645.6	17.00	628.8	18.94	588.1	21.33	565.3
23.69	702.7	27.57	714.2	29.86	707.2	35.25	693.4	41.33	695.8

b. $t = 6\times10^{-3}$ m

c/t=0.03		c/t=0.06		c/t=0.085		c/t=0.14		c/t=0.20	
$(\delta/t)\times100$	P_N	$(\delta/t)\times100$	P_N	$(\delta/t)\times100$	P_N	$(\delta/t)\times100$	P_N	$(\delta/t)\times100$	P_N
0.02	132.0	0.02	136.6	0.02	136.6	0.02	139.0	0.03	139.8
0.11	516.2	0.12	512.8	0.13	509.6	0.15	501.4	0.16	496.8
0.59	828.6	0.64	772.0	0.67	745.2	0.75	688.2	0.84	625.3
2.96	933.8	3.22	899.2	3.38	869.2	3.80	805.1	4.24	720.8
14.83	1335.8	16.14	1316.8	16.92	1274.0	19.00	1206.4	21.21	1120.6
23.80	1407.4	26.86	1422.2	29.27	1424.0	34.97	1419.4	41.24	1388.7

punch penetration at crack initiation is plotted against the variation of percentage clearances for three different values of H'. It is observed from the results that the value of percentage punch penetration at crack initiation increases with the increase of c/t ratio. This may be due to the fact that with larger clearance the material can deform easily, i.e., the severity of deformation decreases, and, thus, requires more punch penetration before crack initiation. With a very high value of c/t ratio more of drawing action takes place. But it can be seen that for the same percentage clearance, by varying the value of H' the percentage penetration required at crack initiation remains nearly constant. Similar observations are made from the plots of the percentage penetration at crack initiation vs. percentage clearance (Fig. 4.9) for different sheet thicknesses, i.e., by varying the sheet thickness for a specific value of c/t ratio the percentage punch penetration at crack initiation remains more or less fixed. So it can be concluded that the percentage punch penetration at crack initiation is insensitive to the work hardening parameter, H', and the sheet thickness, t. But it strongly depends on the local fracture strain of the material of the sheet. The above statement becomes clear when Fig. 4.10 is examined critically. It can be seen that the percentage punch penetration at crack initiation increases with the increase in the value of local fracture strain of the material. This is observed at all the clearances.

4.2.3 Maximum Punch Force

From the results of the analysis an attempt is also made to study the effects of various parameters on the maximum punch force, P_{max}, (i.e., the punch force required for crack initiation). It is described here in brief with the help of graphs. In Fig. 4.11, P_{max} is plotted against the variation of sheet thickness. As the sheet thickness is increased P_{max} increases linearly with it. Similar trend has been also observed from experimental results [25] and even in the analytical work reported [23]. Fig. 4.12 illustrates the effect of varying c/t on P_{max} for various values of H'. Here the value of P_{max} is found to have little variation at smaller values of the c/t ratio but is otherwise almost independent of c/t ratio, within the range of the clearances used. This observation was also made by a number of workers in this field, and is already mentioned in Chapter 1. But maximum punch force is seen to increase with the increase in H'.

4.2.4 Optimum Clearance

In the present work, one of the objective is to arrive at a suitable value of c/t called the optimum clearance (c_o/t) from the results of the analysis. As mentioned earlier it is postulated that the direction of the crack propagation coincides with the direction of the maximum shear strain. When the crack initiates the diagonal angle (Θ) of the deformed continuum and the

direction of the maximum shear strain ($\emptyset$) are calculated with
w.r. to y-axis for various c/t ratios. The results are tabu-
lated in Table 4.3, and Fig. 4.13 shows one set of such results
graphically for $\varepsilon_f = 1.1$. As c/t ratio is increased the angle
Θ also increases in a direct proportion but the angle $\emptyset$ decrea-
ses. Thus both the plots intersect each other at some point
and the value of c/t corresponding to this is taken as the
optimum clearance ratio (c_o/t), for the values of the para-
meters used. The term optimum clearance is used here because
when the direction of the crack propagation coincides with
the diagonal, the fractures meet resulting in clean edges. The
amount of the work required to be done for complete separation
of blank will also be minimum. In Fig. 4.14 and Fig. 4.15
similar graphs are drawn from the results (Table 4.3), for the
values of $\varepsilon_f = 1.25$ and $\varepsilon_f = 1.59$, respectively. The corres-
ponding optimum clearance values are also found in the same
manner mentioned above. The values of the optimum clearance,
thus obtained, are plotted against the ε_f, as shown in Fig.
4.16. It is seen from this plot that as the ductility of the
material (i.e., ε_f) is increased optimum clearance required
between the punch and the die reduces e.g., the optimum
clearance required for blanking aluminium sheet (higher ε_f)
is less than that required for blanking mild steel and brass
(lower ε_f). When the results obtained by the finite element
analysis are compared with the experimental values [25] and the

Table 4.3 Maximum Punch Penetration,Diagonal Angle and
Direction of Maximum Shear Strain for
different Fractional Clearances and Ductility

$t = 3 \times 10^{-3}$ m, $\sigma_{yp} = 8 \times 10^7$

$E = 12500 \times 10^7$ N/m^2, $\gamma = 0.34$, $H' = 25 \times 10^7$ N/m^2

$\emptyset$ = Direction of maximum shear strain with y-axis

Θ = Diagonal Angle with y-axis

c/t	$\varepsilon_f = 1.1$			$\varepsilon_f = 1.25$			$\varepsilon_f = 1.59$		
	$(\frac{\Delta+c}{t}) \times 100$	Θ°	$\emptyset^\circ$	$(\frac{\Delta+c}{t}) \times 100$	Θ°	$\emptyset^\circ$	$(\frac{\Delta+c}{t}) \times 100$	Θ°	$\emptyset^\circ$
0.03	20.42	2.15	13.60	23.69	2.25	14.56	29.8	2.44	13.58
0.06	23.59	4.49	12.00	27.57	4.73	12.54	34.56	5.23	11.80
0.085	26.04	6.56	11.41	29.86	6.91	11.10			
0.14	30.83	11.44	10.40	35.25	12.20	10.64	44.83	14.23	10.30
0.20	35.97	17.34	9.40	41.33	18.82	9.78	53.05	23.07	9.38

theoretical curve from the previous work [23], from the same figure, the trends are observed to be similar and these result match better with the experimental curve. Afterwards using t plot of Fig. 4.9 the values of the optimum percentage punch penetration $((\frac{\Delta + c_o}{t}) \times 100)$ for all the values of ε_f used are obtained, corresponding to the respective c_o/t ratio. Fig. 4.1 shows the variation of $(\frac{\Delta + c_o}{t}) \times 100$ with the variation of ε_f It can be seen that the value of the optimum punch penetration is around 30%, for the range of ε_f selected. When the experi mental [25] as well as the theoretical [23] curves are super- imposed on the finite element solution, it is seen that the results obtained by the finite element method match better with the experimental values.

An attempt was also made to get the crack path in the continuum with the help of the existing programme, which is described in brief here. The crack initiation criterion sta- ted earlier is applied after each displacement step, to check whether crack is initiated at any point or not. Once the indication of crack initiation is obtained, the contribution of that element for the overall stiffness of the continuum is made zero. This is done by assigning zero elastic modulus value (i.e., E = 0) to that element, thus the overall stiffness of the continuum decreases. Then the next convenient increments of the displacement steps are applied and the analysis is

4.2.5 Deformation Pattern and Strain Distribution

Nodal displacements, total stresses and total strains are obtained after each increment step at various points in the material, from the results of the analysis. From these the plots of the deformed grid pattern and the distribution of the strains in the clearance gap are drawn. All the figures which are described below are shown with separate scales for the clearance gap and the other part of the continuum. The clearance gap is exaggerated for clarity and better understanding.

In Fig. 4.18 to Fig. 4.22 the deformation of the various points, from the beginning of the punch penetration till the crack initiation, for c/t ratio of 0.20 is shown. It is seen that until the punch penetrates upto about 0.85% into the sheet there is no appreciable deformation of the nodal points. The deformation becomes pronounced only with the further punch movement. It is seen that the points near the die and the punch corners undergo maximum deformation, while for those away from the corners and towards the centre of the sheet the deformation is less severe. This brings out clearly that the crack should initiate at the punch and the die corners. The effect of change of c/t ratio on the deformation behaviour (at crack initiation) is brought out in Fig. 4.22 to Fig. 4.25. The deformation is more severe for small clearance and becomes less

severe with increase in the clearance. This indicates that for the same value of ε_f, the percentage punch penetration required (upto crack initiation) increases as the clearance is increased.

In Fig. 4.26 to Fig. 4.28 the variation of the maximum and the minimum principal strains, and the effective strains, in the clearance gap are shown for all the displacement steps. They are drawn in a part of the sheet thickness and only near the die for $c/t = 0.20$. It can be seen that, the contours change abruptly till the percentage punch penetration is about 0.847, then there is no further significant change in the shape of the contours. The patterns for the fourth, fifth and the sixth steps look similar in each figure. It is found that the highest numerical values of these strains occur near the lower-most left corner, i.e., the die corner, which indicates that the crack should initiate from that corner only. The gradient of the contours are steepest at the die corner and decreases as one goes away from it. Fig. 4.29 to Fig. 4.31 show corresponding strain contours for four different c/t ratios. The maximum value of the strains are observed near the die corner, for any c/t ratio. But it can be seen that strain distribution in the clearance gap is affected by the c/t ratio, and for c/t ratio in the range of 0.14 to 0.20, the lowest strain occur near the lower right portion of the clearance gap, i.e., opposite to the die corner.

4.2.6 Spread of the Plastic Zone

In order to study the spread of the plastic zone in the sheet material, in relation to the punch penetration, an analysis is performed by prescribing small displacement steps. After each step the number of sampling points which yield are found out. The region enclosed within the points gives the shape and the size of the plastic zone in the material. The plastic enclaves so obtained are superimposed one above the other as shown in Fig. 4.32. It shows that the plastic zone expands slowly in the beginning, and when the value of the percentage punch penetration is about 0.11 all the material in the clearance gap is almost completely plastic. This value of penetration is very low when compared with the value of percentage punch penetration required for crack initiation (which is of the order of 41.33%). Afterwards the plastic deformation of the material in the clearance gap continuously increases with further punch movements. This indicates that during the process of blanking severe plastic deformations are encountered in the clearance gap.
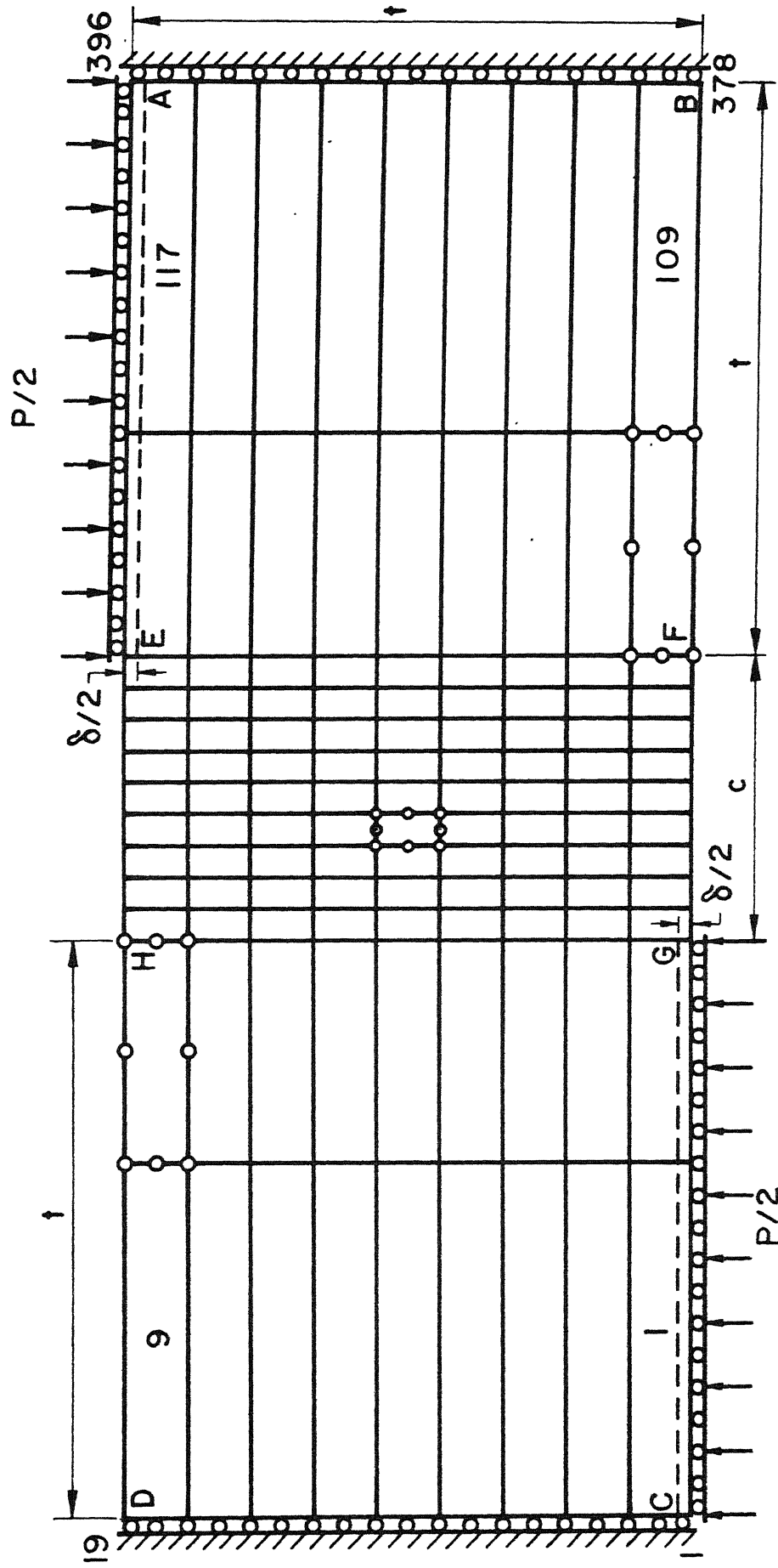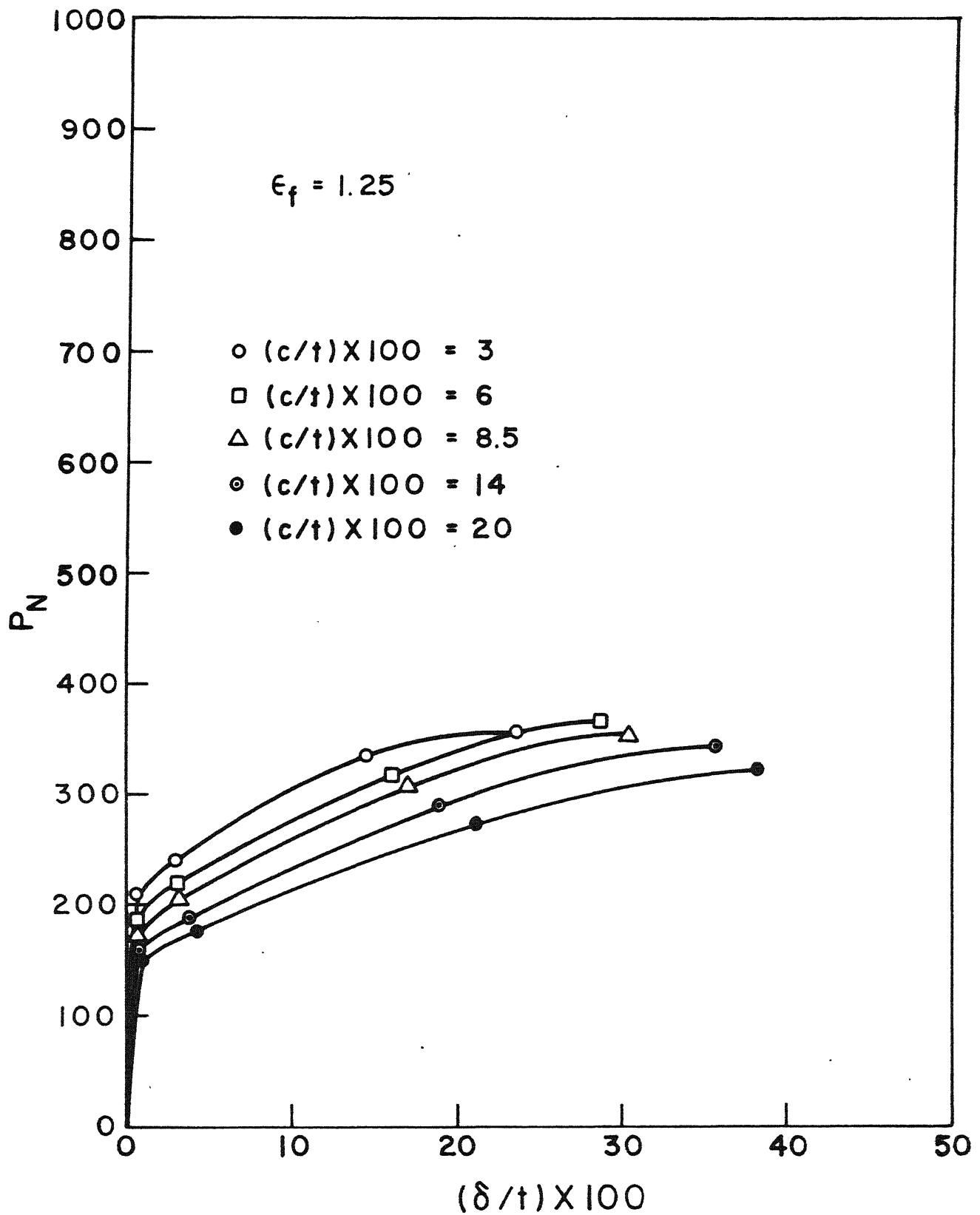
Fig. 4.1 Discretized model of blanking problem.

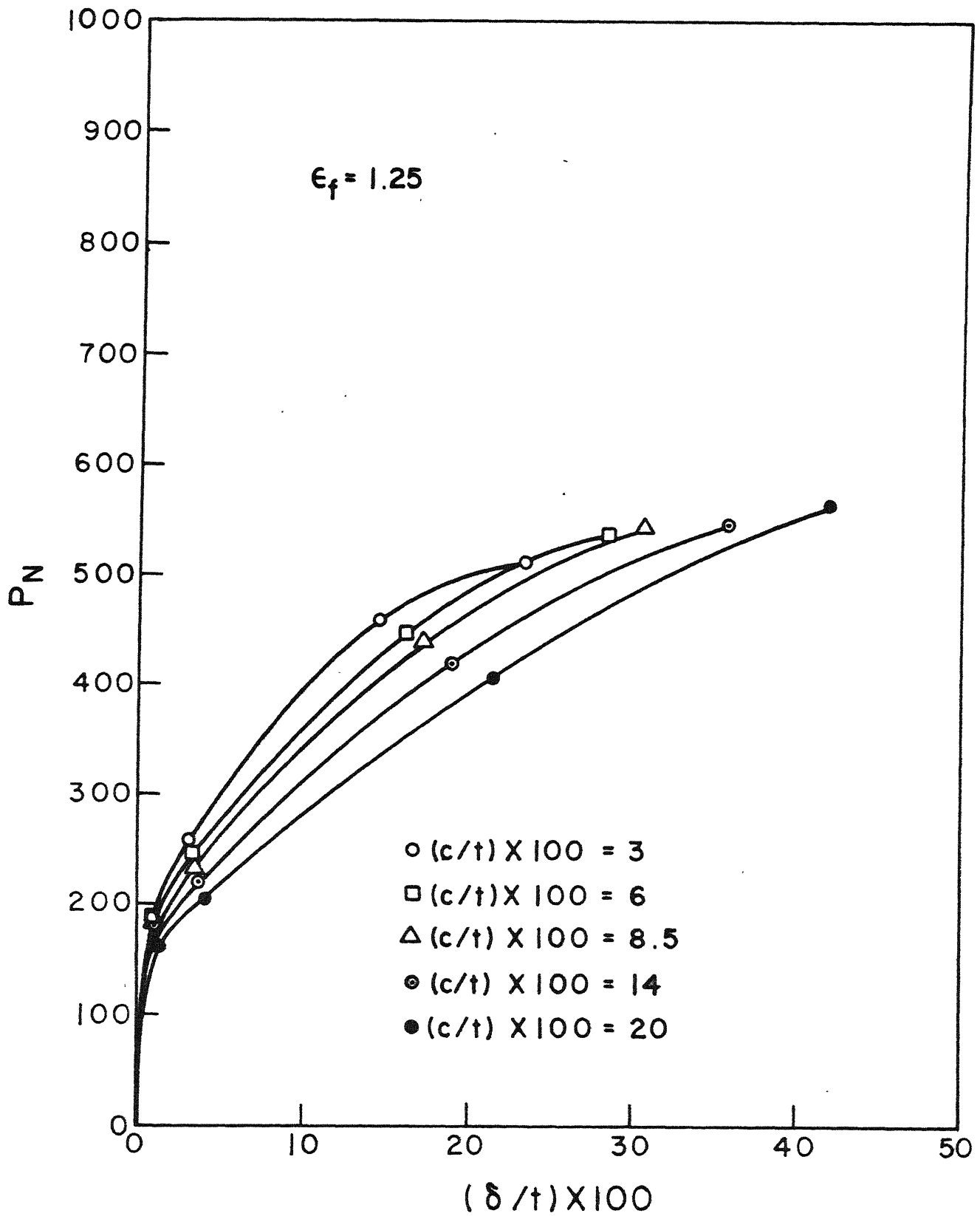Fig. 4.2 Variation of punch force with punch penetration for $t = 1.47 \times 10^{-3}$m and $H' = 25 \times 10^{7}$ N/m².

Fig. 4.3   Variation of punch force with punch penetration for $t = 1.47 \times 10^{-3}$ m   and $H' = 50 \times 10^{7}$ N/m^2
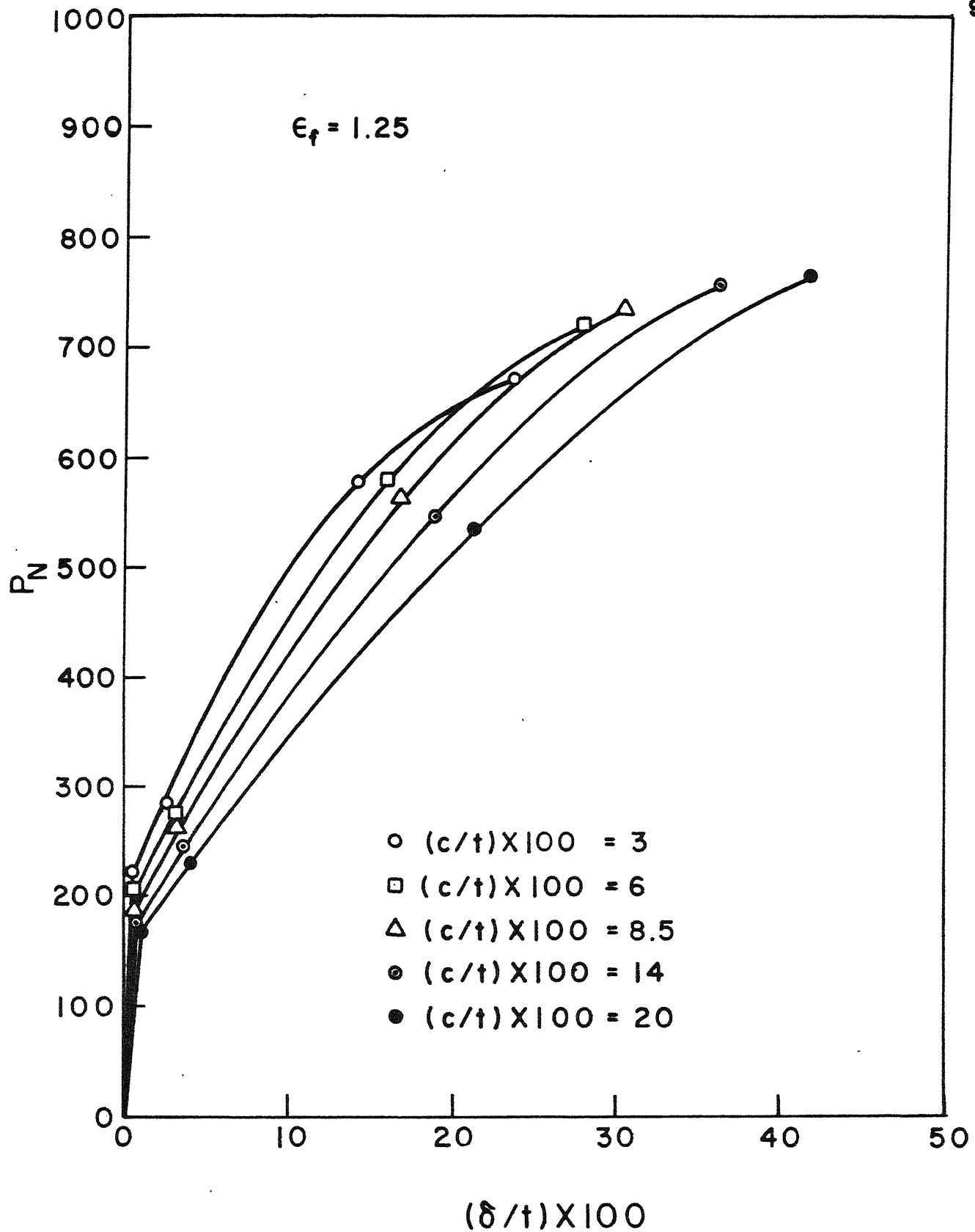
Fig. 4.4 Variation of punch force with punch penetration for $t = 1.47 \times 10^{-3} m$ and $H' = 75 \times 10^{7} N/m^{2}$
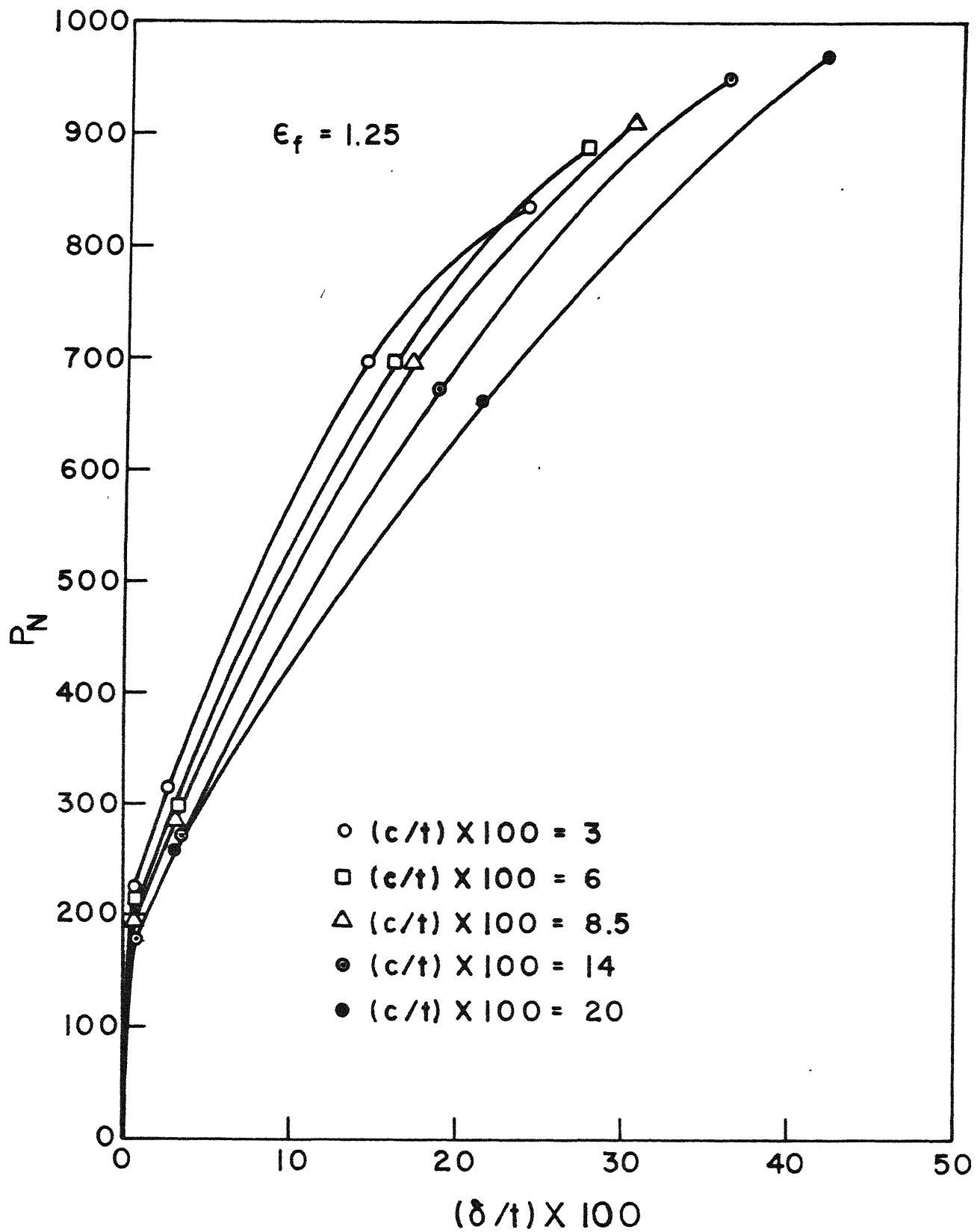
Fig.4.5   Variation of punch force with punch penetration
for $t = 1.47 \times 10^{-3}$ m and $H' = 100 \times 10^{7}$ N/m^{2}
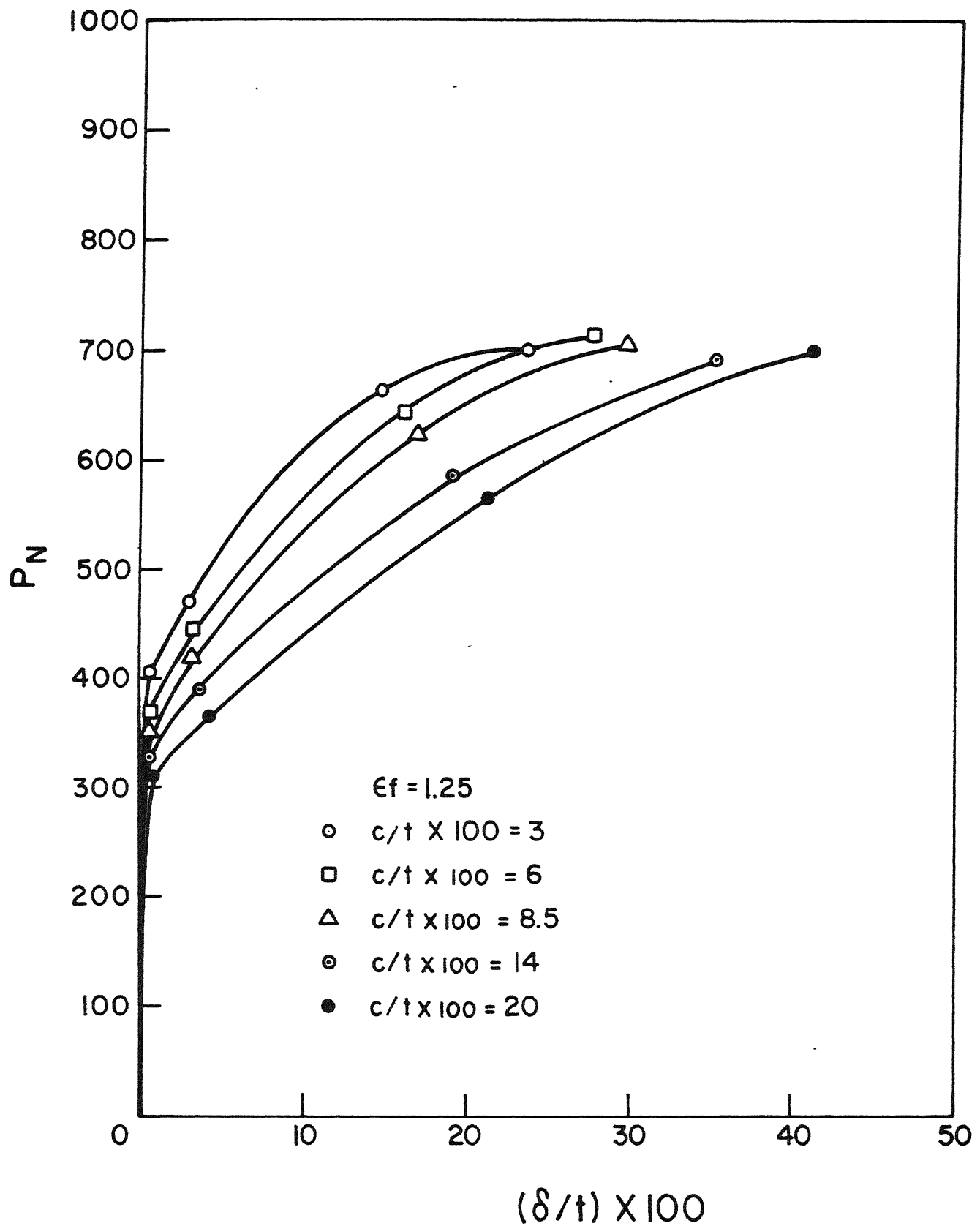
Fig. 4.6 Variation of punch force with punch penetration for $t = 3 \times 10^{-3}$ m and $H' = 25 \times 10^{7}$ N/m^2
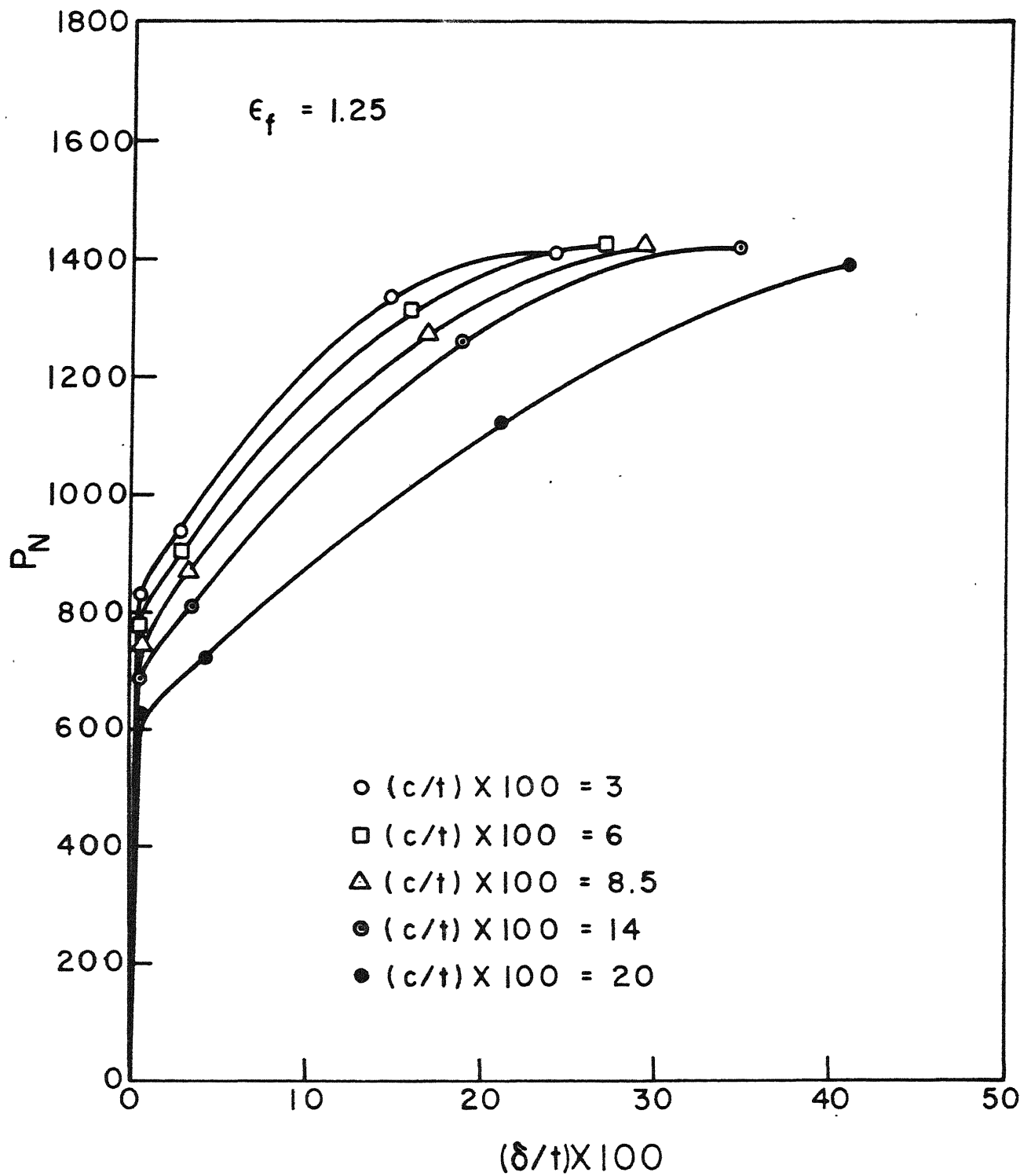
Fig. 4.7 Variation of punch force with punch penetration for $t = 6 \times 10^{-3}$ m and $H' = 25 \times 10^{7}$ N/m²

Legend within figure:

$\epsilon_f = 1.25$

o $(c/t) \times 100 = 3$
□ $(c/t) \times 100 = 6$
△ $(c/t) \times 100 = 8.5$
◉ $(c/t) \times 100 = 14$
● $(c/t) \times 100 = 20$

Axes: P_N (vertical), $(\delta/t) \times 100$ (horizontal)

Fig. 4.8 Variation of punch penetration (at crack initiation) with percentage clearance.
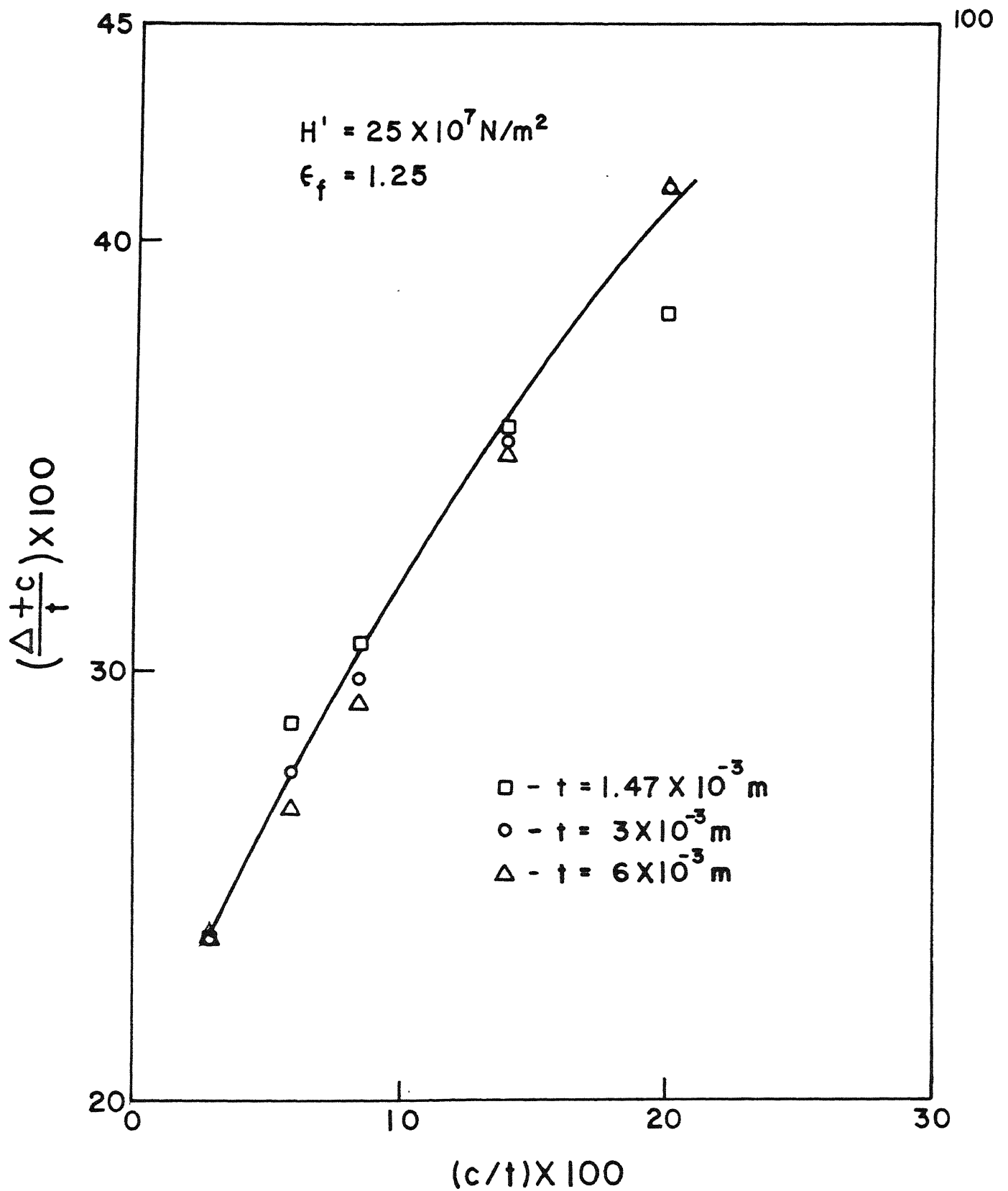
Fig. 4.9   Variation of punch penetration (at crack initiation) with percentage clearance.
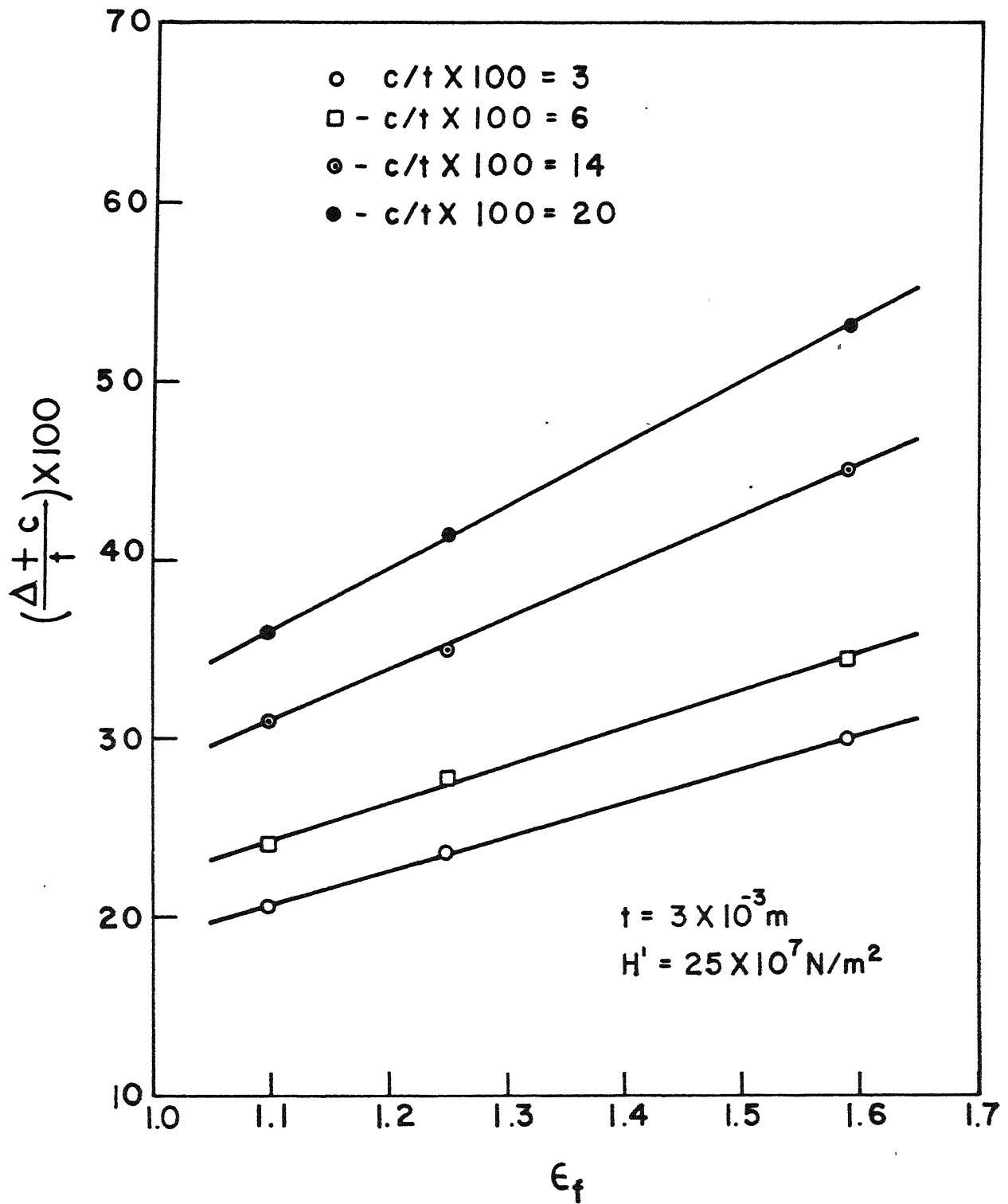
Fig. 4.10 Variation of punch penetration (at crack initiation) with local fracture strain.
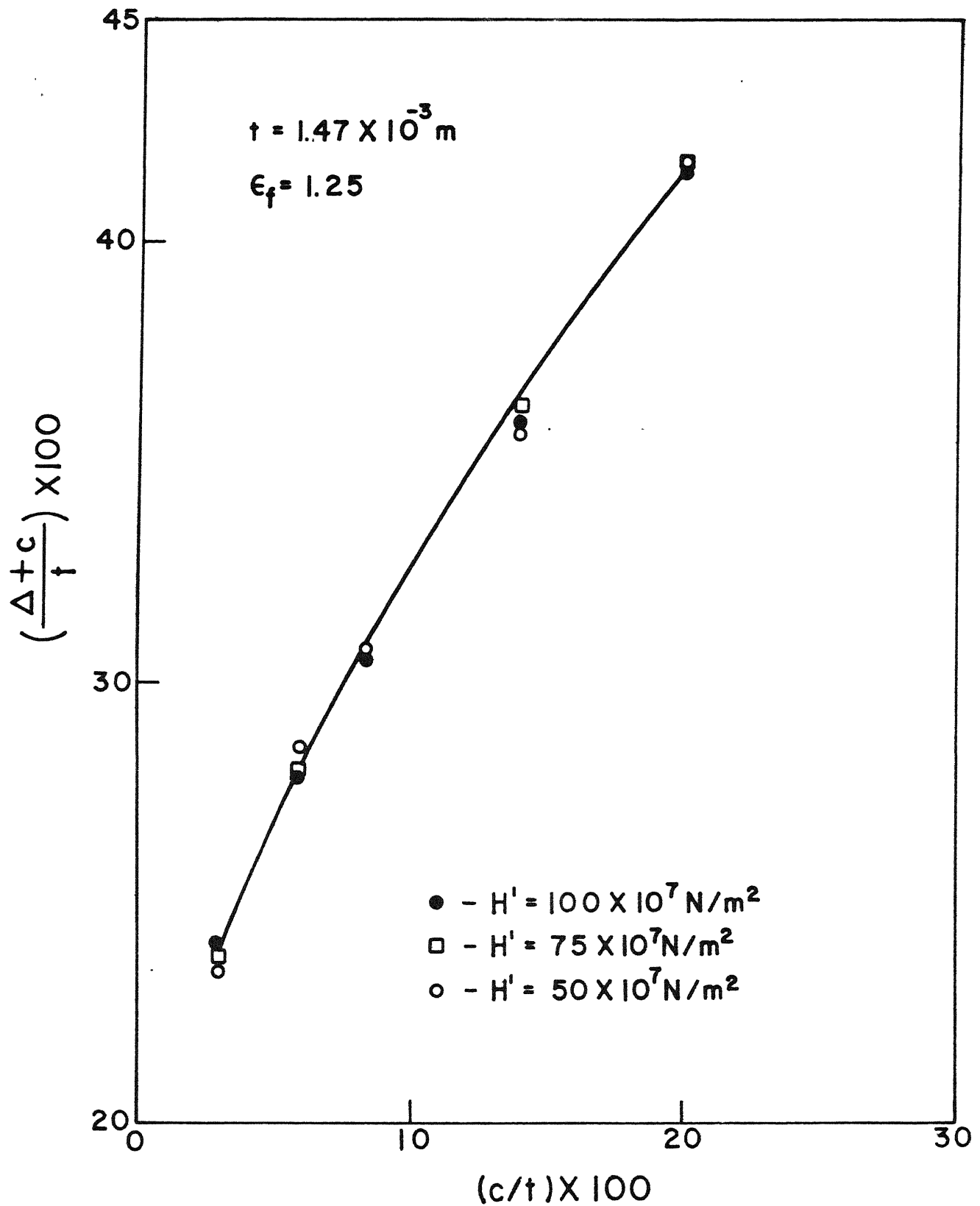
$\epsilon_f = 1.25$

$H' = 25 \times 10^7 N/m^2$

$(c/t) \times 100 = 3$

F.E. Solution

Theoretical [23]

Experimental [25]
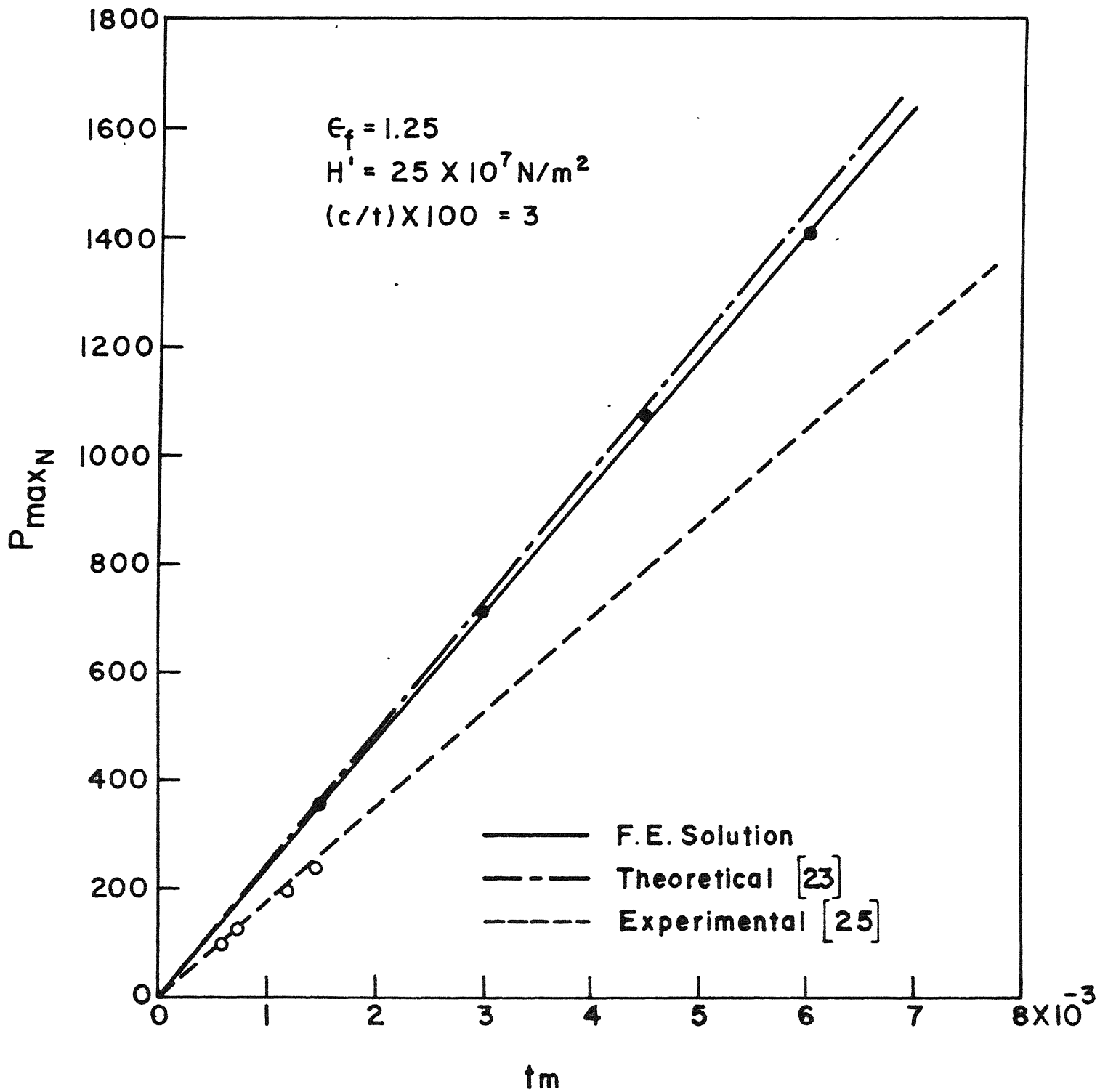
Fig. 4.11   Variation of maximum punch force with sheet thickness.
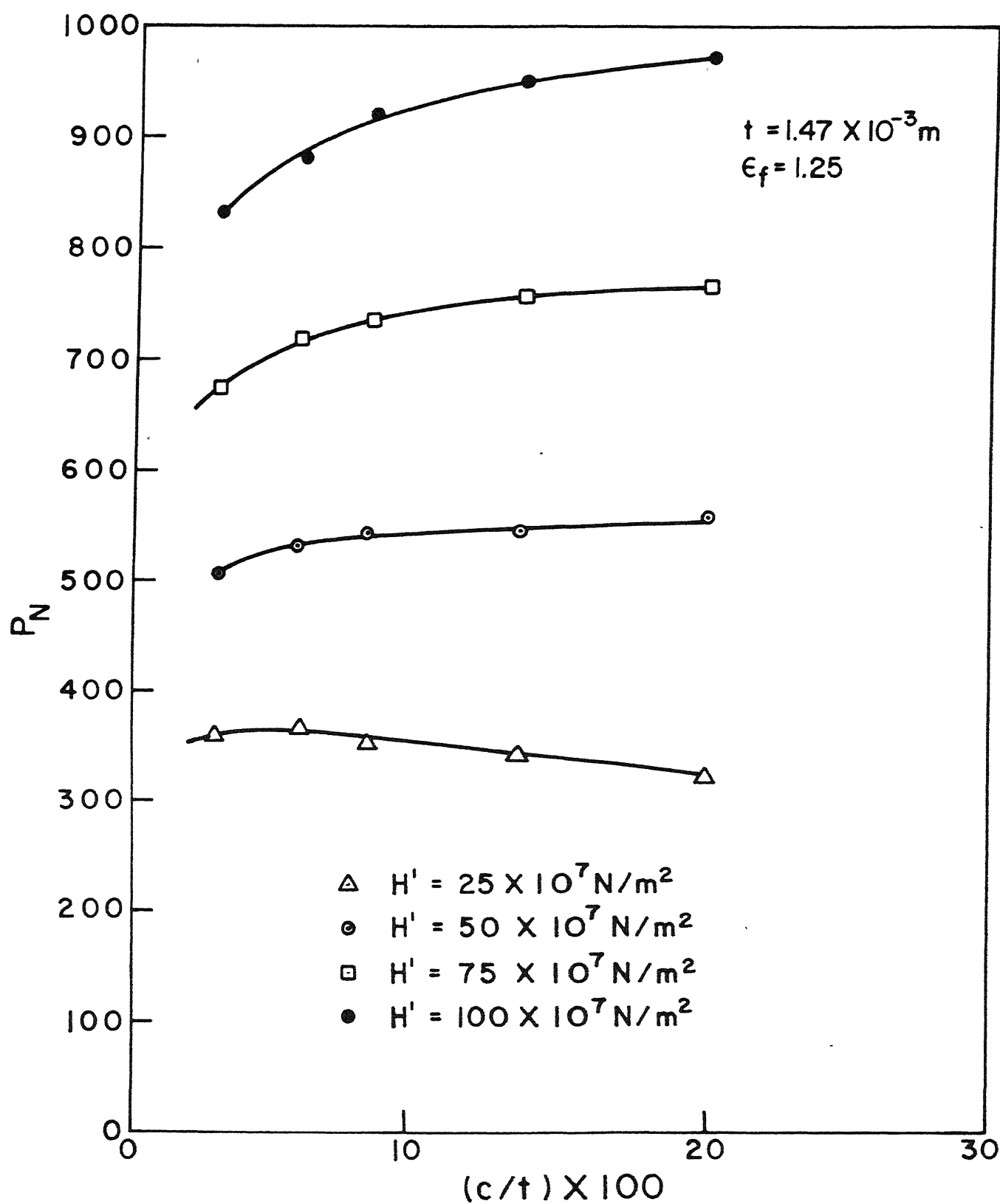
Fig. 4.12 Variation of maximum punch force with percentage
clearance.
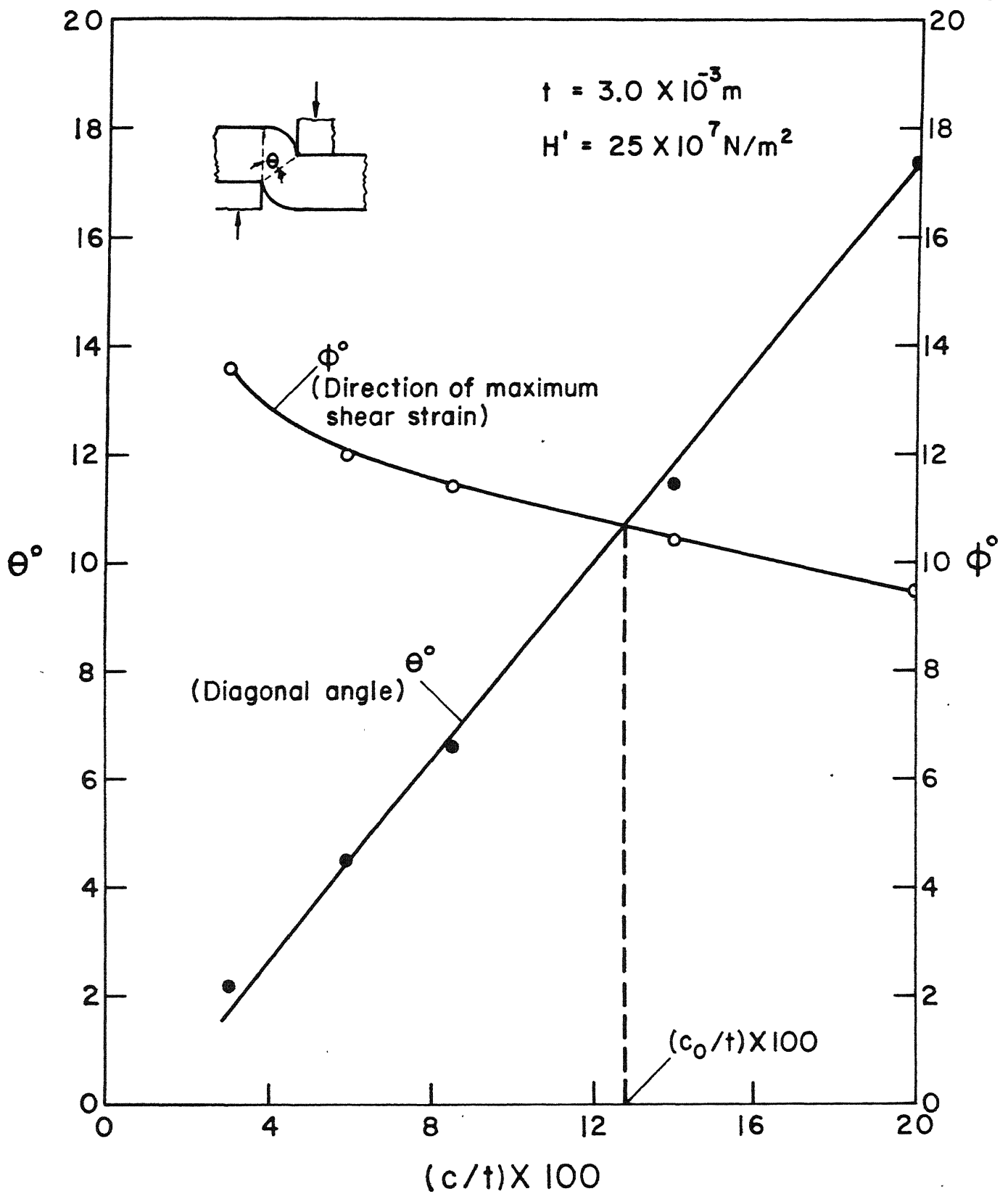
Fig. 4.13   Variation of diagonal angle and direction
of maximum shear strain with percentage
clearance for $\epsilon_f = 1.1$
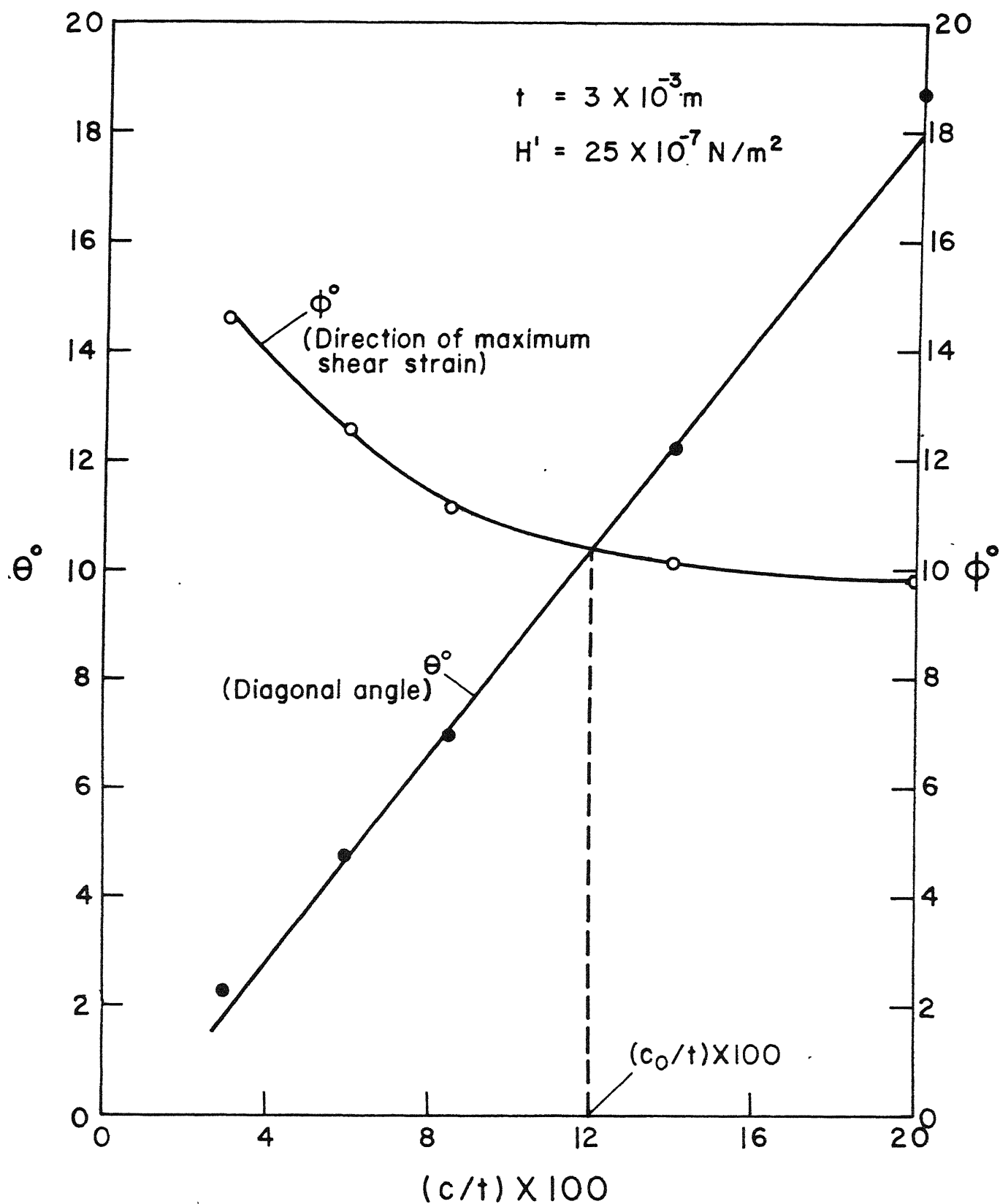
Fig. 4.14   Variation of diagonal angle and direction
of maximum shear strain with percentage
clearance for $\epsilon_f = 1.25$
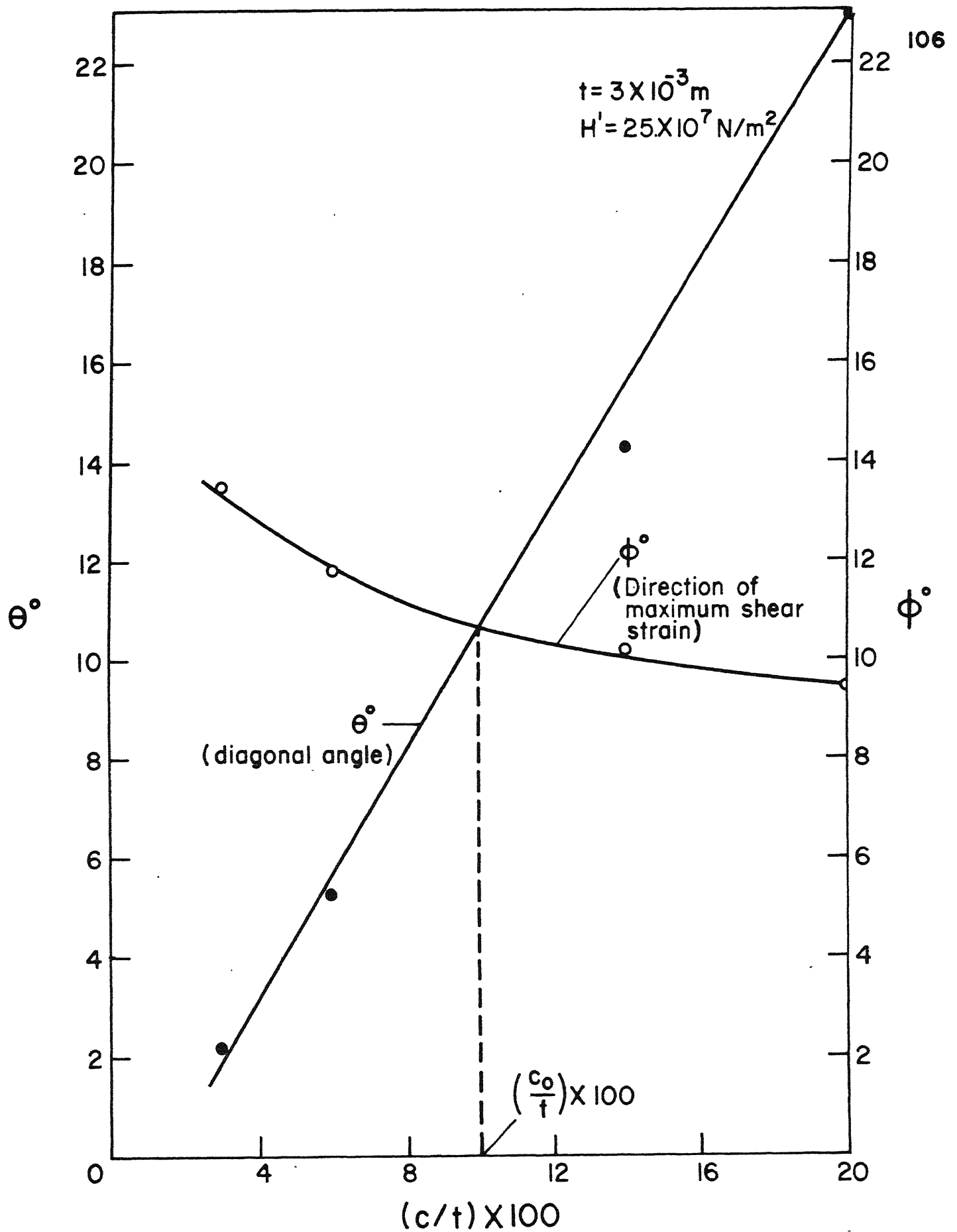
Fig. 4.15 Variation of diagonal angle and direction of maximum shear strain with percentage clearence for $\epsilon_f = 1.59$
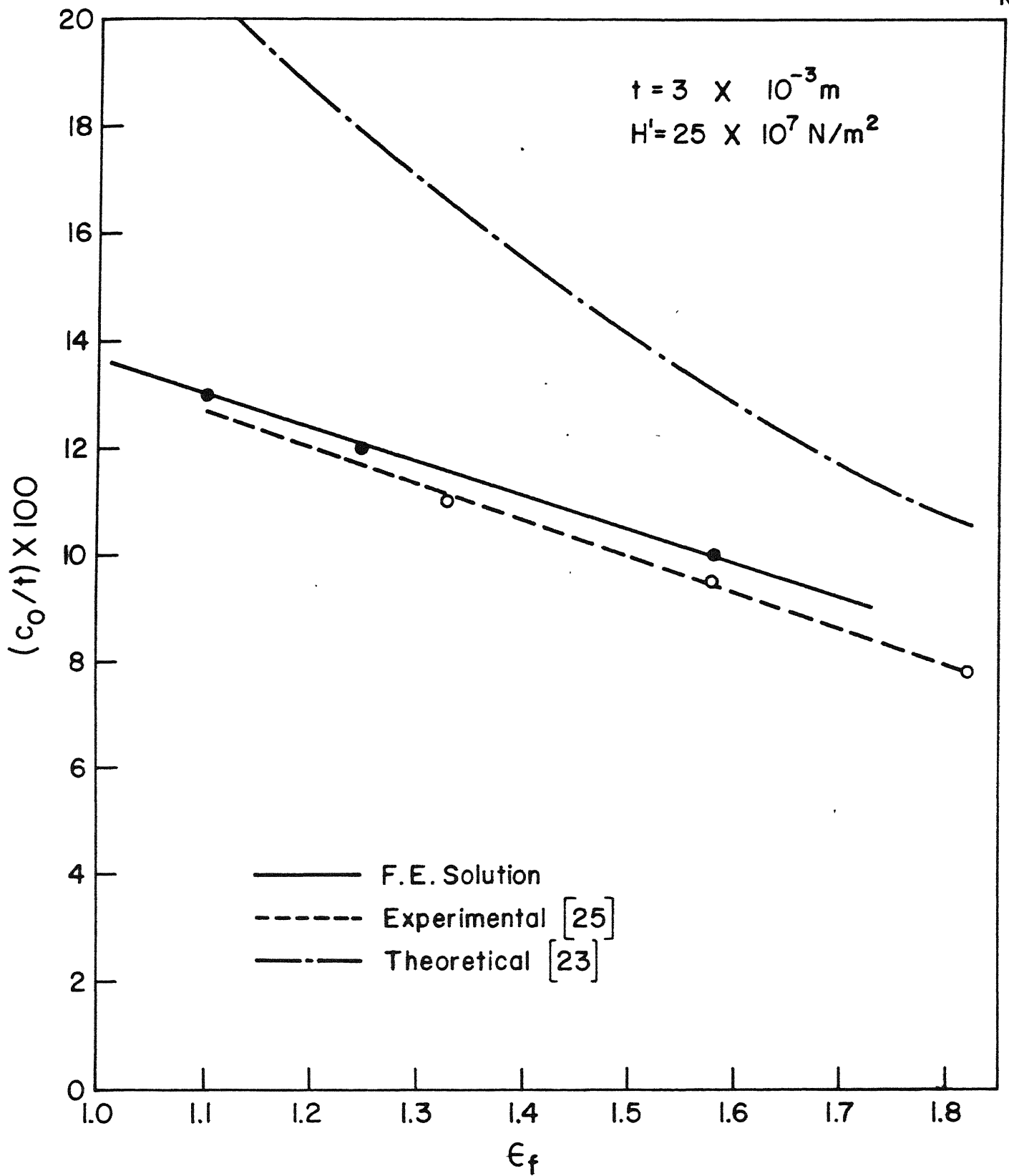
Fig.4.16   Variation of optimum clearance with local
fracture strain
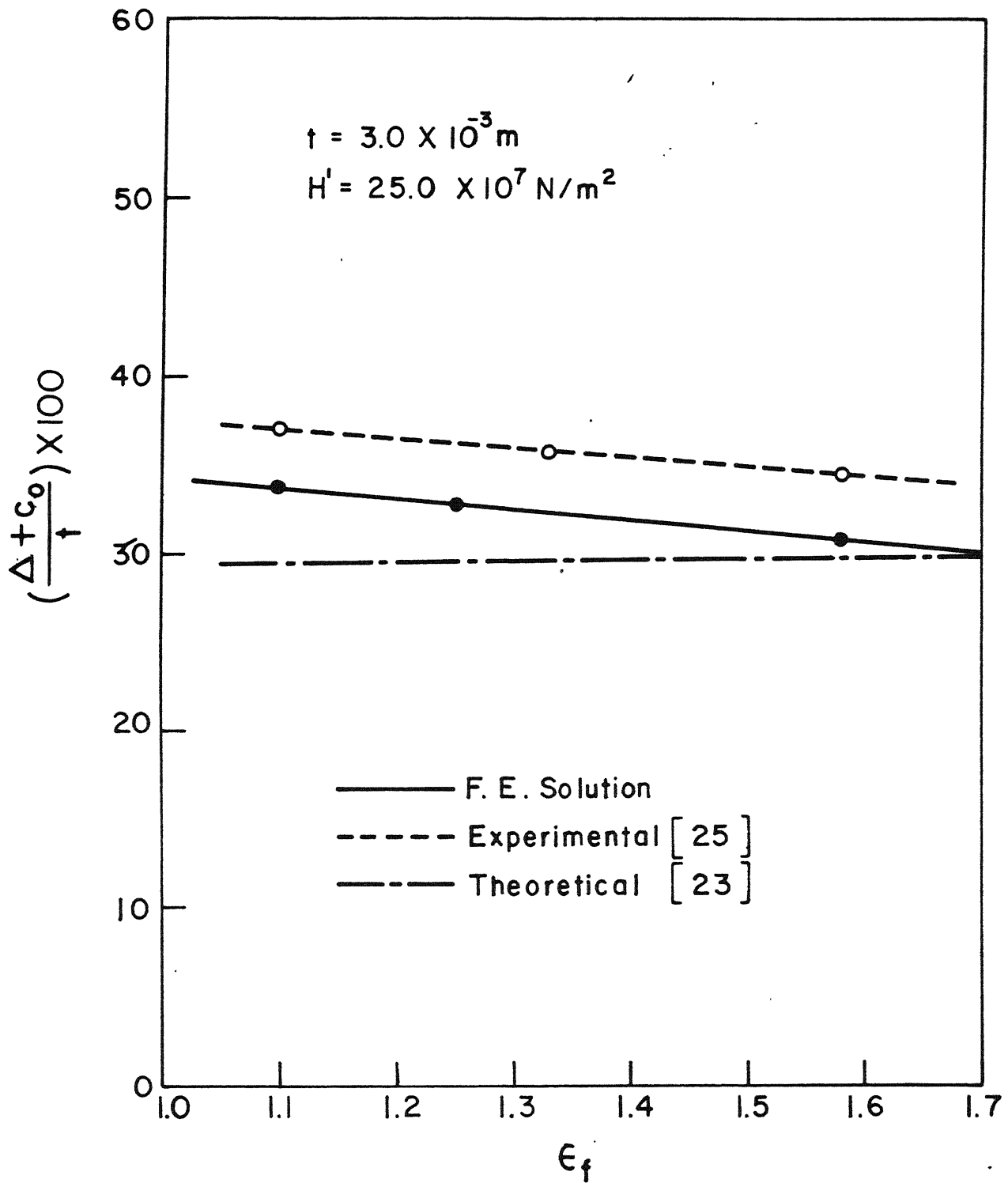
Fig. 4.17 Variation of optimum punch penetration with local fracture strain.

$t = 0.003m$, $H' = 25 \times 10^7 N/m^2$, $\varepsilon_f = 1.25$
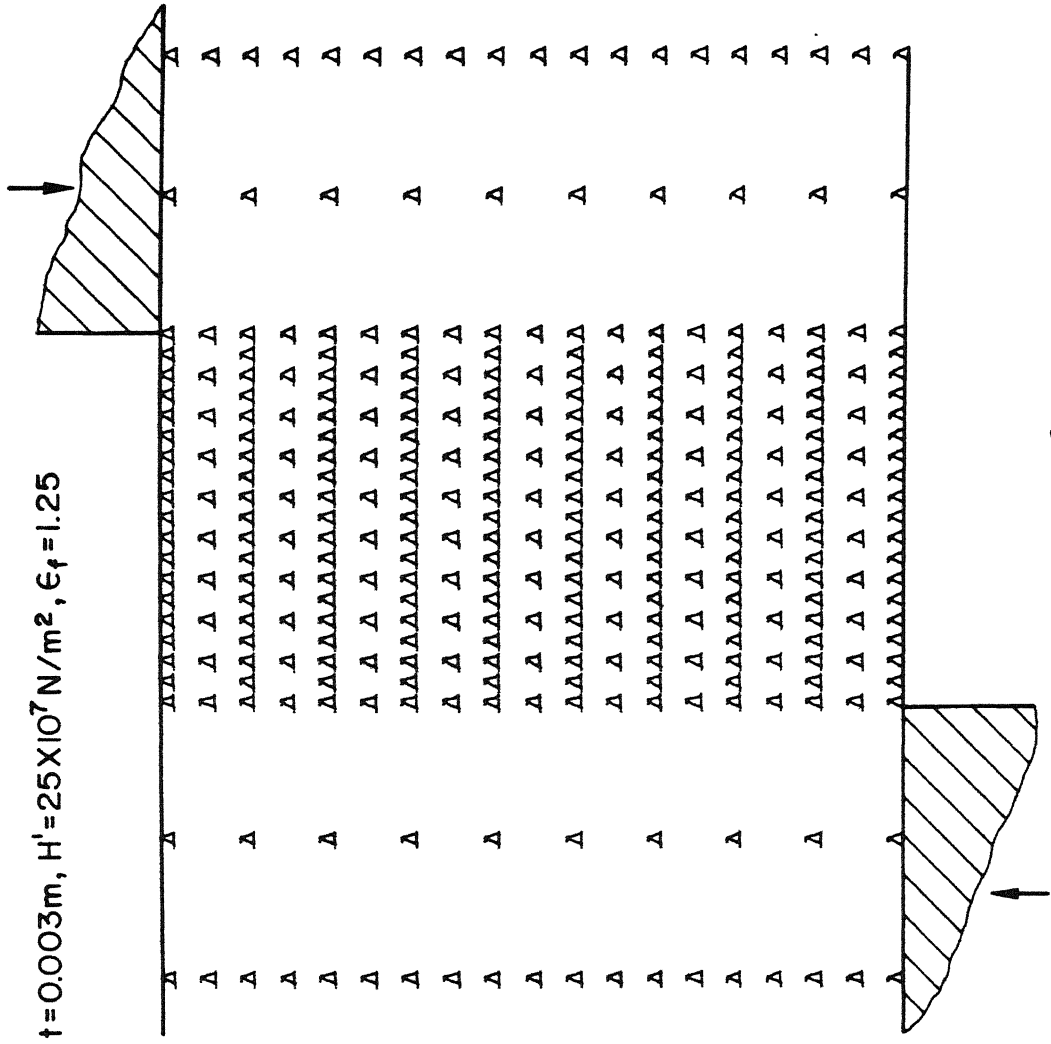
Fig.4.18 Deformation pattern at $\left(\dfrac{\delta}{t}\right) \times 100 = 0.273$ for $c/t = 0.20$

$t = 0.003m, H' = 25 \times 10^7 N/m, \epsilon_f = 1.25$
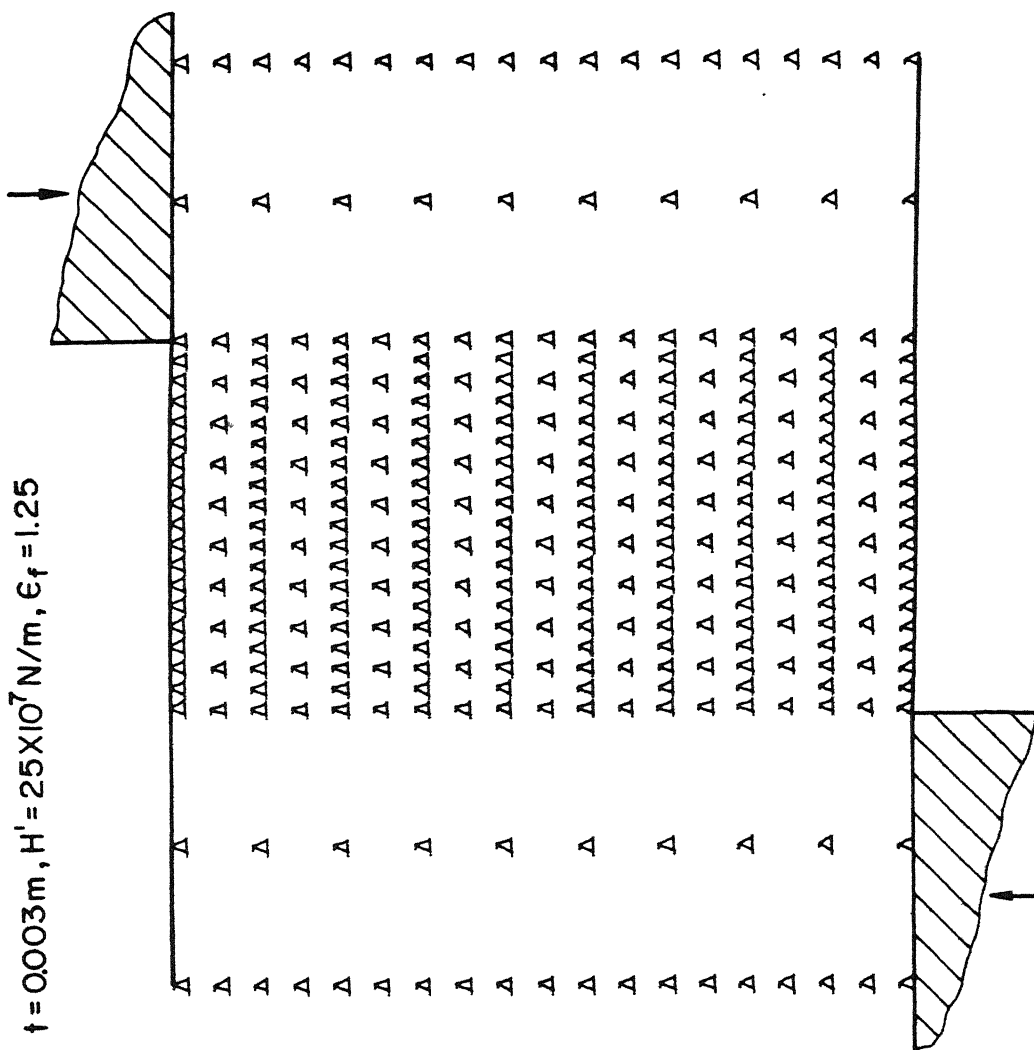
Fig.4.19 Deformation pattern at $(\frac{\delta}{t}) \times 100 = 0.847$ for $c/t = 0.20$

$t=0.003m, H'=25 \times 10^7 N/m^2, \epsilon_f = 1.25$
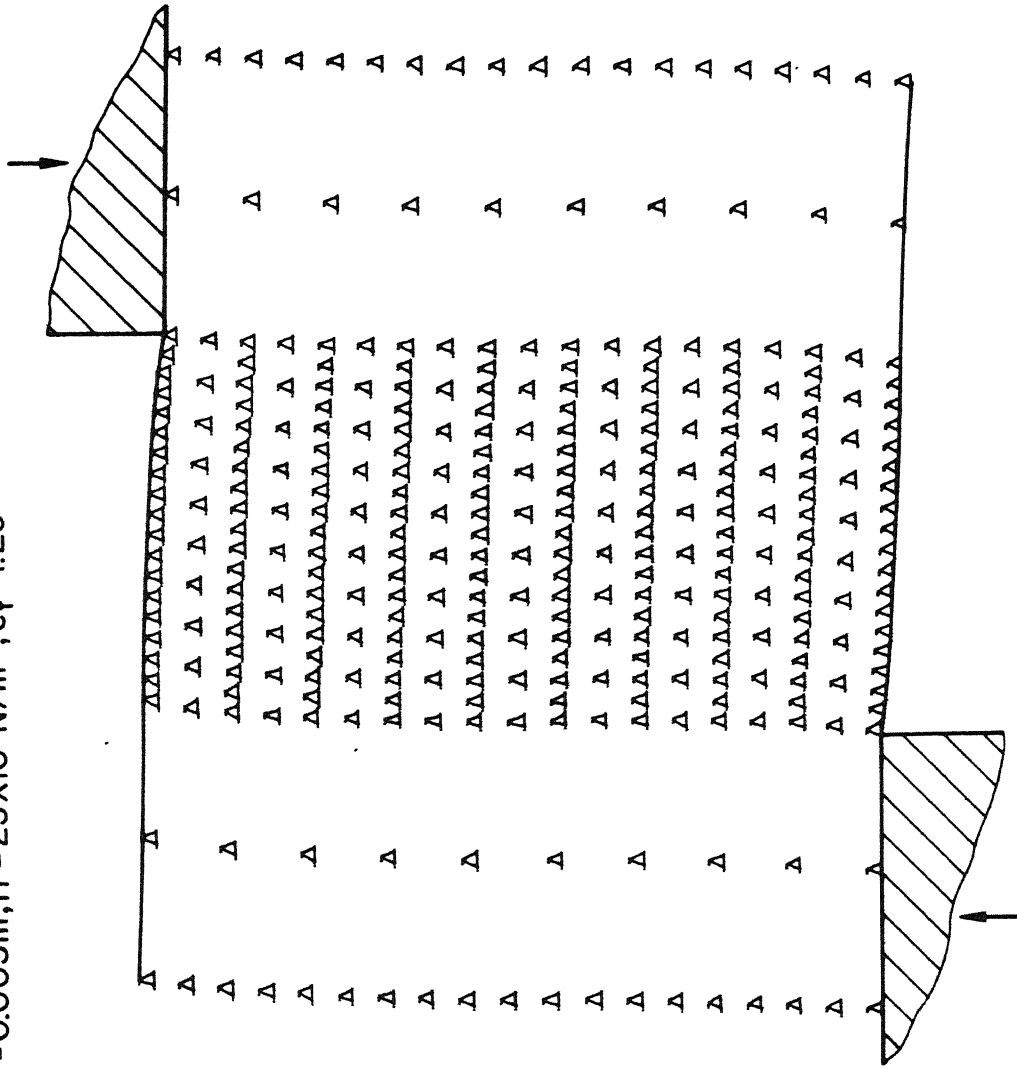
Fig. 4.20 Deformation pattern at $\left(\dfrac{\delta}{t}\right) \times 100 = 4.26$ for $c/t = 0.20$

$t = 0.003 m, H' = 25 \times 10^7 \text{ N/m}^2, \epsilon_f = 1.25$
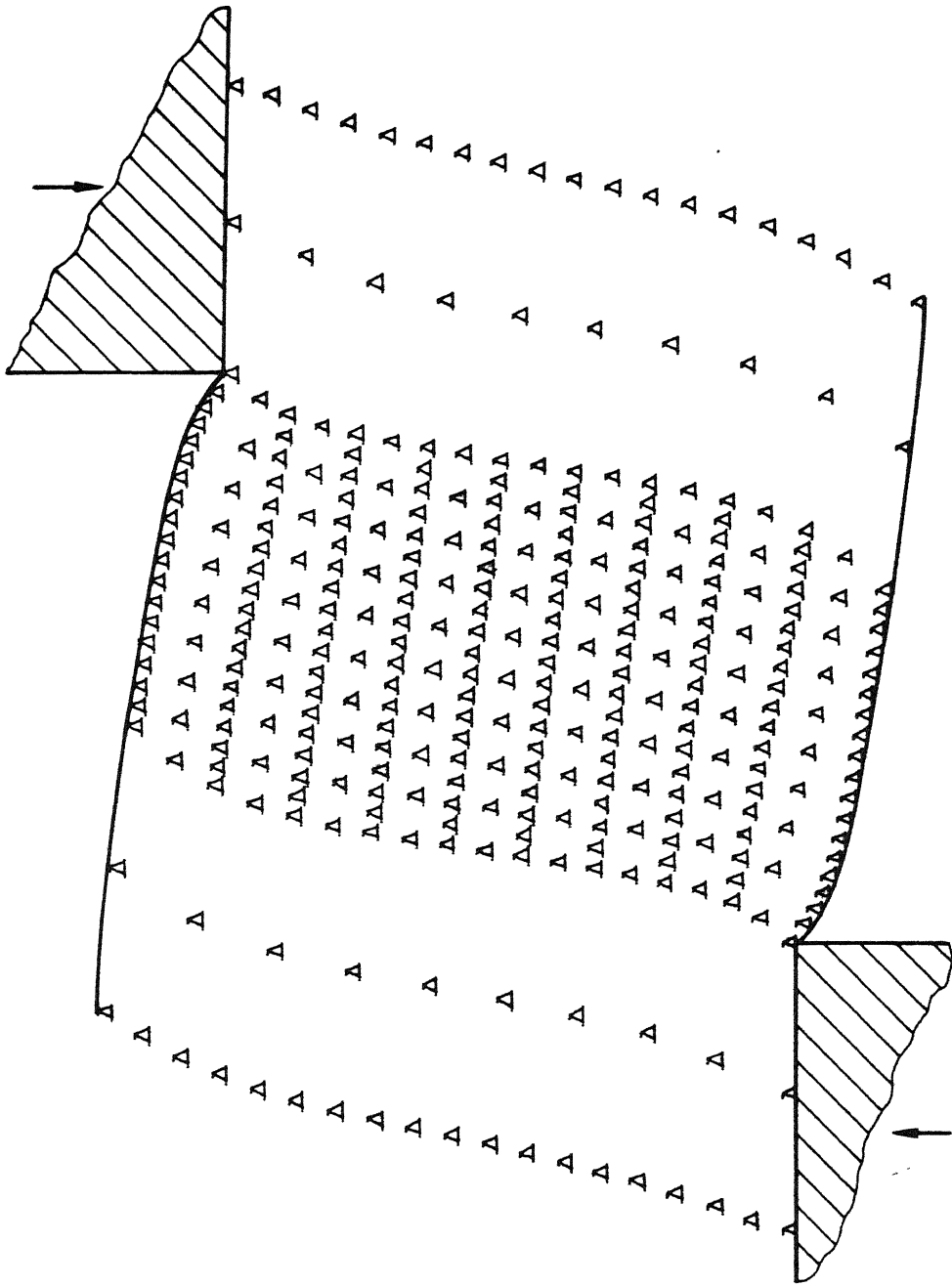
Fig.4.21 Deformation pattern at $\left(\dfrac{\delta}{t}\right) \times 100 = 21.33$ for c/t = 0.20

$t = 0.003m, H' = 25 \times 10^7 N/m^2, \epsilon_f = 1.25$

Note : All calculation are done with respect to original configuration.
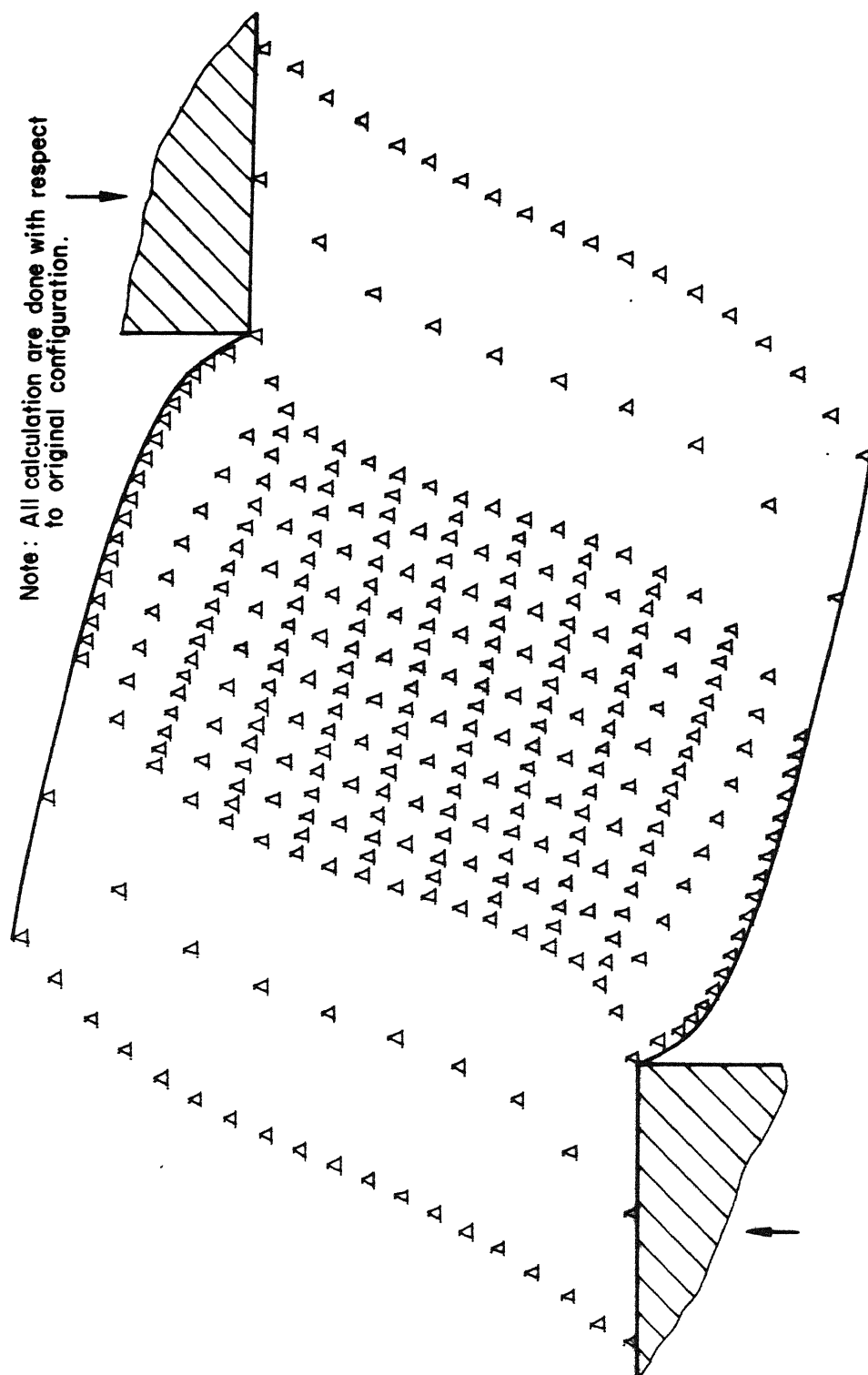
Fig.4.22 Deformation pattern at crack initiation for c/t=0.20

$t=0.003m, H'=25 \times 10^7 N/m^2, \epsilon_f=1.25$
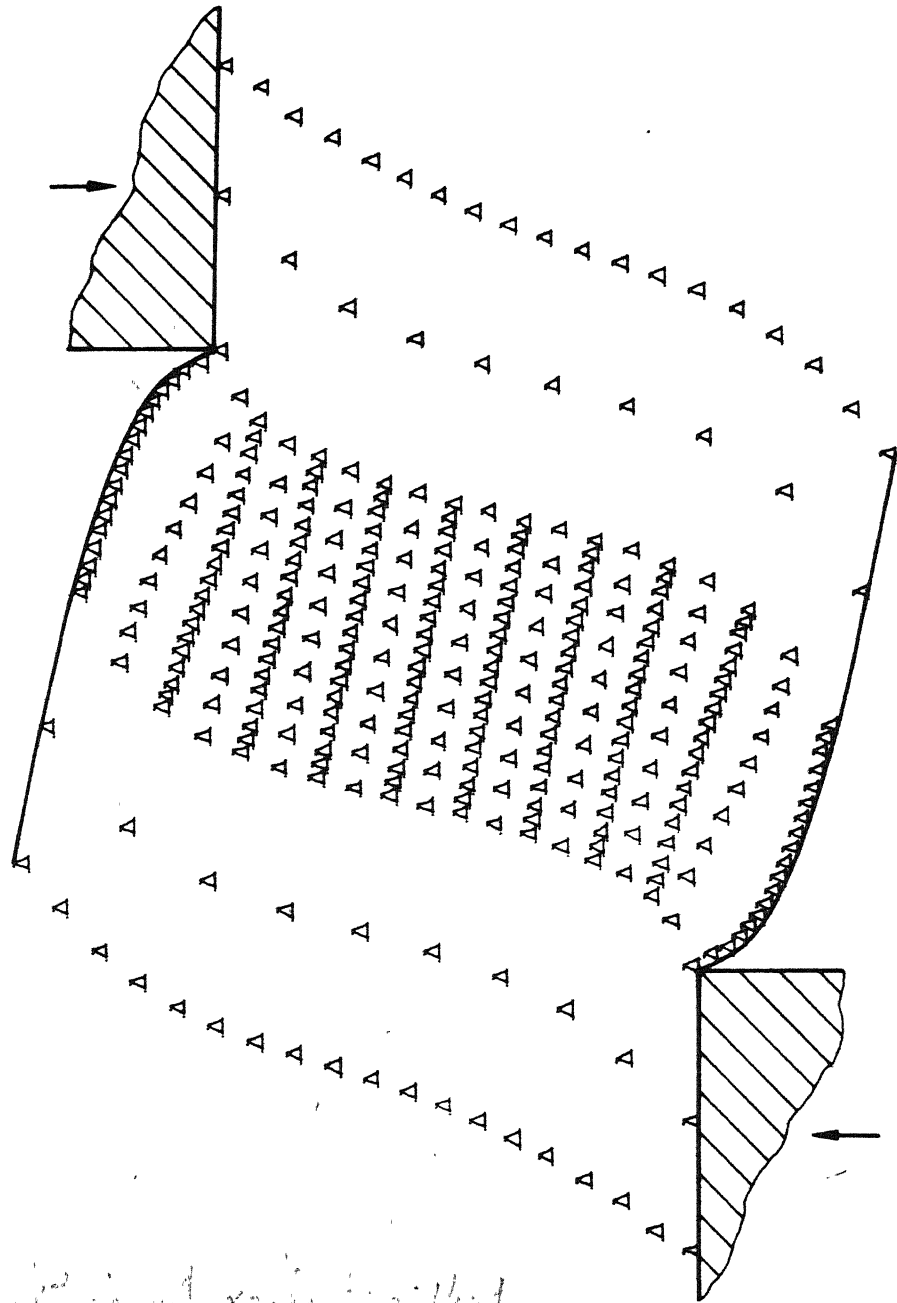
Fig.4.23 Deformation pattern at crack initiation for c/t=0.14

$t = 0.003m, H' = 25 \times 10^7 \text{ N/m}^2, \epsilon_f = 1.25$

Fig.4.24 Deformation pattern at crack initiation for c/t = 0.06

$t = 0.003m, H' = 25 \times 10^7 N/m^2, \epsilon_f = 1.25$
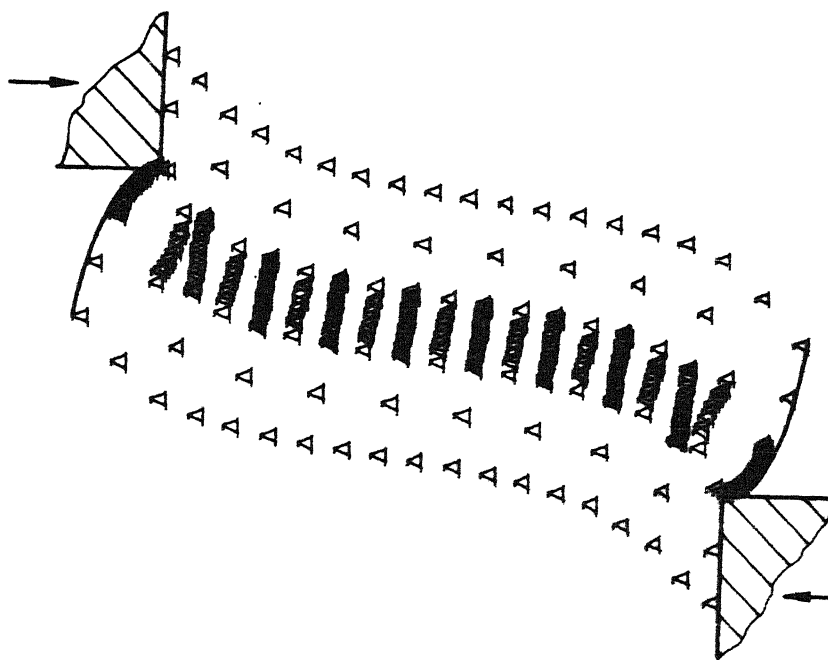
Fig.4.25 Deformation pattern at crack initiation for $c/t = 0.03$

Fig.4.23 Deformation pattern at crack initiation for c/t = 0.14

$t = 0.003m, H' = 25 \times 10^7 N/m^2, \varepsilon_f = 1.25$

Formation of shear drop is explained by this analysis. However, no explanation can not be made on the formation of burnished surface. (bright surface).
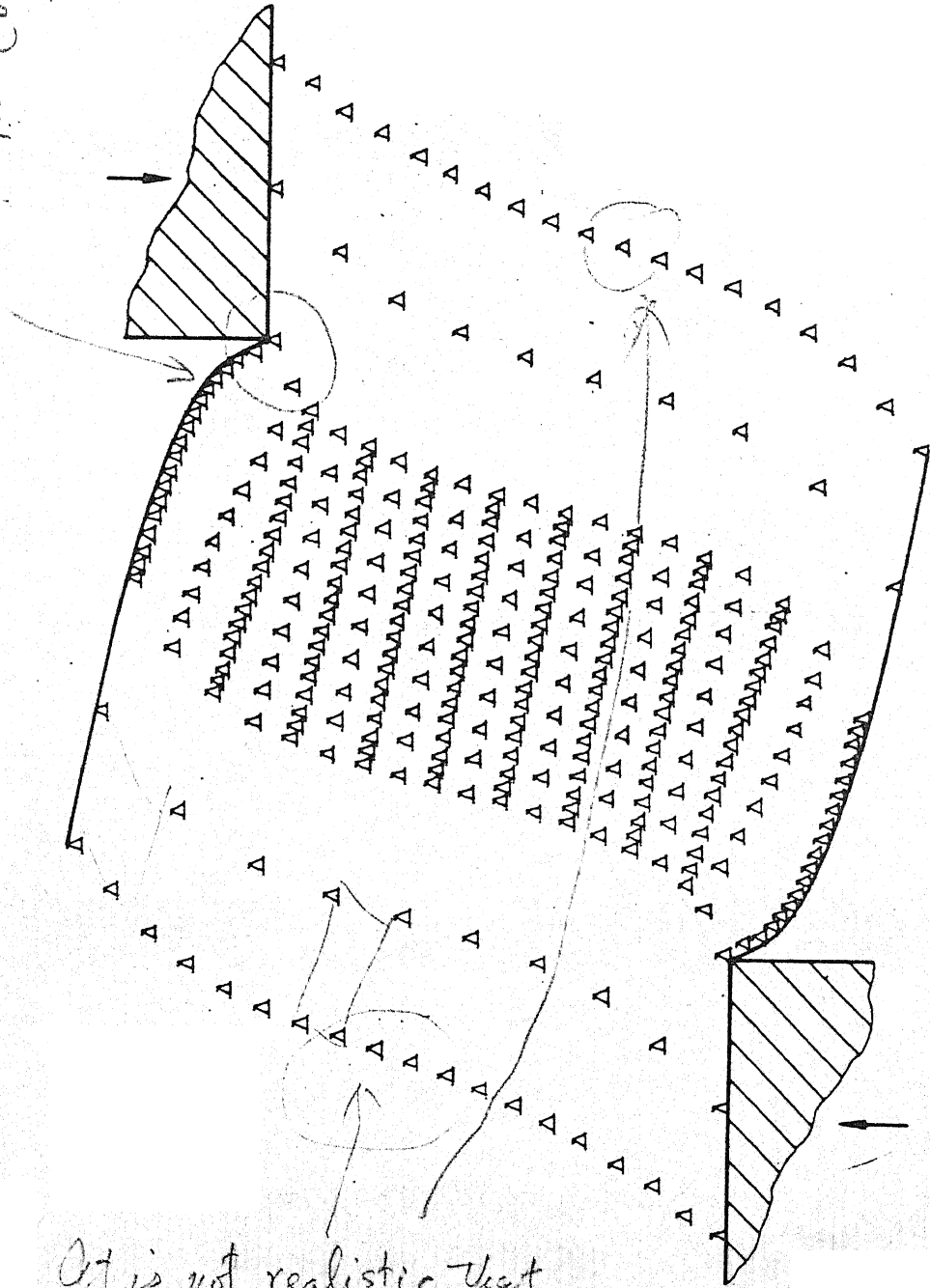
It is not realistic that shear deformation occurs here. Only rigid rotation should take place here.

ALL　　VALUES　　ARE　　NEGATIVE

1 Per.Pun.Pen.=0.0273
-:0.0000RR,=:0.00015
.:0.00022,*:0.00029
+:0.00035,.:0.00042
$:0.00049,#:0.00055
X:0.00062,I:0.00069

4 Per.Pun.Pen.=4.26
+:0.014,-:0.028
*:0.041, :0.055
=:0.068,.:0.082
$:0.095,#:0.11
I:0.12,X:0.14

2 Per.Pun.Pen.=0.164
=:0.0010, :0.0020,*:0.0030
=:0.0040,+:0.0049,.:0.0059
$:0.0069,=:0.0079,I:0.0088
X:0.0098

5 Per.Pun.Pen.=21.83
+:0.069,-:0.13,*:0.18
:0.24,=:0.29,.:0.35
$:0.41,#:0.46,I:0.52
X:0.58

3 Per.Pun.Pen.=0.847
-:0.0039,=:0.0076, :0.011
*:0.015,+:0.019,.:0.022
$:0.026,#:0.030,I:0.033
X:0.037

6 Per.Pun.Pen.=41.33
+:0.13,-:0.24,*:0.34
:0.45,=:0.56,.:0.65
$:0.77,#:0.87,I:0.98
X:1.1

FIG.4.27 DISTRIBUTION OF MINIMUM PRINCIPAL STRAINS IN
CLEARANCE GAP NEAR DIE CORNER FOR t=0.003m AND c/t=0.20

1 Per. Pun. Pen.=0.0273
=:0.00003,*:0.000088
:0.00015,-:0.00021
+:0.00026,:0.00032
#:0.00038,&:0.00044
X:0.0005,I:0.00056

4 Per. Pun. Pen.=4.26
-:0.00081,*:0.016
:0.032,=:0.047
&:0.065,:0.078
&:0.094,#:0.11
I:0.12,X:0.14

2 Per. Pun. Pen.=0.164
:0.00011,*:0.0012,=:0.0023
-:0.0033,+:0.0044,:0.0055
#:0.0066,&:0.0076,X:0.0087
I:0.0098

5 Per. Pun. Pen.=21.33
-:0.015,*:0.079,:0.14
=:0.21,+:0.27,:0.34
&:0.40,&:0.47,I:0.53
X:0.60

3 Per. Pun. Pen.=0.847
=:0.00026, :0.0044,*:0.0086
=:0.013,+:0.017,.:0.021
&:0.025,#:0.030,I:0.034
X:0.038

6 Per. Pun. Pen.=41.33
-:0.028,=:0.15,:0.27
#:0.40,+:0.52,.:0.64
&:0.76,&:0.80,I:1.00
X:1.25

FIG.4.28 DISTRIBUTION OF EFFECTIVE STRAINS IN CLEARACE GAP NEAR
DIE CORNER FOR t=0.003m AND c/t=0.20

a.

t=0.003m c/t=0.03

:0.14,*:0.24,=:0.33,-:0.43
+:0.52,.:0.61,#:0.71,&:0.80
I:0.90,X:0.99

c.

t=0.003m c/t=0.14

=:0.043,*:0.15, :0.25,-:0.35
+:0.46,.:0.56,&:0.67,&:0.77
I:0.87,X:0.98

b.

t=0.003m c/t=0.06

:0.16,*:0.25,=:0.34,-:0.44
+:0.53,.:0.63,&:0.72,&:0.81
I:0.91,X:1.0

d.

t=0.003m c/t=0.20

-:0.024,=:0.13, :0.24,*:0.34
+:0.45,.:0.55,&:0.65,&:0.77
I:0.87,X:0.98

FIG.4.29 DISTRIBUTION OF MAXIMUM PRINCIPAL STRAINS (AT CRACK
INITIATION)IN CLEARANCE GAP NEAR DIE CORNER
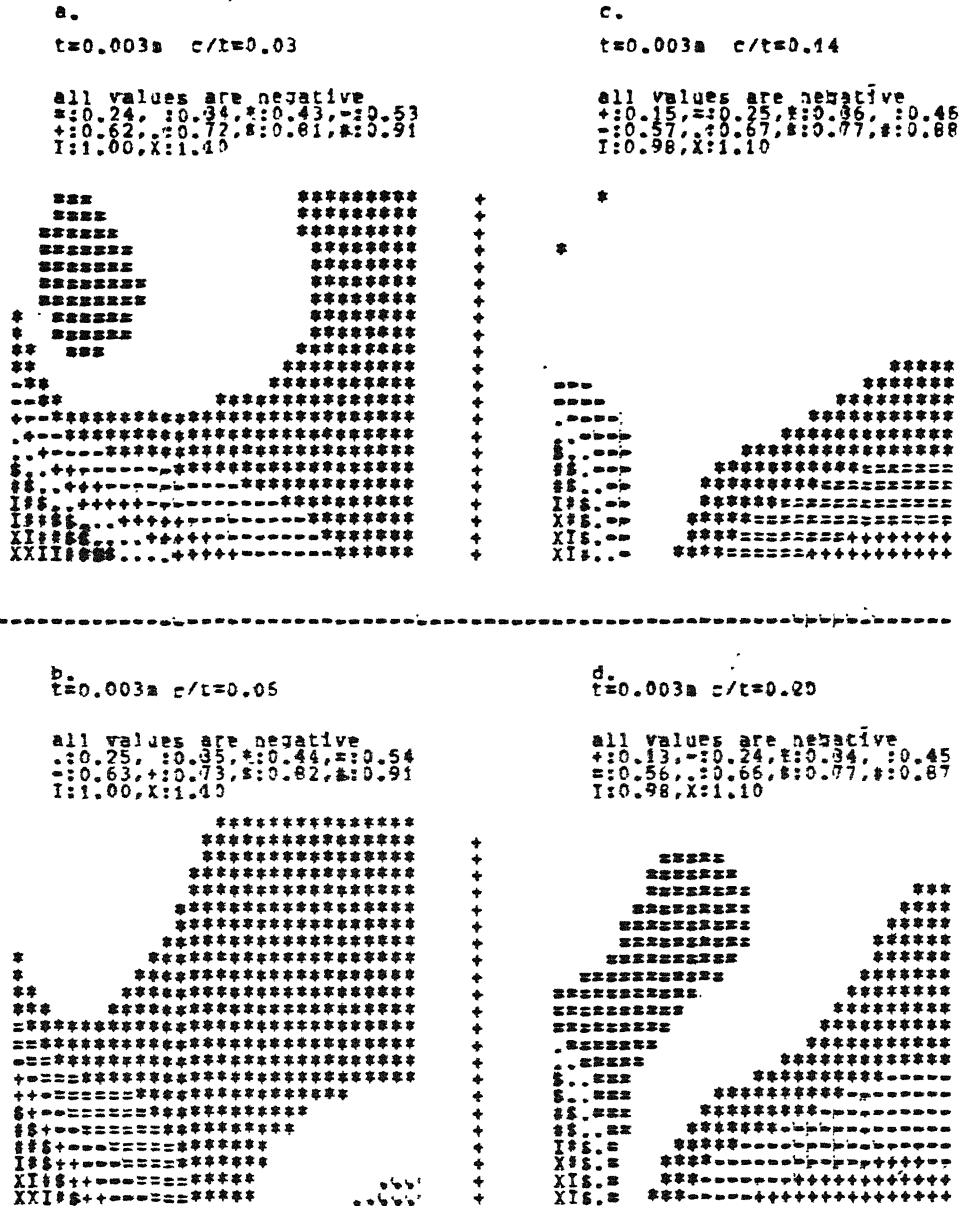
FIG.4.30 DISTRIBUTION OF MINIMUM PRINCIPAL STRAINS (AT CRACK INITIATION) IN CLEARANCE GAP NEAR DIE CORNER

a.

t=0.003 m ,c/t=0.03

:0.17,*:0.28,=:0.38,-:0.49
+:0.60,.:0.71,$:0.82,#:0.93
I:1.0,X:1.25

c.

t=0.003m ,c/t=0.14

=:0.05,*:0.17,.:0.29,-:0.41
+:0.53,.:0.65,&:0.77,#:0.89
I:1.0,X:1.25

b.

t=0.003m c/t=0.06

:0.18,*:0.29,=:0.40,-:0.51
+:0.62,.:0.73,&:0.83,#:0.94
I:1.1,X:1.25

d.

t=0.003m c/t=0.20

-:0.028,=:0.15,.:0.27,*:0.40
+:0.52,.:0.64,$:0.76,#:0.89
I:1.0,X:1.25
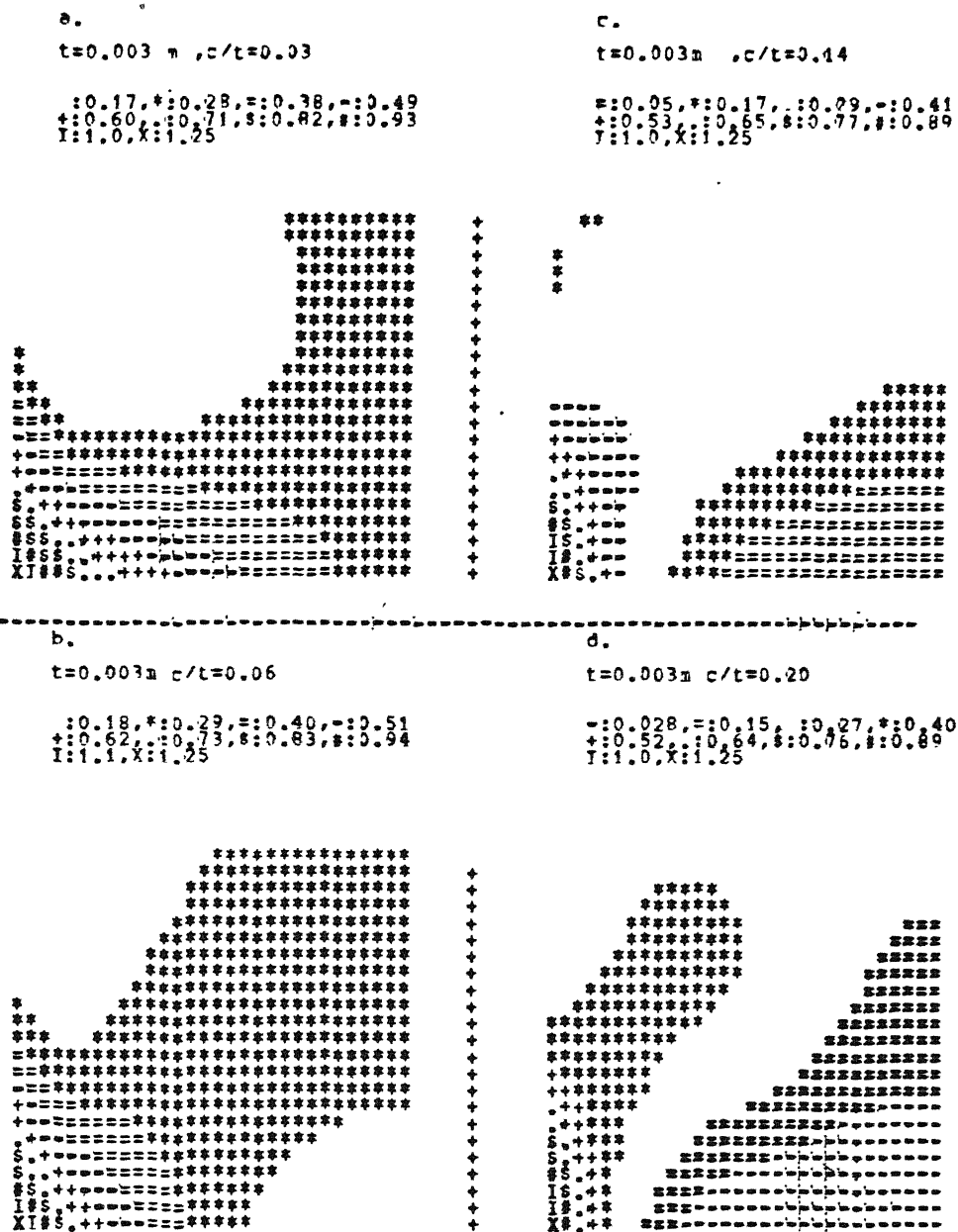
FIG.4.31 DISTRIBUTION OF EFFECTIVE STRAINS(AT CRACK
INITIATION) IN CLEARANCE GAP NEAR DIE CORNER

$t = 3 \times 10^{-3} m$

$H' = 25 \times 10^7 N/m^2$

$(c/t) \times 100 = 20$

The scales for x-axis and y-axis are different.
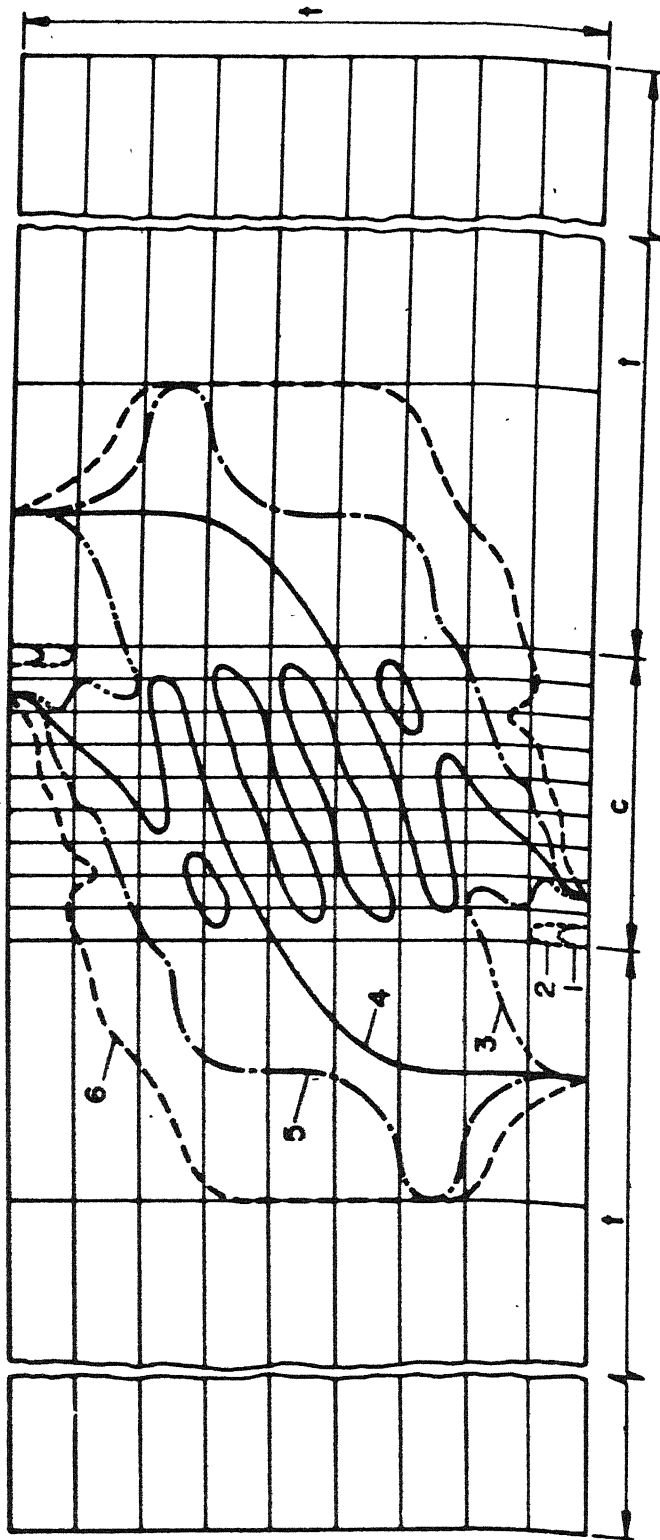
1. $\left(\frac{\Delta + c}{t}\right) \times 100 = 0.0273$ 4. $\left(\frac{\Delta + c}{t}\right) \times 100 = 0.109$

2. $\left(\frac{\Delta + c}{t}\right) \times 100 = 0.0546$ 5. $\left(\frac{\Delta + c}{t}\right) \times 100 = 0.137$

3. $\left(\frac{\Delta + c}{t}\right) \times 100 = 0.082$ 6. $\left(\frac{\Delta + c}{t}\right) \times 100 = 0.164$

Fig. 4.32 Spread of plastic zone with punch penetration.

CHAPTER 5

CONCLUSIONS AND FUTURE WORK

5.1 INTRODUCTION

As mentioned earlier the main objective of this study was to evolve a finite element model for analysing the deformation process during blanking. This model helped in determining the inter-dependance of various process parameters, magnitude of blanking load, optimum punch-die clearance and percentage punch penetration at crack initiation. Besides this, the plots of the deformation pattern, strain distribution and the growth of the plastic region helped in understanding the process in detail.

5.2 CONCLUSIONS

On the basis of the foregoing analyses and discussions the following important conclusions can be drawn :

(i) The developed elasto-plastic finite element model yields acceptable results upto crack initiation.

(ii) By studying the growth of the plastic region with progress of the punch it can be concluded that the material within the clearance gap becomes plastic with a very small punch penetration (compared to the punch penetration required at crack initiation).

(iii) Theoretically obtained punch load agrees well with the results when applied to specific cases studied earlier.

(iv) The maximum punch force required increases with the increase in sheet thickness and work hardening parameter but is independent of the clearance within the range of clearances used.

(v) The percentage punch penetration at crack initiation increases with increase in punch-die clearance and ductility of the material, but the variation of sheet thickness and work hardening parameter has very little effect on it.

(vi) The percentage punch penetration at crack initiation for optimum punch-die clearance does not depend much on the parameters like sheet thickness, work hardening parameter and ductility, and it remains around 30% of the sheet thickness.

(vii) The optimum punch-die clearance depends on the local fracture strain of the material.

(viii) The results yielded by the present model are closer to the experimental results (obtained in previous researches) in comparison to the results from the previous theoretical work.

(ix)   The mode of the metal deformation and variation of strains within the sheet thickness, as seen from the distribution patterns, are found to be most severe at the punch and the die corners, facilitating the initiation of cracks at these two points.

(x)   The hypotheses regarding crack initiation and crack propagation direction, proposed in the work, yield consistantly acceptable results. So these hypotheses may be considered acceptable.

5.3   PRACTICAL UTILITY OF THE MODEL

Besides helping in understanding the deformation process this model has the following practical utility :

(i)   Theoretical analysis, using this model, can give punch load and stress distribution in the sheet metal, which can be used for selecting proper die and punch material.

(ii)   Prediction of proper amount of punch-die clearance (an important parameter of die design) is possible using this analysis, if the sheet thickness and its material properties are specified. Otherwise to obtain an optimum punch-die clearance a good number of actual experiments are required to be performed and their results required to be analysed in detail.

5.4 RECOMMENDATIONS FOR FUTURE WORK

The work, presented in the thesis has been conducted
using a number of simplifying assumptions but for the future
work it is recommended to perform similar type of analysis,
taking into account the actual operating conditions during
the process, as mentioned below. A closed contour blanking
process should be analysed with the present technique using
three dimensional analysis, and the effects of the friction,
tool shear, dullness of cutting edge, clamping forces etc. should
be considered. Anisotropy introduced in the sheet material
during the process, the speed of the blanking and the strain
rate effects should also be included in the finite element
model so as to obtain the more accurate analysis of the
actual operation. By using a suitable element and a very
fine mesh, attempt should be made to get the complete crack
path, i.e., till the blank is separated from the sheet.

REFERENCES

1. Eary, D.F., and Reed, E.A., Techniques of Press Working Sheet Metal, Prentice-Hall Inc., New Jersey, 1974.

2. Crane, E.V., Plastic Working in Presses, John Wiley and Sons, Inc., London, 1957.

3. Ghosh, A., and Mallik, A.K., Manufacturing Science, Affiliated East-West Press Pvt.Ltd., New Delhi - Madras, 1985.

4. Anthony, G.C., 'Pressure Recording Indicator for Punching Machinery', Transactions A.S.M.E., vol. 33, 1911, pp 369-380.

5. Chang, T.M., and Swift, H.W., 'Shearing of Metal Bars', Journal of Institute of Metals, vol. 78, 1950-51, pp 119-146.

6. Chang, T.M., 'Shearing of Metal Blanks', Journal of Institute of Metals, vol. 78, 1950-51, pp 393-414.

7. Biegel, J.E., 'Punch-Die Clearances', Tool and Manufacturing Engineer, vol. 49, no.1, July 1962, pp 89-92.

8. Biegel, J.E., 'The Forces and Work in Metal Stamping as a Function of Clearance', ASTME Creative Manufacturing Seminars, 1961-62, SP62-49, pp 1-13.

9. Hugo, H.H., 'Good Stamping Start with the Dies', Iron Age, May 22, 1969, pp 72-74.

10. Keeler, S.P., 'Circular Grid Warn of Stamping Trouble', The Tool and Manufacturing Engineer, April 1969, pp 18-21.

11. Keeler, S.P., 'Circular Grids Help Solve Stamping Problems', The Tool and Manufacturing Engineer, May 1969, pp 14-17.

12. Santos, W., and Organ, A.J., 'Deformation in the Ductile Fracture Processes Examined by the Visioplasticity Method', International Journal of Machine Tool Design and Research, vol. 13, 1973, pp 217-232.

13.   Kasuga, Y., Tsutsumi, S.,and Mori, T., 'On the Shearing Process of Ductile Sheet-Metals', Bulletin of the JSME, vol. 21, No.154, April 1978, pp 753-760.

14.   Kasuga, Y., Tsutsumi, S., and Mori, T., 'Investigation into the Shearing Process of Ductile Sheet Metals', Memoirs of Faculty of Engineering, Nagoya Univ., Japan, vol. 31, No.1, May 1979, pp 1-46.

15.   Johnson, W., and Slater, R.A.C., 'A Survey of the Slow and Fast Blanking of Metals at Ambient and High Temperatures', Proceedings of the International Conference on Manufacturing Technology, ASTME, 1967, pp 825-851.

16.   Tatsuo, O., and Terunao, Y., 'Effect of Profile in Basal Section in Shearing Process', Memoirs of Faculty of Engineering, Kyusu Univ., V38, n3, Sept. 1978, pp 249-273.

17.   Tatsuo, O., and Susumu, Y., 'Effect of the Geometry of Cutting Edge of Tool in Blanking and Piercing', Memoirs of Faculty of Engineering, Kyusu Univ., V38, n4, Dec. 1978, pp 371-395.

18.   Jimma, T., 'The Theoretical Research on the Blanking of a Sheet Material', Bulletin of the JSME, vol. 6, n23, 1963, pp 568-576.

19.   Jimma, T., 'On the Mechanism of Crack Formation in the Shearing Test of Sheet Metal', The Ninth Japan Congress on Testing Materials-Metallic Materials, March 1966, pp 79-83.

20.   Masuda, M. and Jimma, T., 'Theoretical Research on the Blanking of Sheet Material', C.I.R.P., Annalen, BD.11, 1964, pp 224-228.

21.   Maeda, T., 'Theory of the Shearing Mechanism for Sheet Metals with Punch and Die', Journal of Japan Society of Precision Mechanics, vol. 25, No.6, 1959, p. 248 (In Japanese).

22. Ghosh, A. and Mallik, A.K., 'Mechanics of Stamping and Blanking Operation', Proceedings of the Ninth AIMTDR Conference, IIT Kanpur, Dec. 1980, pp 227-231.

23. Ghosh, A., Raghuram, V., and Popat, P.B., 'A New Approach to the Mechanics of the Blanking Operation: Theoretical Model and Experimental Verification', Journal of Mechanical Working Technology, No.11, 1985, pp 215-228.

24. Shaw, M.C., and Avery, J.P., 'Forming Limits', ASME, Centenial Conference, Aug. 1980.

25. Popat, P.B., 'Experimental Investigation of Blanking Operation', M.Tech. Thesis, Indian Institute of Technology, Kanpur, December 1981.

26. Cook, N.H., Gujral, D.M., and Tipnis, V.A., 'Higher Speed for Punch Presses', The Tool and Manufacturing Engineer, May 1962, pp 97-100.

27. Johnson, W., and Travis, F.W., 'High Speed Blanking of Steel', in Engineering Plasticity , Edited by Heyman J. and Leckie, F.A., Cambridge 1968, pp 385-400.

28. Daneshi, G.H., and Harding, J., 'The High Speed Punching of a Quenched and Tempered 1 1/2 percent CrMo Steel', Institute of Physics Conference, Ser.No. 21, pp 404-416.

29. Johnson, W., and Slater, R.A.C., 'The Effects of Temperature, Speed and Strain-Rate on the Force and Energy Required in Blanking', International Journal of Mechanical Science, vol.9, 1967, pp 271-305.

30. Travis, F.W., and Balendra, R., 'Static and Dynamic Blanking of Steels of Varying Hardness', International Journal of Machine Tool Design and Research, vol.10, 1970, pp 249-271.

31. Dowling, A.R., et al., 'The Dynamic Punching of Metals', Journal of Institute of Metals, vol. 98, 1970, pp 215-224.

32. Eary, D.F., 'Press and Die Alignment-key to Stamping Efficiency', Tool and Manufacturing Engineer, vol. 49, No.6, Dec. 1962, pp 109-112.

33. Lange, K., and Liebing, H., 'Blanking and Piercing without any Burr', Annals. CIRP, vol.27, No.1, 1978, pp 177-181 (In German).

34. Iwate, K., Osakada, K., and Fujino, S., 'Analysis of Hydrostatic Extrusion by the Finite Element Method', Journal of Engineering for Industry, Transactions of ASME, May 1972, pp 697-703.

35. Levy, S., Shih, C.F., Wilkinson, P.D., Stine, P., and McWilson, R.C., 'Analysis of Sheet Metal Forming to Axisymmetric Shapes', Special Technical Publication 647, ASTM, 1978, pp 238-260.

36. Sekhon, G.S., Shishodia, K.S., and Sharma, P.C., 'A Numerical Method for Analysis of Bounded Metal Working Processes', International Journal for Numerical Methods in Engineering, vol. 14, 1979, pp 1165-1182.

37. Oh, S.I., and Kobayashi,S.,'Finite Element Analysis of Plane-Strain Sheet Bending', International Journal of Mechanical Science, vol.22, 1980, pp 583-594.

38. Wifi, A.S., 'Finite Element Correction Matrices in Metal Forming Analysis (with Application to Hydrau-static Bulging of a Circular Sheet)',International Journal of Mechanical Science, vol. 24, No.7, 1982, pp 393-406.

39. Osakada, K., Nakano, J., and Mori, K., 'Finite Element Method for Rigid-Plastic Analysis of Metal Forming-Formulation for Finite Deformation', International Journal for Mechanical Science, vol.24, No.8, 1982, pp 459-468.

40. Oh, S.I., 'Finite Element Analysis of Metal Forming Processes with Arbitrary Shaped Dies', International Journal of Mechanical Science, vol. 24, No.8, 1982, pp 479-493.

41. Tomita, Y., 'A Rigid Plastic Finite Element Perturbation Method for the Effective Prediction of the Influence of the Change in Parameters in the Constitutive Equation Upon Deformation Behaviour', International Journal of Mechanical Science, vol. 24, No.12, 1982, pp 711-716.

42. Mital, N.K., 'Prediction of Binder Wrap in Sheet Metal Stampings Using Finite Element Method', Proceedings, Thirteenth North American Manufacturing Research Conference, SME, Manufacturing Engg. Transactions, May 1985, pp 75-80.

43. Kropp, P.K., and Lahoti, G.D., 'Finite Element Modelling of a Near Net Shape Forming Process for a Bearing Component', Proceedings, Thirteenth North American Manufacturing Research Conference, SME, Manufacturing Engg. Transactions, May 1985, pp 164-169.

44. Guoji, Li, Xianguang, Pan, and Yijian, Huang, 'DIFO-2-A User Oriented FEM Programme for Die Forging', Proceedings, Thirteenth North American Manufacturing Research Conference, SME, Manufacturing Engg. Transactions, May 1985, pp 442-448. .

45. Wu, W.T., and Oh, S.I., 'ALPIDT: A General Purpose FEM Code for Simulation of Nonisothermal Forming Processes', Proceedings, Thirteenth North American Manufacturing Research Conference, SME, Manufacturing Transactions, May, 1985, pp 449-455.

46. Zienkiewicz, O.C., The Finite Element Method, McGraw Hill Book Company (UK) Limited, Third Expanded and Revised Edition, 1977.

47. Bathe, K.J., and Wilson, E.L., Numerical Methods in Finite Element Analysis, Prentice Hall India Pvt.Ltd., New Delhi, 1978.

48. Desai, C.S., and Abel, J.F., Introduction to the Finite Element Method, Affiliated East-West Press Pvt. Ltd., New Delhi, 1972.

49. Reddy, J.N., An Introduction to the Finite Element Method, McGraw Hill Book Company, 1984.

50. Martin, C.H., and Carey, G.F., Introduction to Finite Element Analysis , Tata McGraw-Hill, New Delhi, 1979.

51. Vijayan, C., 'Finite Element Analysis of Strip and Circular Plate Anchors', Ph.D. Thesis, Indian Institute of Technology, Kanpur, February, 1981.

52. Dutta, B.K., 'A 2-D Thermo-Mechanical Finite Element Model for Residual Stress Determination during Welding and Annealing', M.Tech. Thesis, Indian Institute of Technology, Kanpur, July, 1983.

53.   Yamada, Y., Yoshimura, N., and Sakurai, T., 'Plastic
      Stress-Strain Matrix and its Application for the
      Solution of Elastic-Plastic Problems by the Finite
      Element Method', International Journal of Mechanical
      Science, vol. 10, No.5, 1967, pp 343-354.

54.   Marcal, P.V., and King, I.P., 'Elastic-Plastic Analysis
      of Two-Dimensional Stress Systems by the Finite Element
      Method', International Journal of Mechanical Science,
      vol. 9, 1967, pp 143-155.

55.   Marcal, P.V., 'A Stiffness Method for Elastic-Plastic
      Problems', International Journal of Mechanical Science,
      vol. 7, 1965, pp 229-238.

56.   Zienkiewicz, O.C., Valliappan, S., and King, I.P.,
      'Elasto-Plastic Solutions of Engineering Problems;
      Initial Stress Finite Element Approach', International
      Journal for Numerical Methods in Engineering, vol. 1,
      1969, pp 75-100.

57.   Lee, C.H., and Kobayashi Shiro, 'Elasto-Plastic Analysis
      of Plane-Strain and Axisymmetric Flat Punch Indentation
      by the Finite Element Method', International Journal of
      Mechanical Science, vol.12, April 1970, pp 349-370.

58.   Argyris, J.H., 'Elasto-Plastic Matrix Displacement
      Analysis of Three-Dimensional Continua', Journal of
      Royal Aeronautical Society, 1965, pp 633-635.

59.   Nayak, G.C., and Zienkiewicz, O.C., 'Convenient form of
      Stress Invariants for Plasticity', Journal of Structural
      Division, ASCE, vol. 98, 1972, pp 949-954.

60.   Nayak, G.C., and Zienkiewicz, O.C., 'A Note on 'alpha'
      Constant Stiffness Method for the Analysis of Nonlinear
      Problems', International Journal for Numerical Methods
      in Engineering, vol.4, 1972, pp 579-82.

61.   Nayak, G.C., and Zienkiewicz, O.C.,'Elasto-Plastic Stress
      Analysis, a Generalisation for Various Constitutive
      Relations Including Strain Softening', International
      Journal for Numerical Methods in Engineering, vol.5,1972,
      pp 113-35.

62.   Stricklin, J.A., and Haisler, W.E., 'Formulations and
      Solutions Procedures for Nonlinear Structural Analysis',
      Computers and Structures, vol.7, No.1, 1977, pp 125-136.

63. Rice, J.R., McMeeking, R.M., Parks, D.M., and
     Sorenson, E.P., 'Recent Finite Element Studies in
     Plasticity and Fracture Mechanics', Computer Methods
     in Applied Mechanics and Engineering, vol. 17/18,
     1979, pp 411-442.

64. Johnson, W., and Mellor, P.B., Engineering Plasticity,
     Van Nostrand Reinhold Company, 1973.

65. Smith, I.M., Programming the Finite Element Method,
     John Wiley and Sons, 1982.

66. Rowe, R.K., and Davis, E.H., 'Application of the
     Finite Element Method to the Prediction of Collapse
     Loads', Research Report No. R310, Civil Engg. Labora-
     tories, The University of Sydney, School of Civil
     Engg. 1977.

67. Durocher, L.L., and Gasper, A., 'A Versatile Two-
     Dimensional Mesh Generator with Automatic Bandwidth
     Reduction', Computers and Structures, vol.10, 1979,
     pp 561-575.

68. Hill, R., The Mathematical Theory of Plasticity, Oxford
     University Press, 1950.

69. Kukreti, A.R., Khan, A.S., and Iranmanesh, A., 'Fra-
     cture Prediction in Elastic-Plastic Problems Using
     Finite Element Method', Proc. of the International
     Conference on Application of Fracture Mechanics to
     Materials and Structures, FRG, 1984, pp 619-632.

Appendix A

ELASTO-PLASTIC PROGRAMME

This computer programme is developed on DEC-1090 computer system. It is a general purpose programme in which the 'initial stress method' is used for nonlinear elasto-plastic analysis. This incorporates von-Mises yield criterion for two dimensional plane strain problems. The continuum is discretised using eight noded isoparametric element.

The various sub-routines of the programme carry out most of the computational steps and rest of the calculations are done in main programme. Main programme controls various subroutines. Flow chart for MAIN PROGRAMME and STRESS ROUTINE are given in Fig. A.1 and Fig. A.2 respectively.

MAIN
PROGRAMME
Calls GDATA
initialises total displacement, strain,
stress and nodal load vector
calls LOAD
calls FORMK
calls SOLVE
calls DIS
calls STRESS
prints total displacement, total strain, total stress
and net nodal load once solution converges
checks for crack initiation at integration points.

GDATA
ROUTINE

reads and prints number of nodes, number of elements, number of nodes per element, order of numerical integration, number of nodes on which geometric boundary condition are specified, maximum number of iterations in an increment, number of different materials, bandwidth of the global stiffness matrix

reads and prints material properties

reads and prints nodal point data

reads and prints element data

reads and prints boundary data

LOAD
ROUTINE

initialises load vector

reads and prints applied external load, if any, assembles load vector

STIFT2
ROUTINE

initialises element stiffness matrix

calls GAUSS

calls QUAD8

calls FORMJ2

calls DTXY

forms strain-displacement matrix

forms stress-strain matrix

forms element stiffness matrix

QUAD8
ROUTINE

calculates shape function

calculates x and y derivatives of shape function

FORMK
ROUTINE

initialise global stiffness matrix

calls STIFT2

assembles global stiffness matrix

SOLVE
ROUTINE

applies prescribed geometric boundary conditions
at nodes

carries out the triangularisation of the banded

symmetric matrix by Cholesky decomposition

solves for displacement vector by back substitution

for all iterations

DIS
ROUTINE

prints incremental nodal displacements (if required)

calculates incremental strains

STRESS
ROUTINE

initialize residual load vector,

calculates incremental stresses,

checks for yielding at integration points,

calculates elasto-plastic stress-strain

matrix if integrating point yielded,

computes the correction stress vector
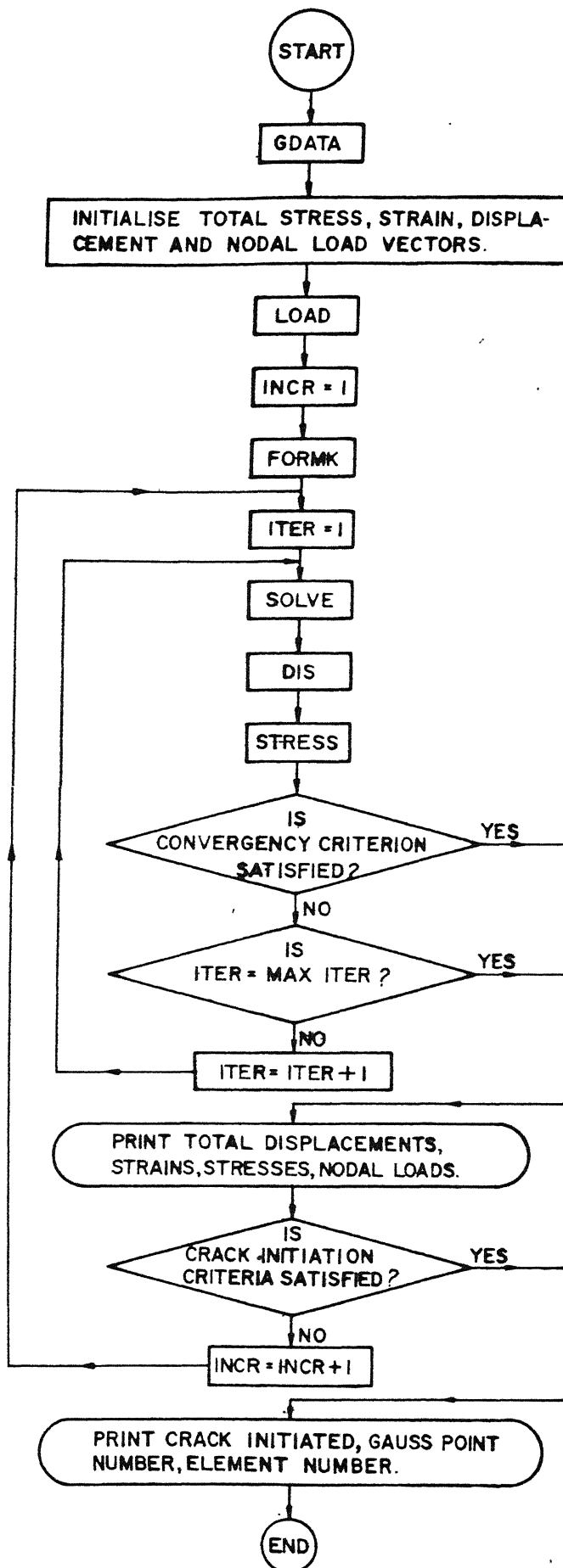
and find residual load vector.

FIG. A.I   FLOW CHART: MAIN PROGRAMME